DIVERSE EFFECTS OF AROUSAL AND LOCOMOTION ON INHIBITORY AND EXCITATORY NEURONS IN AUDITORY CORTEX

by

IRYNA YAVORSKA

A DISSERTATION

Presented to the Department of Psychology
and the Graduate School of the University of Oregon
in partial fulfillment of the requirements
for the degree of
Doctor of Philosophy

December 2019

DISSERTATION APPROVAL PAGE

Student: Iryna Yavorska

Title: Diverse Effects of Arousal and Locomotion on Inhibitory and Excitatory Neurons in Auditory Cortex

This dissertation has been accepted and approved in partial fulfillment of the requirements for the Doctor of Philosophy degree in the Department of Psychology by:

Mathew Smear	Chairperson
Michael Wehr	Advisor, Core Member
Paul Dassonville	Core Member
Cris Niell	Institutional Representative

and

Janet Woodruff-Borden	Vice Provost and Dean of the Graduate School

Original approval signatures are on file with the University of Oregon Graduate School.

Degree awarded December 2019

DISSERTATION ABSTRACT

Iryna Yavorska

Doctor of Philosophy

Department of Psychology

December 2019

Title: Diverse Effects of Arousal and Locomotion on Inhibitory and Excitatory Neurons in Auditory Cortex

Cortical processing of sensory stimuli reflects a complex interplay between bottom-up sensory input and top-down modulatory effects of attention, arousal, and behavioral relevance. The mechanisms by which changes in brain states can modulate the activity of sensory neurons are not well understood. Recent evidence suggests that inhibitory interneurons form specific local circuits across cortical layers that allow them to reshape sensory-evoked responses and modulate spontaneous activity of cortical neurons. Recent advances in optogenetic and multineuronal recording technologies have made it possible to probe local inhibitory circuitry in auditory cortex to elucidate the involvement of VIP-expressing inhibitory cells during endogenous modulation by arousal and locomotion. Here, we describe the effects of endogenous modulatory signals and VIP activation on auditory cortical processing in different cell types and cortical layers. We find that both changes in behavioral state and VIP activation have diverse distributed effects on spontaneous and evoked activity of auditory neurons. Additionally, we show that some aspects of cortical modulation have cellular and layer specificity, although these specific effects do not necessarily overlap in their cellular targets. By separately examining the influence of artificial modulation by VIP activation and endogenous modulation by behavioral state, as well as their combined interactive effects, we conclude that running and arousal changes in auditory cortex are not mediated by VIP-expressing neurons. Finally, we discuss a different subclass of inhibitory interneurons, the main targets of VIP cells, and their known contributions to cortical modulation.

CURRICULUM VITAE

NAME OF AUTHOR: Iryna Yavorska

GRADUATE AND UNDERGRADUATE SCHOOLS ATTENDED:

University of Oregon, Eugene, OR
Indiana University of Pennsylvania, Indiana, PA
Westmoreland County Community College, Youngwood, PA
Volyn State University, Lutsk, Ukraine

DEGREES AWARDED:

Doctor of Philosophy, Psychology, 2019, University of Oregon
Bachelor of Arts, Psychology, 2012, Indiana University of Pennsylvania

AREAS OF SPECIAL INTEREST:

Systems Neuroscience
Electrophysiology

PROFESSIONAL EXPERIENCE:

Graduate Teaching Fellow, Department of Psychology
University of Oregon, Eugene, OR, 2012-2019

PUBLICATIONS:

Yavorska, I., Wehr, M. (2016). Somatostatin-Expressing Inhibitory Interneurons in Cortical Circuits, *Front. Neural Circuits,* 76(10), 1-18

Hoy, J., **Yavorska, I.**, Niell, C., Wehr, M. (2016). Vision Drives Accurate Approach Behavior during Prey Capture in Laboratory Mice, *Current Biology,* 26(22), p. 3046–3052

ACKNOWLEDGMENTS

I would like to thank first and foremost my advisor, Mike, for his support and encouragement that was much needed during many ups and downs of my research work. His kindness and patience allowed me to follow my curiosity and through trial and error learn to become a more rigorous scientist. I would also like to thank many incredible, supportive and intelligent people I was lucky to work with in the Wehr lab: Michael Kyweriga, Allie Moore, Jonny Saunders, and Aldis Weible for teaching me everything that went into my dissertation from programming skills, statistical analysis, mouse surgeries to soldering small electronics and debugging mysterious electrical noise that always found its way into electrophysiological recordings. Additionally, I would like to thank Donna Kayal and Catie Kimsey, two very smart and dedicated undergraduate students and friends who helped me with hours of data processing and analysis. Without immense support that I received at the University of Oregon, this PhD would not have been possible.

I dedicate this work to my dad Ihor.

TABLE OF CONTENTS

Chapter Page

LIST OF FIGURES

Figure Page

LIST OF TABLES

Table Page

CHAPTER I

INTRODUCTION

The role of auditory cortex in processing and encoding different features of sound is still not well understood. Many aspects of hearing, such as frequency and amplitude discrimination as well as sound localization, are computed by subcortical structures. Recent findings in animals as well as humans point to the critical role of auditory cortex in perception of complex sounds and learning. More importantly, new research provides evidence that auditory cortical processing can be strongly influenced by other sensory information, contextual cues, fluctuations in brain states, as well as motor activity. These findings suggest that auditory cortex can act as a hub where auditory information is integrated with other neural signals that reflect an animal's internal state, such as arousal and selective attention, as well as motor activity, such as vocalization and locomotion, thereby contributing to speech perception and auditory motor learning

Most cortical neurons are excitatory and only 20% of cortical cells are inhibitory. Inhibitory neurons play a critical role in shaping neural responses (Liu et al. 2007; Gentet et al. 2010) that are necessary for diverse animal behaviors and cognition. Though cortical inhibitory interneurons are a diverse population, making them difficult to study, using molecular markers has been an effective way to classify them. Neurons that express somatostatin peptide (SOM), vasointestinal peptide (VIP), and parvalbumin (PV) calcium-binding protein form non-overlapping populations that account for the vast majority of inhibitory interneuron in cortex (Xu et al. 2010; Rudy et al. 2011). Most inhibitory neurons in the central nervous system use gamma-aminobutyric acid (GABA) as a neurotransmitter. GABAergic neurons are known to play critical roles in the development, maintenance, and modulation of cortical circuits, however it is still unclear whether and how their diversity is functionally related to specific cortical processes and the extent to which any meaningful differences among them are preserved across cortical regions.

One challenge in studying inhibitory interneurons is that they exhibit remarkable diversity in their morphology, synaptic physiology, firing properties, connectivity, and molecular markers across all cortical layers (Rudy et al. 2011). Recent advancements in

genetic tools have allowed researchers to manipulate the activity of GABAergic neurons that express different molecular markers to understand their impact on local cortical processing (Aston-Jones and Deisseroth 2013). Though these genetic markers do not map cleanly onto other types of differences among these cells, there are some general rules that seem to hold true across multiple studies. For example, SOM cells tend to have low-threshold firing properties, while PV cells tend to be fast spiking (Cauli et al. 2000; Moore and Wehr 2013; Markram et al. 2004). Interneurons that express the VIP marker tend to mostly inhibit other inhibitory cells (Lee and Dan 2012; Hioki et al. 2013; Pi et al. 2013; Dalezios et al. 2002), although they also provide small direct inhibition to other excitatory neurons (Prönneke et al. 2015).

Interneurons are Affected by Modulatory Input

Studies that have looked at cellular mechanisms and effects of locomotion and arousal on sensory cortices in general, and on auditory cortex specifically, have reported different results. Some of the inconsistencies might be attributed to methodologies. For instance, while calcium imaging allows researchers to investigate the activity of many excitatory and inhibitory neuronal subtypes at the same time, it can only show activity in superficial layers, down to layer 4 only, which provides an incomplete picture of cortical modulation. Intracellular patching studies have been indispensable for our understanding of detailed subthreshold and suprathreshold changes in activity and synaptic inputs during locomotion and shifts in arousal. However, these studies, due to difficulty in methodology, often report a small number of neurons, recorded one at a time, which makes it challenging to understand how these modulatory signals affect cortex as a whole. Finally, recent developments in multi-site array technology have allowed researchers to record from an ever-increasing number of neurons across cortical columns as well as horizontally connected cells over a prolonged period of time. Though multi array electrodes only allow extracellular recording of spikes and local field potentials, they usually yield hours of stable recordings of spiking activity of tens to hundreds of neurons. This has led to new challenges, such as high-throughput spike sorting and computationally-intensive analysis of large datasets.

SENSORIMOTOR INTEGRATION

Modulation of evoked auditory responses has been an important topic of research in humans (Houde et al. 2002) as well as animals (Eliades and Wang 2003). Numerous studies in humans, non-human primates, as well as small mammals have shown that spontaneous and evoked activity of most auditory cortical neurons is suppressed during vocalization. A few studies have also pointed to a smaller subset of cells that either show a modest increase or do not change their sound evoked response (Zhou et al. 2014). Though it's still not clear whether modulation during vocalization shares similar mechanisms with the modulation observed during movements, many studies in mammals have described similar suppression of sound evoked responses in cortical neurons during motor activity, regardless of movement types (Schneider et al. 2014; Nelson et al. 2013). Responses to simple and complex sounds have been shown to be suppressed in humans by a variety of movements as well, suggesting that the mechanisms involved are likely preserved across species and are indiscriminate of specific sound properties (Weiss et al. 2011).

Suppression of evoked auditory responses has been viewed as a vital component of speech processing that relies on sensorimotor integration, suggesting that auditory cortex plays an important part in speech production and that the motor system can greatly contribute to speech perception (Hickok et al. 2011). However, previous research that has studied patients with motor deficits, as well as mammalian animal models, has shown that the ability to speak is not necessary for speech perception (Gelding and Sun 2018; Ross et al. 2017; Saunders and Wehr 2019). Motor activity is also not necessary for history-dependent and context-dependent attributes of speech perception. These findings question the exact role of motor modulation of sensory processing, although its ubiquitous influence in all sensory systems has been well established.

In auditory cortex, a variety of movements, such as blinking, grooming, and running, lead to widespread suppression of sound-evoked and spontaneously generated spikes (Schneider et al. 2014; Nelson et al. 2013). Previous work showed that these movements are preceded by activity in secondary motor cortex (M2), which sends projections to both excitatory pyramidal neurons and PV+ inhibitory interneurons in auditory cortex, which results in a net suppression of excitatory neurons (Schneider et al.

2014). Other (non-PV) inhibitory interneurons also show movement-related increases in activity, though they are not targeted by M2 projections (Schneider et al., 2014). Locomotion can also result in suppression of auditory cortical processing via a decrease in thalamic and intracortical drive (Zhou et al. 2014) and ACh-related cortical inhibition (Hangya et al. 2015; Nelson and Mooney 2016). The effects of movement on activity in auditory cortex are thus complex and likely to involve multiple pathways.

Neural Signature of General Arousal

Previous work has shown that the activity of both noradrenergic (NE) neurons in LC and cholinergic (ACh) neurons in the basal forebrain (BF) reliably correlate with pupil diameter in mice (Reimer et al. 2016; Joshi et al. 2016). NE neurons are more closely related to rapid changes in pupil size (Reimer et al., 2016) while ACh neurons are correlated with periods of sustained pupil dilations that are often present during running bursts (Reimer et al. 2016).

Multiple studies have looked at the electrophysiological parameters of brain states and their relationship to a variety of cognitive factors such as arousal, attention, cognitive load, and task performance (Harris and Thiele 2011). Animal studies have revealed that movements, such as locomotion or whisking, are often accompanied by a reduction in low-frequency rhythmic cortical activity, an increase in high-frequency cortical activity, enhanced sensory processing (Fu et al. 2014; Niell and Stryker 2010), a decrease in membrane potential variance (McGinley et al. 2015), and a decrease in input resistance and intrinsic excitability (Schneider et al. 2014). Similar changes in sensory processing are also visible during fluctuations in pupil diameter without movements, often in a nonlinear fashion. In auditory cortex, studies that have looked at pupil changes and locomotion have reported increased neural firing only during intermediate pupil size (i.e., an inverted U-shaped curve), with lower neural firing rates during strong pupil constriction and dilation (McGinley et al. 2015).

Although the effect of modulatory input on cortical sensory processing has been a popular focus of research, many of the underlying mechanisms are still not well understood. This is likely due to a variety of factors such as type of modulation (neurotransmitter and timescale), sensory system, cortical layer, and cellular subtype.

From previous research, we know that modulatory input from the basal forebrain (BF) and locus coeruleus (LC) affects spontaneous and stimulus-evoked neuronal firing during locomotion (Fu et al. 2014; Niell and Stryker 2010; Nelson and Mooney 2016), changes in arousal (Gonchar et al. 2007; Pfeffer et al. 2013), task engagement (Otazu et al. 2009), and the presence of reinforcement/punishment signals (Pi et al. 2013; Hangya et al. 2015) across different sensory modalities.

In visual cortex, it is now well-established that locomotion increases the gain of visually evoked responses without altering tuning of the cells for stimulus parameters (Niell & Stryker, 2010). Recent research has pointed to the VIP-SOM disinhibitory network as one possible way that long-distance projections can communicate the locomotion signal and thereby influence sensory processing (Fu et al. 2014). VIP neurons in V1 are strongly activated via nAChRs during locomotion, which suppresses SOM neurons resulting in an increase in spontaneous and evoked visual responses in principal cells (Fu et al. 2014). Blocking nAChRs leads to a gain reduction in V1 (Herrero et al. 2017). Muscarinic signaling is also involved, although the relative contributions of nicotinic and muscarinic AChR signaling are complex and not completely resolved (Herrero et al. 2017). Indeed, ACh can also directly depolarize SOM neurons over a prolonged period of time, peaking at 10 s, via both nicotinic and muscarinic receptors (Chen et al. 2015). The effect of ACh on cortical neurons can greatly vary depending on the concentration and timing of neurotransmitter release. Experiments *ex vivo* show that in V1 a wide range of ACh concentrations depolarize and evoke action potentials (APs) in SOM interneurons, while only high concentrations of ACh result in APs in VIP and layer I neurons (Chen et al., 2015). Due to high interconnectivity of inhibitory cells, strong depolarization of SOM neurons by ACh results in net inhibition of their VIP and layer I targets at low concentration, counteracting the facilitating effects of ACh in those cells. Additionally, ACh induces SOM-mediated inhibitory currents in PV and principal neurons, leading to robust local field potential (LFP) desynchronization and decorrelation of cortical principal neurons without changing their firing rate (Chen et al. 2015). Suppressing VIP cells using archaerhodopsin (Arch) or activating SOM cells using channelrhodopsin (ChR2) was sufficient to induce LFP desynchronization in anesthetized mice (Chen et al. 2015). Thus, the timescale of cholinergic effects can be reflected in the

activity of different inhibitory cell types, fast disinhibition via VIP-SOM during high-concentration of ACh release and slow prolonged neuronal decorrelation via SOM-PV and SOM-PN during low-concentration of ACh release.

Unlike in visual cortex, increased attention during task performance leads to suppression in responses in auditory cortical neurons, but not in the thalamus (Otazu et al., 2009), though under certain conditions thalamic neurons also show modulation (Jaramillo et al. 2014). The mechanisms of auditory selective attention are still not known. SOM cells in superficial layers contribute to tone habituation in layer 2/3 neurons (Natan et al. 2015; Kato et al. 2015), while sound-guided behavior selectively decreases SOM cell activity, thus releasing PNs from inhibition (Kato et al. 2015), making SOM neurons unlikely candidates of attention-related auditory suppression. Auditory learning seems to engage a different set of neuronal ensembles. Fear-conditioning using tone-shock pairing leads to stronger neural responses to a conditioned tone in mice (Letzkus et al. 2011). During foot-shock, layer I non-VIP auditory neurons that express nAChR inhibit layer 2/3 PV interneurons, thus reducing IPSPs in principal neurons and increasing their responses to a conditioned tone. Pairing tones with nucleus basalis stimulation improves cellular response reliability to a paired stimulus (while also decreasing response to previously-preferred tone) as well as increases an animal's detection rate of paired tones (Froemke et al. 2013). Like movement-related neural modulation of auditory processing, attention, task engagement, and learning-related modulation are also likely to be diverse involving different cellular mechanisms that require temporal specificity.

M2 projections only target a subset of PV and excitatory neurons. Previous work has shown strong projections from M2 to auditory cortex which results in an increase of PV activity and net suppression of excitatory spontaneous and evoked activity (Schneider et al. 2014; Nelson et al. 2013). Similarly, upregulation of PV activity has also been observed in visual cortex via a different mechanism (Fu et al. 2014). Both M2 and BF projections convey motor signals to auditory cortex, and some of their targets overlap, but some do not. Additionally, they receive their input from different brain regions (M2 input comes from motor planning cortical regions, BF input comes from subcortical regions). Additionally, two main inhibitory subtypes, VIP and SOM, show different

patterns of cholinergic receptor expression. Fast VIP recruitment via nicotinic receptors might be involved during locomotion on millisecond time scales, while slower muscarinic receptors might change the excitability of SOM neurons over prolonged periods on the time scale of seconds to minutes. By manipulating the activity of VIP and SOM neurons independently and quantifying the effect of their manipulation on principal cells, we can see if differences in timescales of VIP activation vs SOM suppression map onto specific cortical neurons with similar effects during changes in neural states.

Cortical neurons are estimated to make 3,000 to 10,000 synaptic connections, depending on the region and species (Peters 1987; Schüz and Palm 1989). While many of these synaptic connections are made between cortical and subcortical regions, local intracortical connections are common and play important roles in sensory computations (Seeman et al. 2018; Levy and Reyes 2012). It has been estimated that more than half of the synaptic connections to any given neuron come from neurons within 100 - 200 μm radius, resulting in a highly redundant and interconnected local network of cells that can be stimulated by a similar external stimulus (Peters and Sethares 1991; Pfeffer et al. 2013). The complexity of cortical computations is also reflected in neuronal electrophysiological properties (input resistance, firing threshold, synaptic adaptation, etc.) that can have a dramatic effect on how different cells integrate their input. Numerous electrophysiological properties of neurons that can be dictated by biophysical properties of membrane channels and probabilistic neurotransmitter release lead to highly variable neuronal output, typically with noisy firing rates and irregular interspike intervals. The vast interconnectedness of neurons as well as their irregular spiking makes deciphering neural computations quite challenging. The work summarized in this dissertation focuses on quantifying changes in neuronal output for auditory stimuli as well as for spontaneous activity during different behavioral states: quiescent (stationary), high arousal (stationary), and high arousal with locomotion. Using optogenetic tools, I will also examine the contributions of three main inhibitory neuronal subtypes to the modulatory effects of those behavioral states.

CHAPTER II

MODULATION OF AUDITORY CORTEX BY VIP-EXPRESSING INTERNEURONS

INTRODUCTION

VIP neurons comprise a small fraction (10-15%) of all inhibitory neurons, corresponding to only 1-2% of all cortical cells (Gonchar et al. 2007; Pfeffer et al. 2013). Though they are found in all cortical layers, their density is the highest in layer 2/3 (Xu et al. 2010). Similarly to SOM neurons, VIP neurons most commonly coexpress CR, NPY, and CCK as additional molecular markers (Xu et al. 2010; Kubota et al. 2011; Cauli et al. 2014). Most VIP neurons are continuous adapting (70%), bursting and irregular spiking. Thirty percent of 5HT3aR-expressing cells also express VIP. VIP cell axons are primarily dendrite-targeting. A substantial portion (80%) of their targeted subcellular structures are dendrites, with the exception of layer 6 where ~40% of the synapses they make are axosomatic (Zhou et al. 2017).

VIP neurons do not take part in cortical critical period plasticity and have little effect on thalamic input to cortical layer 4 neurons in A1 (Takesian et al. 2018). Response properties of VIP neurons vary in V1 and A1. In layer 2/3 of auditory cortex they respond later than PV neurons and are selective for lower intensity sounds (Mesik et al. 2015).

VIP interneurons also show diversity in their connectivity and morphology across cortical layers. In layer 2/3 they typically exhibit bipolar/ bitufted dendritic morphology, while in deeper layers 4-5 their shapes expand to other varieties such as tripolar, multipolar, and atypical types (Bayraktar et al. 2000; Prönneke et al. 2015). VIP neurons in superficial layers tend to send their axons to all layers in columnar fashion while keeping their dendrites in layers 1 and 2/3. On the other hand, VIP cells in layers 4-5 restrict their axons to deeper layers while spreading dendrites across all cortical columns, suggesting that effects of VIP activation in infragranular layers may not only be specific to their column but also to their layer.

VIP neurons have been shown to participate in a disinhibitory circuit in mouse auditory cortex (Pi et al. 2013; Pfeffer et al. 2013). This disinhibitory circuit is recruited during performance of an auditory discrimination task: reinforcement signals activated

VIP neurons for an extended period of time, while punishment signals activated VIP neurons only for a brief duration. This activity then inhibited SOM and a fraction of PV inhibitory neurons, resulting in a net increase of neural responses to tones (Pi et al., 2013). A similar disinhibitory circuit has also been reported in barrel cortex during locomotion, where VIP neurons receive input from motor cortex (Lee et al. 2013). In auditory cortex, the BF projects to all major types of cortical neurons, including VIP, resulting in depolarization in auditory neurons, during stimulation of BF axons in ChAT-ChR2 mice and locomotion (Nelson and Mooney 2016). Though both M2 and BF convey movement related signals to the auditory neurons, the extent of convergence of this input and the timescale of its strongest recruitment and influence on auditory processing remains unknown.

The functional roles of VIP neurons in auditory cortical processing remain unclear. Characterization of VIP cells and their effect on other neurons has been mostly restricted to upper layers or a small number of patched cells in deeper layers (Fu et al. 2014; Nelson and Mooney 2016; Lee et al. 2013; Pi et al. 2013; Pfeffer et al. 2013). About 60% of VIP neurons are located in layer 2/3. The fact that they maintain their dendrites in superficial layers with local axonal projections only within their own layer or to layer 5a suggests that these VIP cells are the ones that have been implicated in the disinhibitory motif and likely correspond to those that have been described previously (Fu et al., 2014). The other 40%, in layers 4-5 seem to exhibit a different connectivity pattern, the function of which is still not described. Although it is known that VIP neurons have diverse morphology and show diverse inhibition of principal neurons, the functional implications of VIP inhibition of excitatory neurons are still not well-understood. The differences in dendritic and axonal projection between VIP cells in superficial and deep layers suggest that their role might not be restricted to state modulation via a disinhibitory circuit alone.

We recorded from auditory neurons in awake mice that expressed ChR2 in VIP-positive neurons, during natural changes in arousal and locomotion. Though activating VIP cells produced an overall facilitating effect on cortical neurons, this effect was not homogeneous, with about 44% of neurons increasing their firing and 27% decreasing. Inhibited and disinhibited neurons were found in all cortical layers, but the distribution of

inhibited cells was shifted towards supragranular layers, while disinhibited neurons were more likely to be found in infragranular layers. Running and changes in arousal also led to diverse effects on neuronal activity. Running led to an increase in spontaneous activity but a suppression of evoked activity, whereas increases in arousal without locomotion led to modest increase in both evoked and spontaneous activity. Changes in neuronal firing when the animal was running during VIP activation trials were well-predicted by the sum of VIP activation and running effects separately. Similar results were observed when an animal's arousal level changed without locomotion. Taken together, these results suggest that the modulatory effects of running and arousal are not mediated by VIP inhibitory network.

EXPERIMENTAL PROCEDURES

Mice

All procedures were performed in accordance with National Institutes of Health guidelines, as approved by University of Oregon Institutional Animal Care and Use Committee. We recorded from offspring (N = 16, age range 60 - 210 days) of a cross between a homozygous cre-dependent ChR2-eYFP line (Madisen et al., 2012; JAX Stock No. 012569) and a homozygous PV-IRES-Cre line, n = 6 (Hippenmeyer et al. 2005; JAX No. 008069) or a homozygous VIP-IRES-Cre line, n = 10, (Taniguchi et al. 2011 JAX No. 010908) using linear array silicone probes.

Surgery

Mice were anesthetized with isoflurane (1.25-2.0%). A headpost was secured to the skull and a mark was made on the skull over auditory cortex for a future craniotomy (AP: -2.9 mm, ML: 4.4 mm, relative to bregma). Mice were housed individually following the surgery and were allowed at least 5 days of post-operative recovery. On the day of recording, mice were anesthetized with isoflurane (1.25-2.0%), the head was clamped with the headpost, and a small craniotomy was made over auditory cortex (1x1 mm). The craniotomy was covered with a thin layer of agar and the animal was allowed to recover for at least an hour before recording.

Electrophysiology

All electrophysiological recordings were performed while the animal was awake and head-fixed on a styrofoam ball inside a double-walled acoustic isolation booth. The ball was mounted on an axle that allowed it to rotate forwards or backwards; rotation of the ball produced by locomotion of the animal was measured with an optical mouse. Neurons in auditory cortex were recorded with either a 32-channel silicon probe (25 μm spacing between sites, single 750 μm shank, Neuronexus A1x32-Poly2-5mm-50s-177) or a 64-channel probe (25 μm spacing between sites, two 750 μm shanks, Neuronexus A2x32-Poly2-5mm-25s-200-177), Intan RHD2000 board, and Open Ephys software (Siegle et al. 2017). The silicon probe was positioned with a micromanipulator (MP- 285, Sutter) orthogonal to the cortical surface such that the electrode sites spanned cortical layers. Spiking and local field potential data were filtered online (600-6000 Hz and 0.1-400 Hz, respectively) and recorded. Single neurons were identified offline using Kilosort spike sorting software (Pachitariu et al. 2016). To measure the depth of recorded cells, we used current source density analysis of the local field potential evoked by 600 ms white noise bursts. We identified the robust sink with the shortest latency at the L3-L4 boundary and assigned it a depth of 400 μm (Intskireli & Metherate 2012). We assigned the depths of individual neurons relative to this, based on the channel exhibiting the maximum waveform amplitude for each neuron. This allowed us to relate recording depth to our histological analysis and laminar boundaries (Anderson et al 2009). Recordings for which current-source density did not yield unambiguous depth information were excluded from any analysis based on depth of recorded cells, such as laminar analysis.

Acoustic stimuli

Sound was delivered from a free field speaker on the contralateral side of recording site. To test effects of locomotion, arousal, and VIP activation on evoked activity 600 ms white noise (WN) bursts were presented at 80 dB amplitude with a one second interstimulus interval. Acoustic stimuli were randomly interleaved with a period of silence (SS) of the same duration, used for measuring spontaneous activity. Both white noise and silent stimuli presentations were presented with and without a laser illumination (wavelength 470, fiber diameter 800 μm), randomly interleaved as well (See

Fig. 1A for experimental design). Stimuli were presented as least 30 times in each combination (WN, SS, WN + laser, SS + laser).

Behavioral state recording

Running speed was recorded using width pulse modulation (WPM) via an optic mouse that was connected to a Raspberry Pi. Movements of the ball were detected by the optic mouse which modulated the width of a 10 ms pulse that the Raspberry Pi send to the Intan board. Pupil size was recorded using a Pi camera and another Raspberry Pi computer at a sampling rate of 30 Hz. Pupil data was analyzed with DeepLabCut software (Mathis et al. 2018) for each mouse separately. Pupil size was quantified as the diameter of a circle fit to the measured pupil.

Analysis

Modulation Index

Spiketimes of individual neurons were binned into 5 ms windows. On responses, Sustained responses, and Off responses were quantified as the average firing rate (FR) in 0 - 100 ms, 100 - 600 ms, and 600 - 700 ms time windows relative to stimulus onset, respectively. Unless otherwise specified, modulation of evoked responses was computed over a 650 ms time window, during the 600 ms of sound presentation plus 50 ms after stimulus offset to include Off responses. Significant evoked responses were identified by a ranksum test between neuronal firing rate during sound presentation and spontaneous neural firing rate during an equivalent period of silence (SS) in laser-off trials ($p < 0.01$). Analysis of the evoked responses included all cells that responded significantly to sound, either with an activated response (increase in firing rate) or a suppressed response (decrease in firing rate), unless specified differently. Modulation index (MI) was defined as the difference in mean firing rate of a neuron in two compared conditions divided by the sum of those means.

$$Run\ MI = (mean\ FR_{run} - mean\ FR_{sit}) / (mean\ FR_{run} + mean\ FR_{sit})$$

$$Pupil\ MI = (mean\ FR_{large\ pupil} - mean\ FR_{small\ pupil}) / (mean\ FR_{large\ pupil} + mean\ FR_{small\ pupil})$$

$$VIP\ MI = (mean\ FR_{laser\ on} - mean\ FR_{laser\ off}) / (mean\ FR_{laser\ off} + mean\ FR_{laser\ on})$$

Modulation index varies from -1 to 1, and measures the amount of firing rate modulation induced by one condition compared to another. For example, a neuron with a Run MI close to 1 fired much more during running than when the mouse was sitting still. A neuron with a Run MI of -1 was completely suppressed during running compared to when the mouse was sitting still. We computed each MI during different states; for example, 'VIP MI sit' compares laser-on to laser-off trials, all recorded when the mouse was sitting still.

Interaction analysis

To obtain predicted values for each neuron, we computed modulation index for each experimental condition separately. Running and arousal (pupil) modulation index was computed in laser off trials, without VIP activation. VIP modulation index was computed in laser on trials during stationary periods or trials during low arousal state, for running and pupil respectively. The predicted value for each cell was the sum of the effects of behavioral modulation (run or arousal) and VIP activation (laser on).

$$Predicted\ run = run\ MI_{laser\ off} + VIP\ MI_{sit}$$

$$Predicted\ pupil = large\ pupil\ MI_{laser\ off} + VIP\ MI_{small\ pupil}$$

To obtain modulation index for each cell when two experimental conditions were present simultaneously (running + VIP activation, or high arousal + VIP activation), a new modulation index was computed. For running, we used the mean firing rate of neurons when animals were running on laser-on trials, and compared to the mean firing rate of neurons on laser-off trials when animals were sitting. Similar computation was performed for high arousal state.

$$Run{+}VIP\ MI = (FR_{run\ +\ laser\ on} - FR_{sit\ +\ laser\ off}) / (FR_{run\ +\ laser\ on} + FR_{sit\ +laser\ off})$$

$$Pupil{+}VIP\ MI = (FR_{large\ pupil\ +\ laser\ on} - FR_{small\ pupil\ +\ laser\ off}) / (FR_{large\ pupil\ laser\ on} + FR_{small\ pupil\ +\ laser\ off})$$

Current source densities

Current source densities (CSDs) were computed on local field potentials (LFPs) recorded during presentation of acoustic stimuli (white noise at 80 dB). LFPs were bandpass filtered from 1 to 300 Hz to remove spikes. CSDs were computed using the standard method; i.e., the second spatial derivative of LFPs were replaced with the corresponding spatial differences (for more details, see Pettersen et al. 2006). This resulted in easily identifiable evoked sources and sinks which are characteristic spatiotemporal patterns in the laminar structure of auditory cortex (Fig. 1F).

$$CSD_j = (trace_{j-1} + trace_{j+1} - 2 * trace_j) / distance^2$$

Cell type categorization

To categorize cells into fast and regular spiking we measured spike width and peak to trough ratio of spike waveforms in recorded neurons. Width was measured from 20% of the peak to 20% of the trough. Neurons showed clear separation into two clusters based on their spike width, thus cells that has a spike width of less than 0.9 ms were classified as fast spiking cells, while cells that had spike with of 0.9 ms or greater were classified into regular spiking cells (Fig. S4, Moore and Wehr 2013; Niell and Stryker 2008).

VIP activation experiments

We recorded from ten VIP-ChR2 mice, n = 27 recording sessions, n = 1009 total cells, regular spiking: n = 834, fast spiking: n = 175. For a subset of recorded neurons (n = 648), we were able to assign the cortical layer they belonged to by identifying sources and sinks from current source density analysis to a white noise stimulus. Modulation induced by running or changes in arousal were calculated for a subset of recordings in which we were able to obtain a sufficient number of trials in each condition (n = 11 recording sessions for running, n = 17 recording sessions for arousal).

Spike correlation analysis

For correlation analysis between neural activity and pupil size or running, we binned spike times of individual neurons into 50 ms time bins and smoothed data over 10 time bins. Binned and smooth firing rate was correlated with pupil trace or running speed

(Spearman's correlation, Fig. 5A). For spike correlations among individual simultaneously recorded neurons, spiketimes were binned into one ms time bins (Fig. 5C). To avoid a bias due to uneven sample size in each condition, Spearman's correlations were bootstrapped using random samples from each condition. Mean correlation values at zero were computed for each neuron in three behavioral conditions: running, stationary low arousal (pupil < 60% of maximum size), and stationary high arousal (pupil > 60% of maximum size).

Distance correlation

Distance correlation values were computed between binned firing rate of simultaneously recorded neurons (100 ms bins) and pupil size or running speed. Because distance correlation measures linear and nonlinear relationship between two variables, the values of the relationship between two variables can be only positive. A distance correlation value of zero can be obtained only if there is no observed dependency between two variables. Additionally, distance correlation can be computed between two variables of different dimensions. Neuronal activity was defined by an n by t matrix where n is the number of neurons in the recording and t is the duration of the recording. Behavioral state, either running or arousal, were defined by an array of t duration of simultaneously recorded running speed or pupil size.

RESULTS

Individual Differences

Previous research has reported variable results of modulatory effects of arousal and locomotion. We hypothesized that some of those differences might be cell-type specific, while some might be due to individual differences between animals, recording sites, or both. To measure the variability of state modulation in our data, we computed distance correlation values for each recording site and each individual neuron separately (see Székely et al. 2007 for details). The idea is to measure how much firing rate is affected by arousal (for example), by measuring the correlation between them. If firing rates are strongly modulated by arousal, the correlation between them should be high, whereas if arousal has no effect on firing rate then the correlation should be close to zero. Since

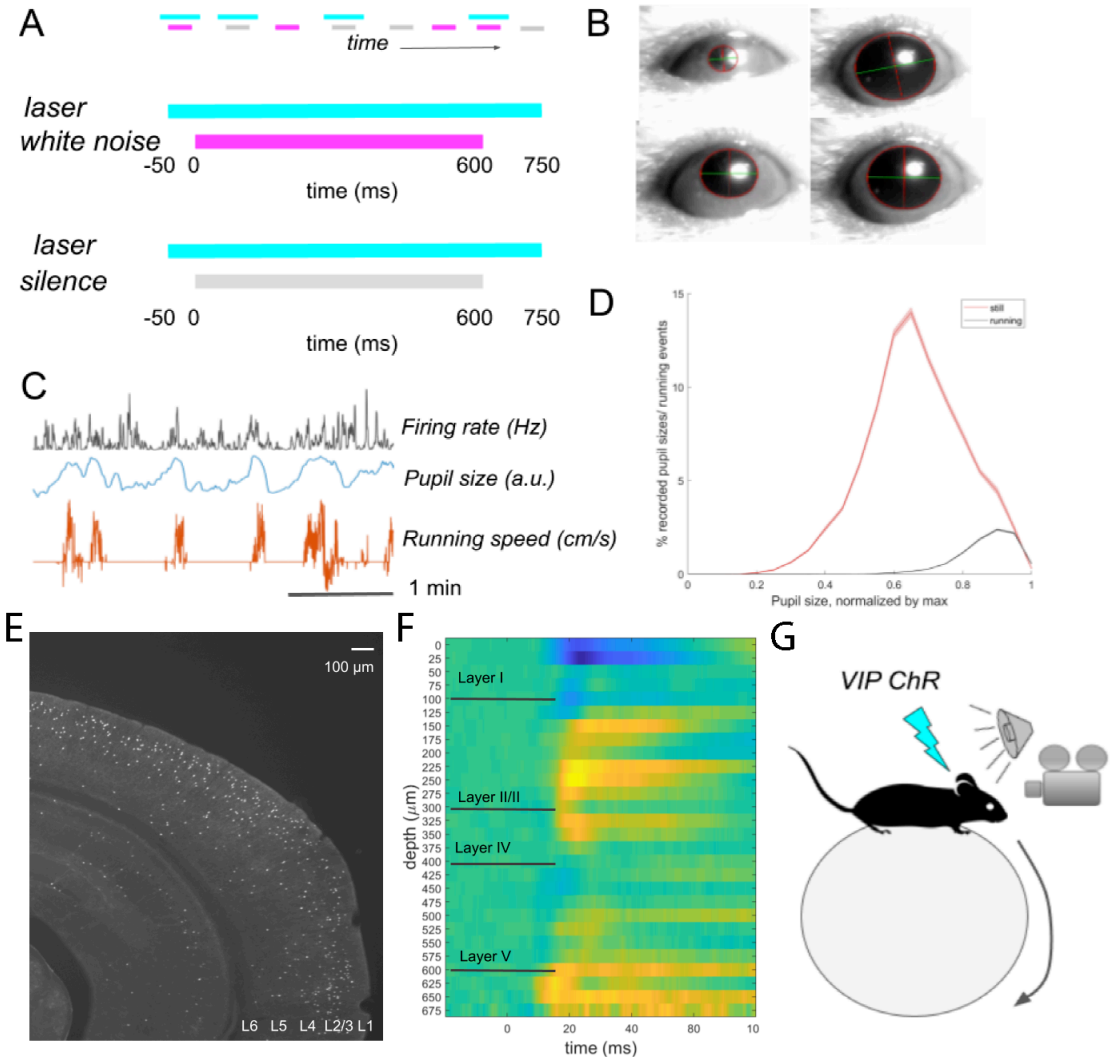

Figure 1. Experimental design and measurements. A. Stimulus presentation. Laser pulses were presented with and without 80 dB WN bursts, the conditions were randomly interleaved, with a one second ISI. When presented, LED pulse began 50 ms before the start of the sound and ended 150 ms after sound offset. **B.** Examples of different states of arousal as measured by the pupil size. Small pupil sizes indicate low arousal state. **C.** Example traces of neuronal FR (100 ms time bins), pupil size, and running speed. Animals frequently oscillated between low and high arousal states. **D.** Percentage of recorded pupil sizes for stationary (red) and running (black) trials. **E.** Expression pattern of VIP-positive interneurons in auditory cortex in a VIP-Cre-Ai14 Mouse. **F.** Sum of CSDs across recordings used for cortical depth analysis (n =18). Sources are shown in blue, sinks are shown in yellow. Two main sources are found in layers 1 and 5. Layers 2/3 and 4 are indicated by a large sink. **G.** Experimental setting. Awake behaving mice were allowed to run on a ball. Sounds were presented randomly interleaved with LED trials. Pupil size was measured on the contralateral side from neural recording site (recordings in left auditory cortex and right pupil).

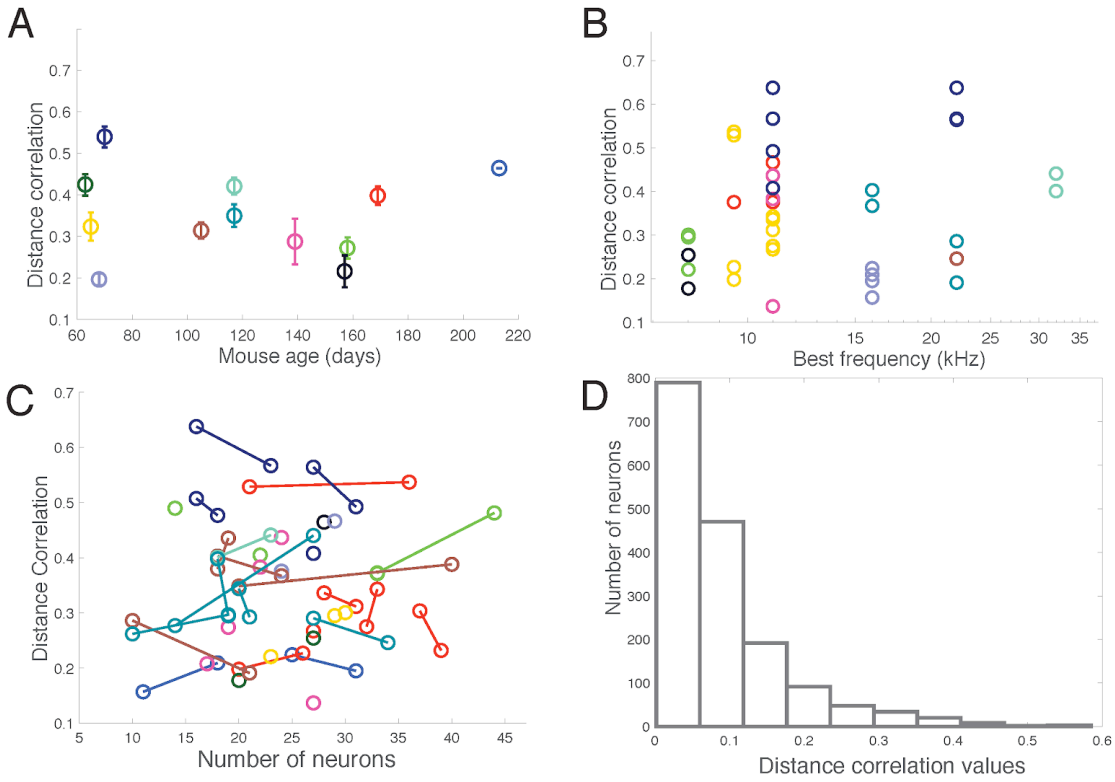

Figure 2. Modulation of neural activity by running speed. Firing rate was calculated by binning spiketimes in 100 ms time bins and smoothing over 500 ms sliding window. Distance correlation values are computed between all simultaneously recorded neurons (for **A** - **C**) or firing rate of a single neuron (**D**) and recorded running speed during a prolonged period of silence. **A.** Variability in the strength of neural modulation by running speed does not depend on animal's age. Average distance correlation values computed for recordings from each animal by age, *Spearman's rho* = - 0.10, $p = 0.52$. Each color represents one animal. **B.** Distance correlation values for each recording site sorted by best frequency of the site, recordings from the same animals are in the same color, showing no frequency dependency, *Spearman's rho* = 0.16, $p = 0.35$. **C.** Strength of neural modulation by running does not depend on the number of simultaneously recorded neurons. Distance correlation values sorted by number of neurons recorded with a linear silicone probe. Two-shank 64-channel probes are separated into two recordings, linked with a line *Spearman's rho* = - 0.004, $p = 0.97$. Each color represents recordings from one animal. **D.** Modulation of single units by running follows a Poisson distribution - firing rate of most single neurons shows weak dependency on running speed.

some studies have reported U-shaped relationships between running and arousal, which is a non-linear relationship, a linear correlation metric might not be appropriate (i.e. could yield a linear correlation of zero even though arousal strongly modulates firing rate). Distance correlation is a recently introduced measure of dependence between two random vectors. Here we used it to measure the dependence between a two dimensional matrix array of binned firing rate from simultaneously recorded neurons (see Experimental Procedures) and pupil size or running speed. The greatest advantage of distance

correlation analysis over Spearman's correlation is the ability to account for nonlinear dependencies, thus a distance correlation of zero can only be obtained if two vectors do not show any linear or nonlinear dependencies. While comparing distance correlation values in recordings from different mice as well as recordings from the same animal, we noticed large differences between them. Distance correlation values were slightly higher for pupil size than for running speed, but not significantly different (mean ± SEM, running = 0.25 ± 0.02, pupil = 0.28 ± 0.02, ranksum p = 0.19, Fig. 4B), suggesting that neural activity shows strong interdependence with both running speed and pupil size.

Because modulatory signals from arousal and running activate the ACh system in the BF (Nelson and Mooney 2016), and previous research has also shown that the effects of ACh decline with age (Rogers et al. 1998), we first tested whether the distance correlation values varied by animal's age. We found that age did not correlate with behavioral state modulation (pupil $p = 0.15$, running $p = 0.52$, Fig. 2A, 4A). Distance correlation values were significantly correlated with best frequency of the recorded site for pupil, but not for running (Fig. 2B, 4B, pupil $p = 0.01$, running $p = 0.35$). Since the number of animals in the study was relatively small and most of the recording sites from one animal had similar best frequencies due to our use of a small craniotomy, this significant correlation is likely not meaningful. We also wondered if the number of simultaneously recorded cells might cause such drastic differences in modulatory effects. Because some recordings were done with a 32-channel probe and some with a 64-channel probe, which could yield different numbers of simultaneously recorded neurons, it's important to test whether the presence of more neurons contributed to greater distance correlation values for a given mouse or a recording site. Cortical neurons show great variability in their firing rate over time (Kuebler and Thivierge 2014), therefore averaging over a time window or averaging them together could in principal smooth variability of individual neurons and produce higher correlation values. We found that strength of neural modulation by state did not correlate with the number of recorded neurons in individual recording (Fig. 2C, 4C, pupil $p = 0.41$, running $p = 0.97$), suggesting that a small number of strongly modulated neurons can still lead to higher distance correlation values than a large number of weakly modulated cells. Distance correlation values for individual neurons were smaller than recording sites and followed a

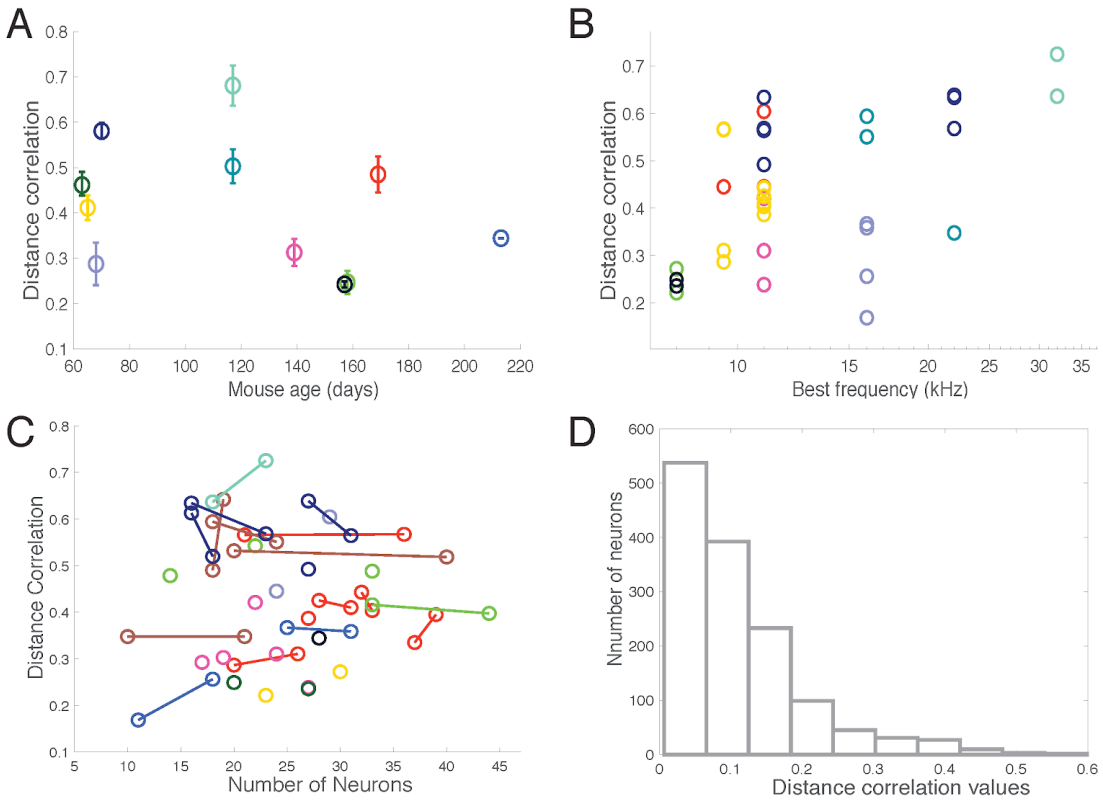

Figure 3. Modulation of neural activity by arousal level, approximated by pupil size. Firing rate was calculated by binning spiketimes in 100 ms time bins and smoothing over 500 ms sliding window. Distance correlation values are computed between all simultaneously recorded neurons (for **A** - **C**) or firing rate of a single neuron (**D**) and recorded pupil size during a prolonged period of silence. **A**. Variability in the strength of neural modulation by arousal level does not depend on animal's age. Average distance correlation values computed for recordings from each animal by age. Each color represents one animal, colors are the same as in Figure 2, *Spearman's rho* = - 0.24, $p = 0.15$. **B.** Distance correlation values for each recording site sorted by best frequency of the site, *Spearman's rho* = 0.41, $p = 0.01$. **C.** Strength of neural modulation by running does not depend on the number of simultaneously recorded neurons. Distance correlation values sorted by number of neurons recorded with a linear silicone probe. Two-shank 64-channel probes are separated into two recordings, linked with a line, *Spearman's rho* = - 0.11, $p = 0.41$. Each color represents recordings from one animal. **D.** Modulation of single units by state of arousal follows a Poisson distribution - firing rate of most single neurons shows weak dependency on pupil size.

Poisson distribution (Fig. 2D, 4D), indicating variability in modulatory effect at the single neuron level as well.

Though previous work has shown that the effects of locomotion and arousal generally follow a U-shaped modulatory curve, suggesting nonlinear effects (McGinley et al. 2015), other studies have reported mostly linear changes in neural activity (Zhou et al. 2014). These differences might arise if recording sessions do not capture the full spectrum of behavioral changes, from lowest arousal to highest, thus revealing only one side of the U-curve (usually the right side of high arousal). We normalized pupil traces for each animal and computed the distribution of pupil sizes over all experiments (Fig.

1D). This revealed that the distribution of pupil sizes in these experiments was negatively skewed, that is, animals spent most of their time in medium to high states of arousal during our experiments, with a proportionately shorter period of time in low states. This suggests that a linear approximation could provide an accurate measure of modulatory effects in our data. We tested this further by comparing residual mean squared errors for linear regression and regression with a quadratic term, which revealed that both models explain similar amount of variance in the neural data, using pupil size trace as a predictor (Fig. S3). Additionally, as expected, running bursts occurred only in high states of arousal, at above 60% of the maximum pupil size (Fig. 1D). Therefore, we classified times when animals had large pupil size but without locomotion as "high arousal stationary state," which we used for distinguishing the effects of locomotion from effects of general arousal.

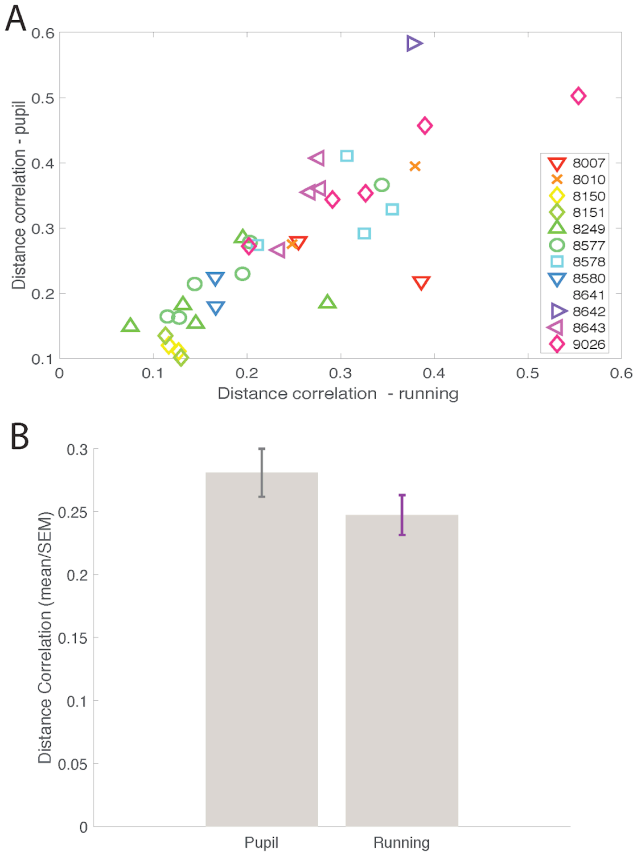

Figure 4. Modulation by locomotion and arousal level correlate. A. Average distance correlation values for running and for pupil size per each recording site show strong correlation, data binned in 50 ms time bins and smoothed over 500 ms. **B.** Neurons are equally modulated by changes in arousal and locomotion, Pupil *mean* = 0.28, *SEM* = 0.02, Running *mean* = 0.25 ± 0.02 (mean ± SEM), *ranksum* , $p = 0.19$.

Locomotion Reduces Signal to Noise Ratio

Understanding modulatory effects on sensory processing requires a thorough understanding of which modulatory signals are involved. Previous research has shown that layer 2/3 and layer 5 neurons in auditory cortex receive corollary discharge signals from motor cortex that activate a subset of excitatory and PV-expressing neurons in A1, resulting in net inhibitory effect of spontaneous and evoked activity (Nelson et al. 2013). This signal can be seen during a variety of different movement types (Schneider et al. 2014) but does not appear to be a general signature of arousal (Nelson et al. 2013). Other research in awake behaving mice revealed that in auditory cortex active behaviors suppress excitatory and inhibitory inputs in layer 2/3, but not in layer 4. The scaling down in excitation and inhibition led to suppression in layer 2/3 responses but preserved their tuning properties (Zhou et al. 2014). Thus, it appears that modulation by locomotion has an inhibitory effect on cortical neurons, though whether this effect is similar in all cortical layers remains unclear. Additionally, how this suppressive effect during locomotion interacts with modulatory signals from the BF during running to influence cortical dynamics is not well understood (Nelson and Mooney 2016). Changes in arousal strongly modulate activity in BF, which has wide-spread facilitating effects on cortical neurons (Hangya et al. 2015; Sarter et al. 2005; Fu et al. 2014; Eggermann et al. 2014). In auditory cortex, BF projections innervate inhibitory and excitatory neurons in all cortical layers (Nelson and Mooney 2016), and their activity has been associated with both locomotion and general increase in arousal. Activation of BF projections evokes excitatory and inhibitory postsynaptic potentials, though its net effect on spiking output is an overall facilitation (Nelson and Mooney 2016).

A complicating factor in studying the effects of arousal and locomotion is that these two signals inherently correlate with each other. To understand their separate contributions to cortical dynamics, we split recordings into three states: (1) stationary — when the animal was sitting and their arousal was low (below 60% of max pupil size), (2) high arousal but stationary — when animal's pupil was above 60%, similarly to running, but without locomotion, and (3) running — when the animal exhibited both a heightened state of arousal and locomotion. Bursts of running occurred only during high arousal states; in the rare cases when some motion was detected during low arousal, it was not

associated with a running burst and was excluded from the analysis. Recording sessions in which an animal's state did not fluctuate often, leading to low numbers of trials in one or more conditions, were excluded from analysis. Neural activity during high arousal was compared to the low arousal state, while running was compared to stationary trials across all arousal conditions. We found that running effects were similar when compared to stationary trials in low arousal state only, or to both arousal states, thus sitting trials were combined to increase the number of mice and recordings in the analysis.

As described below, results of our experiments show that running increases spontaneous activity and suppresses all types of evoked responses (On, Off, and Sustained) to white noise bursts resulting in an overall decrease in signal to noise ratio of sound-evoked activity (Fig. 6, Fig. 7). Effects of arousal change without locomotion were overall smaller and resulted in a general increase in neuronal activity, evoked and spontaneous (Fig. 6).

Spontaneous activity

We found that most auditory neurons increased their spontaneous firing rate during periods of locomotion (signrank = 7.58, p = 0.01e-8, Fig. S1, Fig. 6A,C). This increase was similar in all neuronal types across cortical layers (ranksum = 0.05, p = 0.40, Fig. 6C). Spontaneous activity during stationary high arousal state (sit + large pupil) increased slightly for all neurons, but generally the effect of modulation by arousal was much smaller than by locomotion, and it tended to vary a lot across cortical layers and cell types (mean ± SEM, running MI = 0.09 ± 0.03, arousal MI = 0.02 ± 0.01, ranksum z = 2.31, p = 0.02). Spontaneous firing rate modulated arousal and running in all cortical layers similarly (Kruskal Wallis ANOVA, running chi sq. = 3.65, p = 0.31, pupil chi sq. = 1.81, p = 0.61, Fig. 6C).

Correlation values between neuronal firing rate and behavioral traces (pupil size or running speed) showed a slightly different picture of modulatory effect. Mean of correlation values between neurons and running trace were lower for fast spiking and regular spiking neurons than between pupil size (mean ± SEM, fs running = 0.030 ± 0.003, pupil = 0. 044 ± 0.004, n = 276, rs running = 0.018 ± 0.002, pupil = 0.023 ± 0.002, n = 1065, Fig. 5A). This is likely due to the nonlinearity of the running trace, in which

stationary state is a non changing zero value while spontaneous activity still exhibits some degree of fluctuation, and does not indicate lesser modulatory effect. When we compared distance correlation values, a measure that accounts for nonlinear effects, for running and pupil size among recorded sites, we found that mean dependency of neuronal activity on running speed or pupil size were not significantly different from each other (Fig. 3B). A notable difference was apparent between fast and regular spiking cells, fast spiking cells were consistently more strongly modulated by animal state as indicated by their higher correlation values with running and pupil traces as well as stronger modulation index (Fig. 5A, Fig 7A).

To investigate whether changes in animal's state can modulate the strength and dynamics of synaptic connections, we computed cross-correlations of spikes among simultaneously recorded neurons during bursts of running and sitting still (detailed in Methods, as well as Gilbert and Wiesel 1985; Ts'o et al. 1986). Similarly to previous analysis, correlation values between pairs of fast spiking neurons were significantly higher than between regular spiking pairs (Fig. 5C; Kruskal Wallis ANOVA chi sq = 50.64, p = 0.11e-12). These correlation values were not significantly different when animal was running versus sitting still or during periods of high stationary arousal for fast spiking neurons Kruskal Wallis ANOVA chi fs sq = 2.52, p = 0.28, n = 104), but regular spiking neurons showed lower correlation values with other neurons during stationary trials and low arousal than during running or stationary trials with high arousal (Kruskal Wallis ANOVA chi sq = 35.14, p = 2.33e-8, n = 731, mean correlation values at time zero, running = 0.0026, sitting + small pupil = 0.0024, sitting + large pupil = 0.003). These mean correlation values across all neurons are small and higher correlations can be driven by higher spontaneous firing rate during high arousal and running.

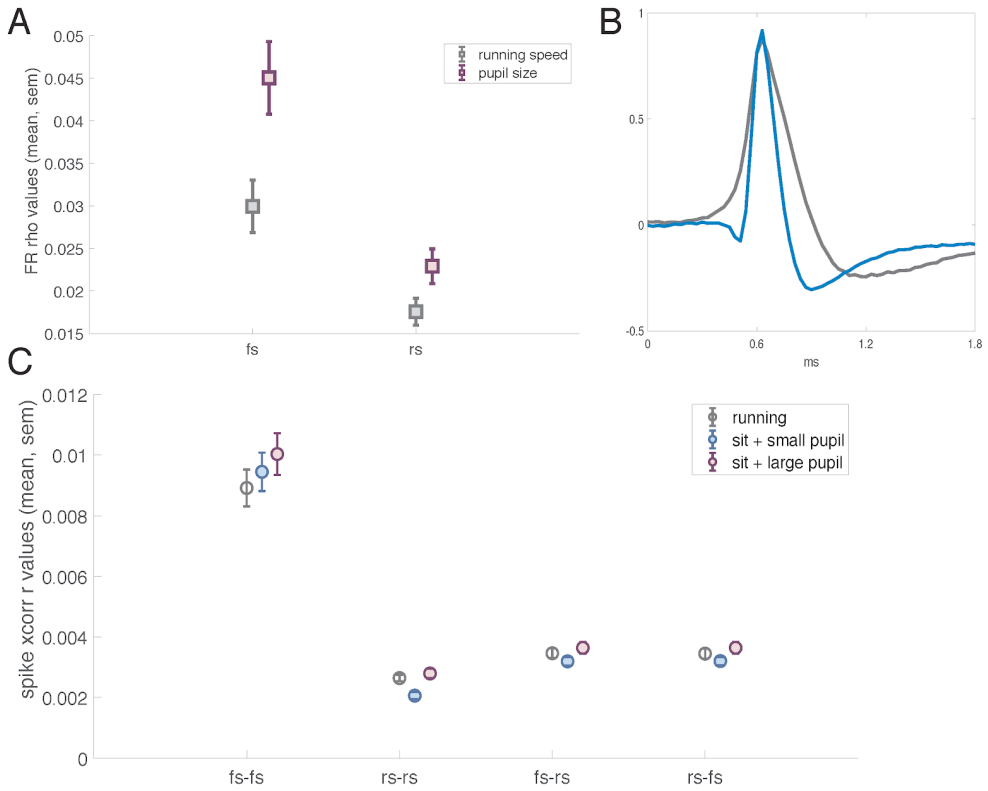

Figure 5. Fast spiking cells are more strongly modulated by state and activity of other fast spiking neurons. A. Mean and SEM Spearman's correlation values between spontaneous firing rate of isolated neurons with running speed or pupil size. **B.** Example waveforms of a regular spiking neuron (rs, grey) and fast spiking neuron (fs, blue). Spike waveform examples are normalized to their max. **C.** Mean and SEM correlation values of spike times among simultaneously recorded neurons at time zero in three state conditions: running, quiescent (sit + small pupil), stationary high arousal (sit + large pupil).

White noise evoked activity

We measured the effects of an animal's state on sound-evoked activity, using 600 ms white noise bursts to drive cortical responses. Using a prolonged sound allowed us to partition evoked activity into On responses (0 - 100 ms after sound onset), Sustained responses (100 - 600 ms), and Off responses (600 - 700 ms, i.e. 0 - 100 ms after sound offset). We also used the entire response (0 - 650 ms after sound onset) to capture all three of these components together. Overall, we observed that evoked responses to sound during a 650 ms window were suppressed by locomotion in most auditory neurons. Locomotion had somewhat stronger overall effect on evoked activity of regular spiking than of fast spiking cells, though it was not statistically different (ranksum $z = 1.30$, $p = 0.19$, Fig. 6A, Fig. 8). Further analysis showed that running exhibited slightly different strength of suppression across different response types. It suppressed On, Sustained, and

Off activated responses. Even neurons that responded to sound with suppression exhibited greater degree of suppression during running, with the exception of Off responses. Suppressed Off responses showed facilitation during running, which can be the result of misclassification of suppressed Off responses due to prolonged suppression of spontaneous activity after sound offset (Galazyuk 2015; Galazyuk et al. 2017). The mechanism of prolonged suppression post sound offset is not well understood though it has been related to residual inhibition. This mechanism likely differs from a brief suppression post sound offset (100-200 ms) that can be classified as a true suppressed off response, though both will result in smaller spiking output post stimulus offset.

Separating locomotion effect by cortical layer revealed that superficial layers exhibited the strongest suppression. Neurons in layer 6 were either strongly inhibited or disinhibited by running, resulting in a net not significant modulation. Subdividing neurons further into regular and fast spiking categories indicated that in most layers they are modulated similarly, besides layer 4. In layer 4 regular spiking cells were strongly inhibited while fast spiking cells increased their firing rate. This result is consistent with previous work showing that locomotion can suppress auditory neurons via PV inhibition (Schneider et al. 2014), but it was inconsistent with previous research that reported no modulation of layer 4 neurons by running (Zhou et al. 2014). Because cells show a remarkable diversity in their sound evoked responses, we wondered whether brief activated On responses (0 -100 ms), which are often studied in auditory research, are modulated differently than evoked activity over 650 ms in our experiments. Furthermore, because previous research has shown that On and Off responses are mediated by a nonoverlapping set of synapses (Scholl et al. 2010), we decided to investigate whether activated On and Off responses exhibited a different pattern of modulation across cortical layers. Indeed, running modulation index of On responses revealed a distinct but familiar pattern of suppression observed in the analysis of full 650 ms time window. The strongest suppression was observed in layers 2/3 and 6, while layers 5 and 4 showed a modest and variable modulation (Fig. 9, bottom panel). Though suppression of Off and On responses was not statistically different ($p = 0.15$), Off responses showed a slightly different pattern of suppression across cortical layers. The greatest difference between them was observed

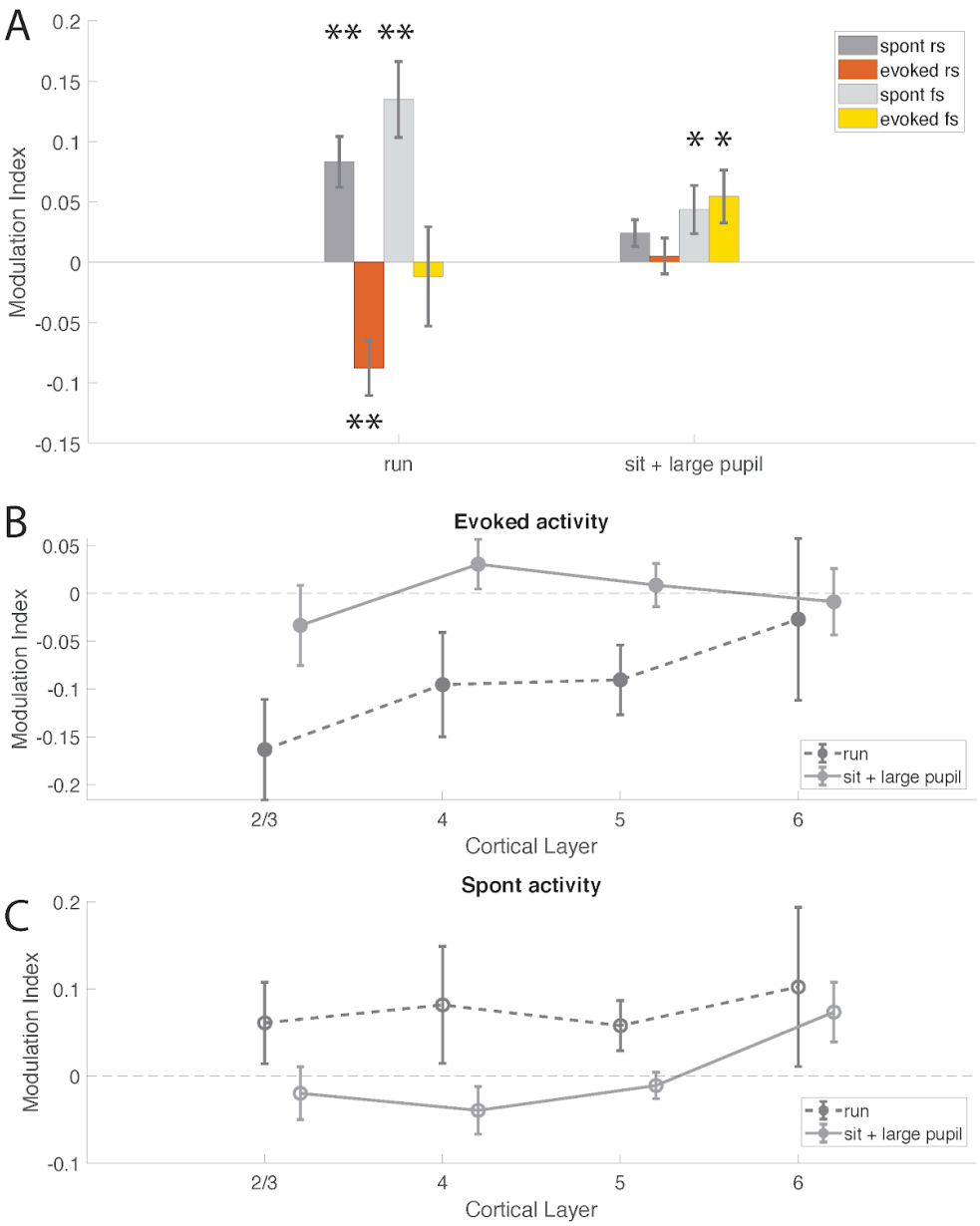

Figure 6. Modulation of evoked and spontaneous activity. A. Mean and SEM modulation index during running and high arousal states (sit + large pupil) in regular spiking (rs) and fast spiking (fs) cells. Spontaneous activity: regular spiking cells, mean ± SEM, running = 0.08 ± 0.02, n = 283; sit + large pupil = 0.02 ± 0.01, n = 335. Fast spiking cells, running = 0.15 ± 0.04, n =71; sit + large pupil = 0.04 ± 0.02, n = 96. Evoked activity: regular spiking cells, running = -0.09 ± 0.03, n = 203; sit + large pupil = 0.01 ± 0.02, n = 348. Fast spiking cells, running = -0.01 ± 0.04, n = 53; sit + large pupil = 0.06 ± 0.02, n = 78. **B.** Modulation of evoked activity separated by cortical layers. Running (mean ± SEM) L2/3 = -0.16 ± 0.05, n = 23, L4 = -0.10 ± 0.05, n = 20, L5 = -0.10 ± 0.04, n = 50, L6 = -0.03 ± 0.08, n = 15; Sit + large pupil (mean ± SEM) L2/3 = -0.03 ± 0.04, n = 33, L4 = 0.03 ± 0.03, n = 42, L5 = 0.01 ± 0.02, n = 160, L6 = 0.02 ± 0.03, n = 41. **C.** Modulation of spontaneous activity separated by cortical layers. Running (mean ± SEM) L2/3 = 0.06 ± 0.04, n = 32, L4 = 0.08 ± 0.05, n = 42, L5 = 0.06 ± 0.03, n = 85, L6 = 0.10 ± 0.09, n = 23; Sit + large pupil (mean ± SEM) L2/3 = -0.02 ± 0.03, n = 43, L4 = -0.04 ± 0.03, n = 55, L5 = 0.01 ± 0.02, n = 216, L6 = 0.07 ± 0.03, n =67.

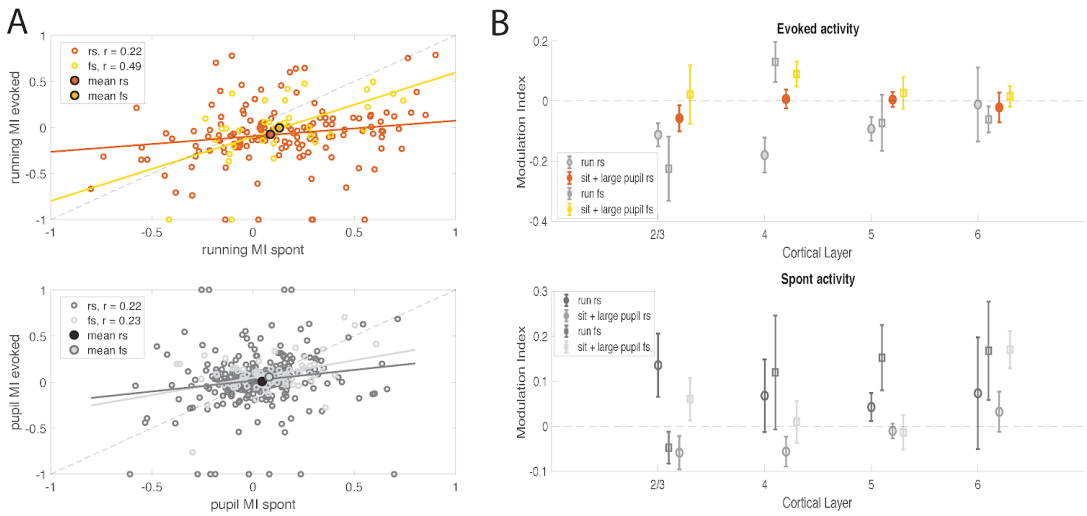

Figure 7. Effects of locomotion and arousal on evoked and spontaneous activity by cell type and cortical layers. A. Neurons show positive relationship in modulation of spontaneous and evoked activity during running and state of high arousal (pupil). Running rs n = 148, r = 0.22, fs n = 36, r = 0.49. Pupil rs n = 348, r = 0. 22, fs = 98, r = 23. **B**. Means and SEM of modulation indices for rs (dark grey and orange) and fs (light grey and yellow) across cortical layers during running or during high arousal state (sit + large pupil) separated by evoked and spontaneous activity. Regular spiking evoked running L2/3 n = 11, L4 n = 16, L5 n = 50, L6 n = 11; sit + large pupil L2/3 n = 23, L4 n = 30, L5 n = 130, L6 n = 27. Fast spiking evoked running L2/3 n = 9, L4 n = 6, L5 n = 7, L6 n = 5; sit + large pupil L2/3 n = 10, L4 n = 12, L5 n = 27, L6 n = 14. Regular spiking spontaneous running L2/3 n = 20, L4 n = 23, L5 n = 57, L6 n = 13; sit + large pupil L2/3 n = 32, L4 n = 36, L5 n = 139, L6 n = 41. Fast spiking evoked running L2/3 n = 10, L4 n = 7, L5 n = 9, L6 n = 6; sit + large pupil L2/3 n = 12, L4 n = 12, L5 n = 27, L6 n = 17.

n layer 2/3, where On responses were significantly more strongly suppressed than Off responses (p = 0.001). Overall, suppression patterns of On and Off responses were complementary to one another, suggesting that they are potentially modulated by a different mechanism. Fast spiking and regular spiking cells showed similar pattern of suppression though modulation of fast spiking cells was more variable.

Despite overall suppressive effect of locomotion and facilitating effect of stationary arousal state, both regular and fast spiking cells showed substantial diversity in the strength and direction of modulation (Fig. 7A, VIP ChR2 experiment, laser off trials, Fig. 8B-D, laser off trials). Though the population mean is slightly below zero (filled orange dot for regular spiking and yellow for fast spiking), individual cells had modulations that were distributed widely above and below zero (Fig. 7A). Evoked modulation showed positive relationship with modulation of spontaneous activity for both regular spiking and fast spiking neurons, in locomotion and stationary arousal

conditions (Fig. 7A). Modulation of suppressed On and Off responses during locomotion showed the strongest correlation with modulation of spontaneous activity (Fig 9B, D, dark grey lines). Neurons that are strongly and positively modulated by running show a similar effect in both evoked and spontaneous instances, though evoked responses might exhibit a lesser modulatory effect overall. The slope of this relationship appears to be stronger for fast spiking than regular spiking neurons (fs slope = 0.61, rs slope = 0.28), it is still less than one indicating that running has a stronger effect on spontaneous activity than evoked.

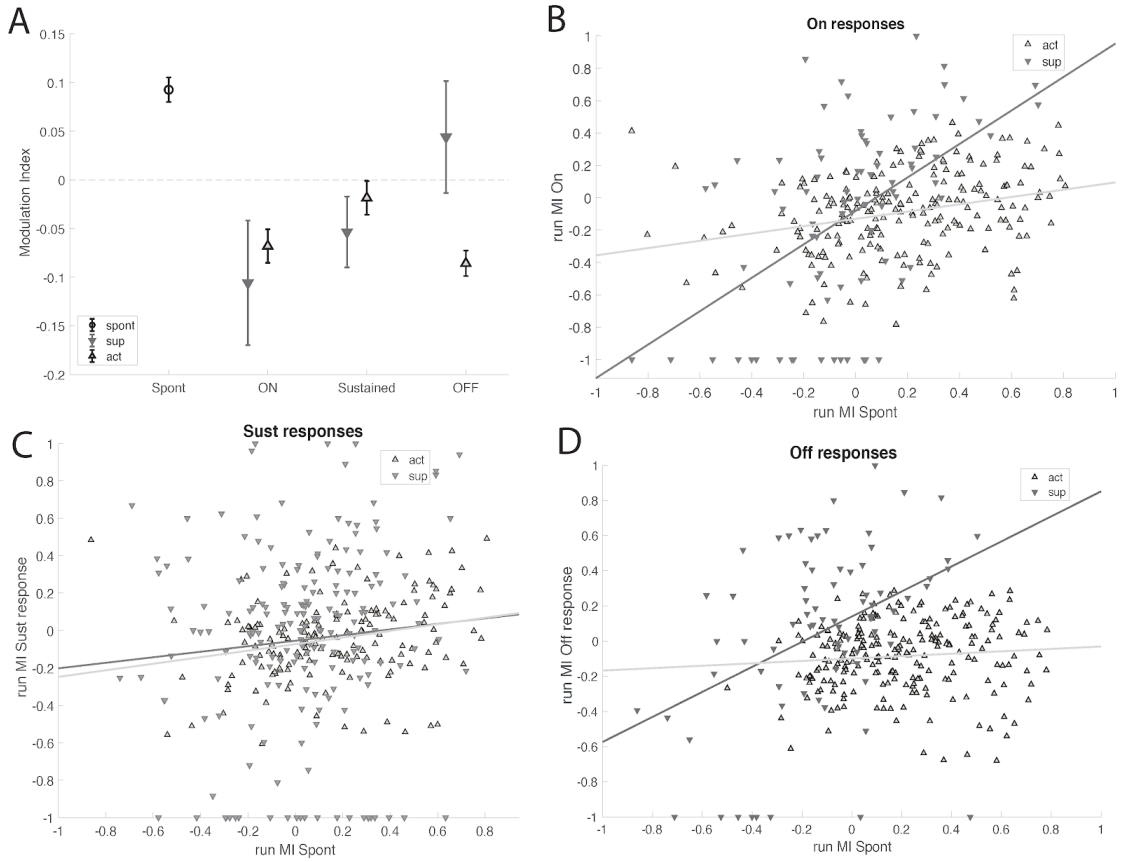

Figure 8. Locomotion modulates all subtypes of evoked responses. A. By response type (mean ± SEM): On activated = -0.08 ± 0.02, n = 242, suppressed -0.11 ± 0.05, n = 84, Sustained activated = -0.02 ± 0.02, n = 180, suppressed -0.5 ± 0.04, n = 202, Off activated = -0.09 ± 0.01, n = 248, suppressed 0.04 ± 0.06, n = 81. **B.** Modulation Index (MI) of On responses by MI of spontaneous activity. Lines of best fit are shown separately for suppressed and activated responses, dark grey and light grey respectively. **C.** MI of Sustained responses plotted against MI of spontaneous activity. **D.** MI of Off responses plotted against MI of spontaneous activity. Dark grey lines indicate lines of best fit for suppressed responses and light grey lines represent lines of best fit of activated responses.

Separating sound evoked responses into On, Sustained, and Off responses that are either suppressed or activated showed that all types of sound responses were suppressed

by running (Fig. 8A). The only not suppressed subtype of evoked responses, suppressed Off, showed facilitation. This unexpected difference is likely due to misclassification of a few suppressed Off responses to a forward suppression of spontaneous activity after stimulus offset (Galazyuk et al. 2017; Galazyuk 2015), which is thought to be the result of lasting inhibition. Since running increases spontaneous activity, the facilitating effect on suppressed Off can be attributed to alleviation of prolonged post stimulus suppression, rather than a rapid suppressed Off response that usually lasts less than 200 ms.

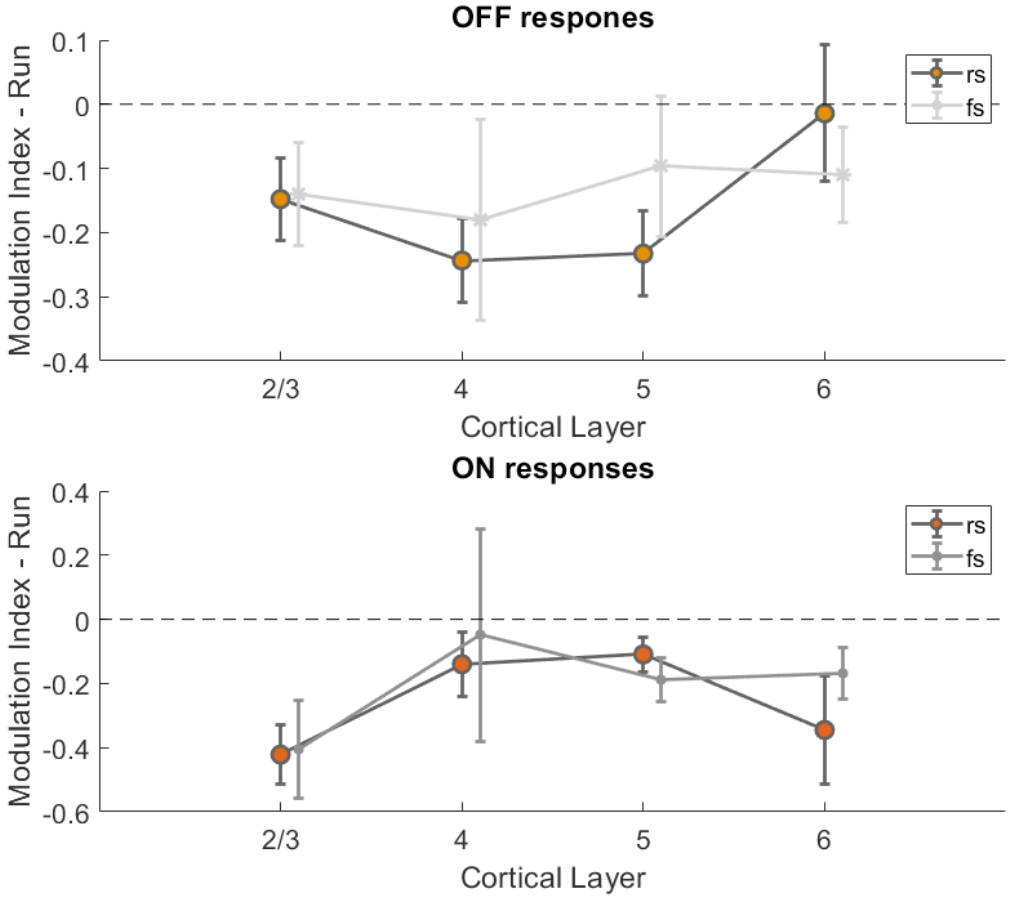

Figure 9. On and Off responses show a different pattern of suppression by locomotion. Overall mean ± SEM MI, On responses L2/3 = -0.41 ± 0.07, L4 = -0.12 ± 0.11, L5 = -0.12 ± 0.05, L6 = -0.24 ± 0.09; Off responses L2/3 = -0.14 ± 0.05, L4 = -0.21 ± 0.09, L5 = -0.20 ± 0.06, L6 = -0.06 ± 0.06. On responses in L2/3 are significantly different from On responses in L4 and L5 (*tukey - kramer p* = 0.01, *p*=0.02, respectively) and from L2/3 Off responses (*ranksum z* = -3.20, *p* = 0.001). On responses by cell type, rs L2/3 n = 16, L4 n = 23, L5 n = 126, L6 n = 30; fs L2/3 n = 10, L4 n = 9, L5 n = 23, L6 n = 21. Off responses were not significantly different across layers (Kruskal-Wallis ANOVA, *chi* = 2.24, *p* = 0.52). Off responses by cell type rs L2/3 n = 18, L4 n = 22, L4 n = 65, L5 n = 20; fs L2/3 n = 8, L4 n = 13, L4 n = 29, L5 n = 18; and overall On and Off did not differ in total suppression (mean ± SEM On = -0.24 ± 0.05, n = 258, Off = -0.17 ± 0.03, n = 193, *ranksum z* = -1.45, *p* =0.15).

Activating VIP Cells Disinhibits Neurons in Infragranular Layers

Research on functional connectivity of VIP interneurons has consistently shown that they form a disinhibitory circuit with SOM inhibitory cells (Pfeffer et al. 2013; Fu et al. 2014; Lee et al. 2013; Pi et al. 2013), though they also provide lesser amounts of inhibition to excitatory and SOM-negative inhibitory cells. Most VIP interneurons (60%) are located in layer 2/3 but their axonal projections usually span the full cortical column, suggesting that even manipulation of supragranular VIP neurons can produce an effect all cortical layers (Prönneke et al. 2015). Additionally, most inhibitory targets of VIP neurons are located in infragranular layers indicating that the disinhibitory effects of VIP are not restricted to layer 2/3 (Prönneke et al. 2015).

We activated VIP neurons in VIP-Cre-ChR2 mice during white noise and silent trials that were randomly interleaved into four different trial types: white noise alone, white noise with laser on, silence alone, silence with laser on. Trials were randomly presented during different behavioral states: quiescent, high stationary arousal, and running. We computed modulation index for evoked and spontaneous activity by calculating the mean firing change in laser on versus laser off trials across all behavioral states (see Experimental Procedures). As predicted from established disinhibitory role of VIP neurons, their activation resulted in a net increase in spontaneous and evoked cortical activity. This increase was similar in regular spiking and fast spiking neurons, suggesting that both types are affected by VIP activity. Interestingly, VIP activation had a much stronger effect on suppressed evoked responses than activated evoked responses, suggesting that some aspect of sound suppression in the cortex might be mediated by local inhibition.

Because VIP neurons exhibit different patterns of connectivity across cortical layers, we decided to examine whether this facilitating effect was similar in all layers. Separating neurons by their depth revealed that activation of VIP interneurons produced different effects in superficial and deep cortical layers. While most neurons in all layers showed some degree of modulation by VIP activation, the strongest disinhibitory effect on spontaneous activity was found in layer 5 and layer 6. Multiple comparison analysis revealed that layer 2/3 and layer 5 neurons exhibited the greatest difference in modulation (tukey - kramer $p = 0.04$). This result is consistent with previous research showing that

most of the GABA-ergic dendrites that are targets of VIP neurons are located in layer 5 (Zhou et al. 2017). Layer 5 is also the most populated by Martinotti cells, which belong to the group of SOM - expressing neurons (Wang et al. 2004). Thus the strong disinhibitory effect that we see in our experiments (Fig. 10A) is likely driven by a familiar VIP-SOM disinhibitory circuit. Comparing regular spiking and fast spiking neurons showed that they exhibit a similar pattern of modulation of spontaneous activity by VIP.

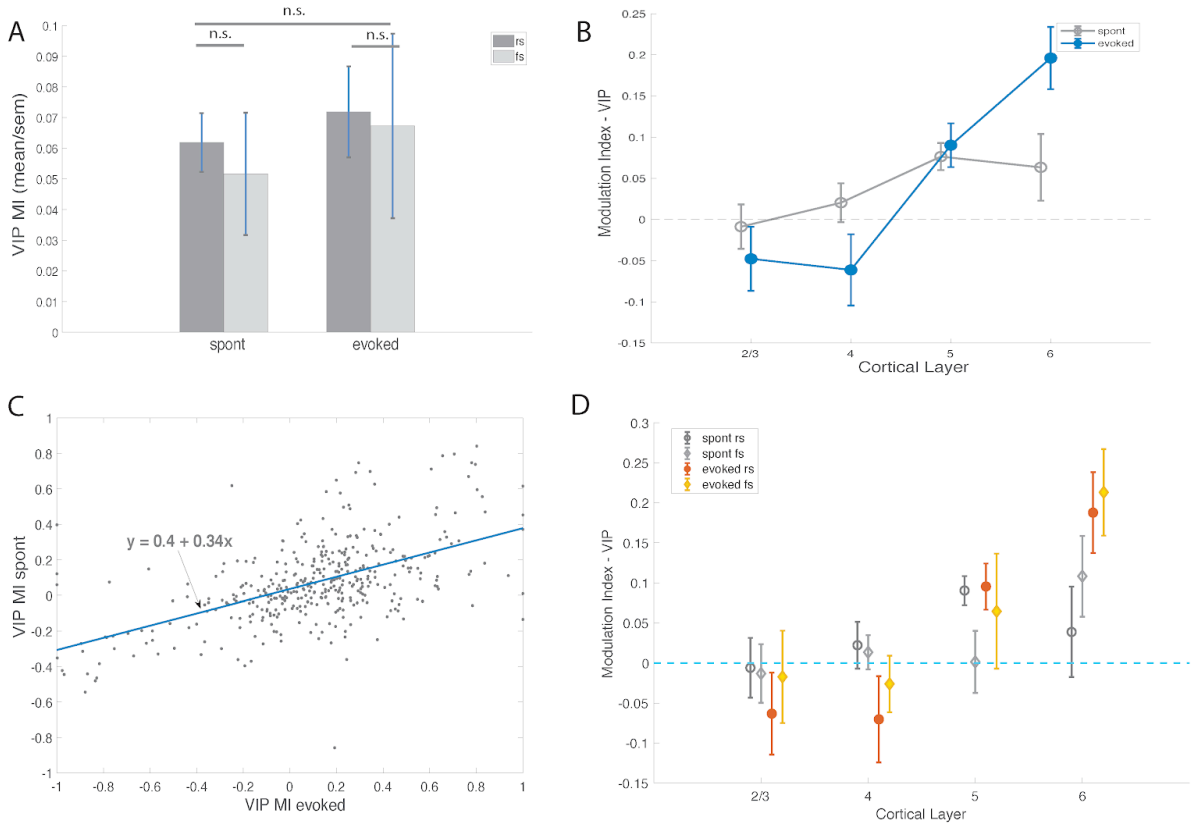

Figure 10. Effects of VIP activation on cortical neurons. A. VIP enhances evoked and spontaneous activity of both regular (rs) and fast spiking (fs) neurons, ranksum z = -1.25, p = 0.20, n = 291. **B.** VIP activation produces inhibitory effect in superficial and disinhibitory effect in deep layers. Evoked: Kruskal Wallis ANOVA, df = 290, chi-sq = 25.05, p = 1.51e-05; tukey - kramer, L 2/3 and L4 are significantly different from L5 and L6, p = 0.02. Spontaneous: Kruskal Wallis ANOVA, df = 272, chi-sq = 9.64, p = 0.02; tukey - kramer, L2/3 and L5 are significantly different, p = 0.04. **C.** Modulation of spontaneous and evoked activity of cortical neurons by VIP shows a positive relationship. **D**. Distribution of VIP activation effects across cortical layers by cell type (rs, fs) and activity type. Evoked fs n = 66 (L2/3 = 13, L4 = 12, L5 = 27, L6 = 14), rs n = 225 (L2/3 = 27, L4 = 24, L5 = 136, L6 = 28). Spontaneous fs n = 66 (L2/3 = 15, L4 = 12, L5 = 22, L6 = 17), rs n = 207 (L2/3 = 23, L4 = 31, L5 = 122, L6 = 31).

In evoked responses, neurons in superficial layers showed effects of inhibition and disinhibition that added to a net smaller modulatory effect in layer 2/3 and suppressive effect in layer 4 (Fig. 10 B,D). This result is consistent with previous

research showing that most synaptic targets of VIP neurons in superficial layers are GABA-negative (Zhou et al. 2017). Strong suppression of evoked responses by VIP in layer 4 may suggest that VIP neurons are position to modulate input to auditory cortex, since layer 4 neurons are the main target of thalamocortical projections and are the first to receive sound evoked synaptic input (Fig. 10B). Separating effects for regular spiking and fast spiking neurons revealed that suppression of evoked responses was found in both fast spiking and regular spiking neurons (rs mean = -0.08, SEM = 0.5, n = 48, fs mean = -.03, SEM = 0.3, = 14), though regular spiking cells showed slightly greater suppression (Fig. 10D, rs in orange, fs in yellow).

VIP neurons had the strongest facilitating effect on evoked responses in layer 6, though their effect on spontaneous firing rate in these neurons was similar to other cortical layers (Fig. 10B). This was not due to sound - evoked suppression; in fact, layer 6 neurons had the strongest evoked firing rate (evoked, mean ± SEM (Hz): layer 2/3 = 4.82 ± 0.69, layer 4 = 6.99 ± 0.90, layer 5 = 7.83 ± 0.69, layer 6 = 14.03 ± 3.03; spontaneous means ± SEM: layer 2/3 = 4.33 ± 0.70, layer 4 = 6.44 ± 0.65, layer 5 = 5.70 ± 0.57, layer 6 = 7.12 ± 0.92). Because Martinotti cells are also found in layer 6, some of this disinhibition is likely to be mediated by local SOM interneurons, however the difference in effect for the evoked and spontaneous activity indicates involvement of neurons that receive sound-evoked thalamic or recurrent excitation. Layer 6 neurons also showed a strong correlation in modulation of spontaneous and evoked activity by VIP (n=42, rho = 0.39, p = 0.01, slope = 0.26, intercept = 0.16), suggesting that their spontaneous firing and evoked responses are mediated by overlapping input.

Previous research in patched cortical slices showed that VIP provide stronger inhibition to SOM interneurons in layer 2/3 than layer 5 (Pfeffer et al. 2013), which is inconsistent with the strength of disinhibitory effects that we see in our results. While VIP engage in disinhibitory network with SOM interneurons, this not the only known existing disinhibitory motif in cortical circuits. This unexpected result can be attributed to the differences of SOM interneurons connectivity to other inhibitory and excitatory cells. SOM neurons are known to inhibit PV interneurons (Pfeffer et al. 2013), which suggests that their inhibition can lead to an increase in activity in some PV neurons, thus leading to more inhibition. Additionally, previous work has shown that recurrent inhibition in

L2/3 neurons can lead to supralinear increase in inhibition via facilitating synaptic input from SOM interneurons in L2/3 and 5 (Kapfer et al. 2007), suggesting that the tendency of cortical networks to balance excitation and inhibition via a complex inhibitory network may override selective activation of VIP neurons, leading to either a net of zero difference between them or even a stronger suppression when excitatory drive increases.

Effects of Arousal and Locomotion Are not Mediated by VIP Network

Because VIP interneurons receive cholinergic input from basal forebrain (Nelson and Mooney 2016) and have a disinhibitory effect on visual cortical neurons during running (Fu et al. 2014), we wondered whether their activity contributed to modulatory effects of locomotion or stationary arousal in auditory cortex. To test whether activating VIP neurons changes state dependent effects, we compared modulatory effects of locomotion and arousal in the same neurons during laser on and laser off trials (Fig. 11). Activating VIP had a net facilitating effect on cortical neurons (Fig. 10), but did not change the overall strength of state dependent effects for regular or fast spiking cells. Modulation effect by running or arousal change was similar in strength during laser off and laser on trials overall (Fig 11A), as well as across cortical layers for evoked (Fig. 11B) and spontaneous activity (Fig. 11C). VIP activation did not differ in all behavioral conditions (Fig. S2).

Regular and fast spiking neurons showed modest positive relationship in modulation by running during laser off trials and VIP activation modulation during stationary trials, suggesting that neurons that are modulated by locomotion are also to some degree are modulated by VIP interneurons (Fig. 13B). Similar positive relationship was observed between modulation in stationary arousal in laser off trials and VIP modulation during low arousal trials (Fig. 14B). Correlatory relationships in behavioral effects and VIP activation are not surprising, considering the degree of interconnectivity among cortical neurons. They also do not imply a causal relationship since correlations can be a result of a latent variable. Locomotion and arousal can modulate the same neurons that are modulated by VIP but via a different mechanism. Therefore, to test whether behavioral state modulates neurons via VIP network, we computed predicted values for each neuron that consisted of summed modulatory effect of running (or

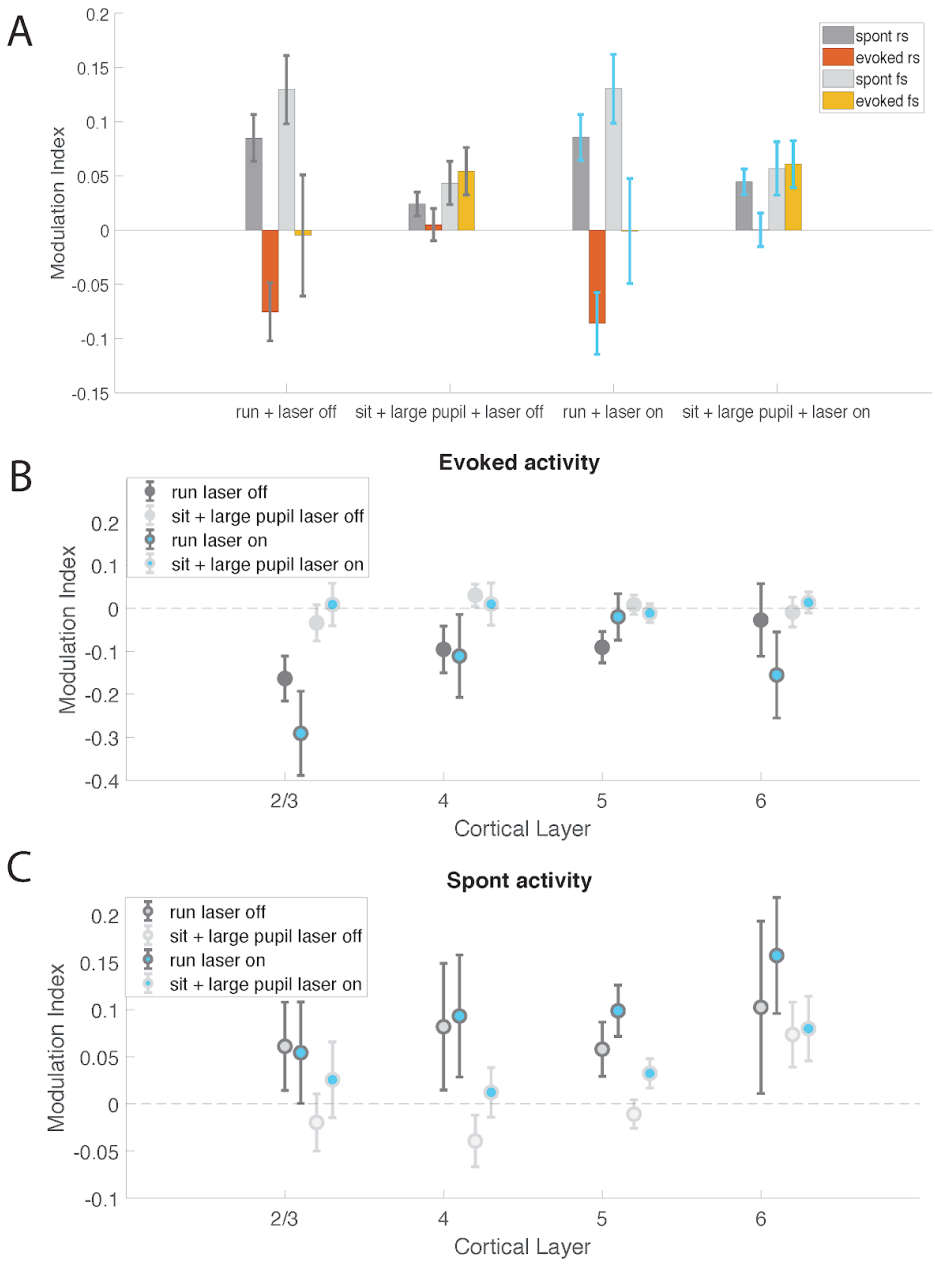

Figure 11. VIP activation does not disrupt state modulation of neural activity. A. Mean ± SEM of modulation index for running and high arousal state (pupil + sit) with (laser on) and without (laser off) VIP activation trials, for regular spiking (rs) and fast spiking (fs) respectively. Mean ± SEM laser off/on comparison, evoked: running rs = - 0.08 ± 0.03 / -0.09 ± 0.02, signrank z = -1.04, p = 0.30, n = 148, fs = -0.004 ± 0.06 / -0.002 ± 0.05, signrank z = 1.12, p = 0.23, n = 36, pupil + sit rs = 0.005 ± 0.02 / 0.005 ± 0.02, signrank z = 0.16, p =0.88, n = 348, fs = 0.06 ± 0.02 / 0.07 ± 0.02, signrank z = 0.56, p = 0.60, n = 96. Laser off mean ± SEM, spont: running rs = 0.09 ± 0.02 / 0.09 ± 0.01, signrank z = 0.50, p = 0.69, n = 248, fs = 0.13 ± 0.03 / 0.14 ± 0.03 , signrank z = 0.64, p = 0.64, n = 65; pupil + sit rs = 0.05 ± 0.01 / 0.06 ± 0.01, signrank z = -0.12, p = 0.91, n = 400, fs = 0.08 ± 0.02 / 0.09 ± 0.02, signrank z = -0.29, p = 0.77, n = 109. **B.** Modulation index of running and arousal (pupil + sit) by layer on evoked activity, comparing laser on and laser off trials, L2/3 - L6: running n = 17, n = 12, n = 29, n = 8, pupil + sit n = 22, n = 26, n = 67, n = 18. **C.** Modulation index of running and arousal (pupil + sit) by layer on spontaneous activity, comparing laser on and laser off trials, L2/3 - L6: running n = 22, n = 26, n = 67, n = 18, pupil + sit n = 35, n = 45, n = 164, n = 47.

arousal) in laser off trials and VIP modulation in stationary low arousal trials and compared it with actual modulation index of the same neurons when both modulatory mechanisms were present.

$$Predicted = run\ MI_{laser\ off} + VIP\ MI_{sit}$$

$$Run{+}VIP\ MI = (FR_{run+laser\ on} - FR_{sit+laser\ off}) / (FR_{run+laser\ on} + FR_{sit+laser\ off})$$

If VIP modulation and running (or arousal) modulation are independent, their predicted value that's computed based on the effect of two modulatory signals separately should be similar to recorded value when two modulatory signals were present. We compared predicted values to recorded values in two behavioral states and found that they were strongly correlated and not statistically different from one another (Fig. 13, Fig. 14).

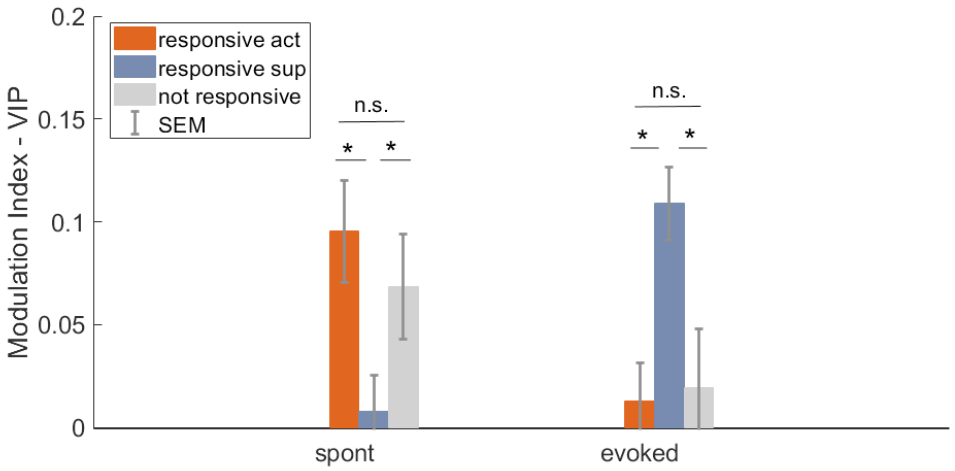

Figure 12. VIP activation has the strongest effect on suppressed auditory responses. VIP activation increases spontaneous activity in activated cells and evoked activity in suppressed cells. Spont Krusal-Wallis ANOVA chi-sq = 10.33, p = 0.005, Evoked: Krusal-Wallis ANOVA chi-sq = 11.65, p = 0.003, activated n = 286, suppressed n = 331, not responsive n = 441.

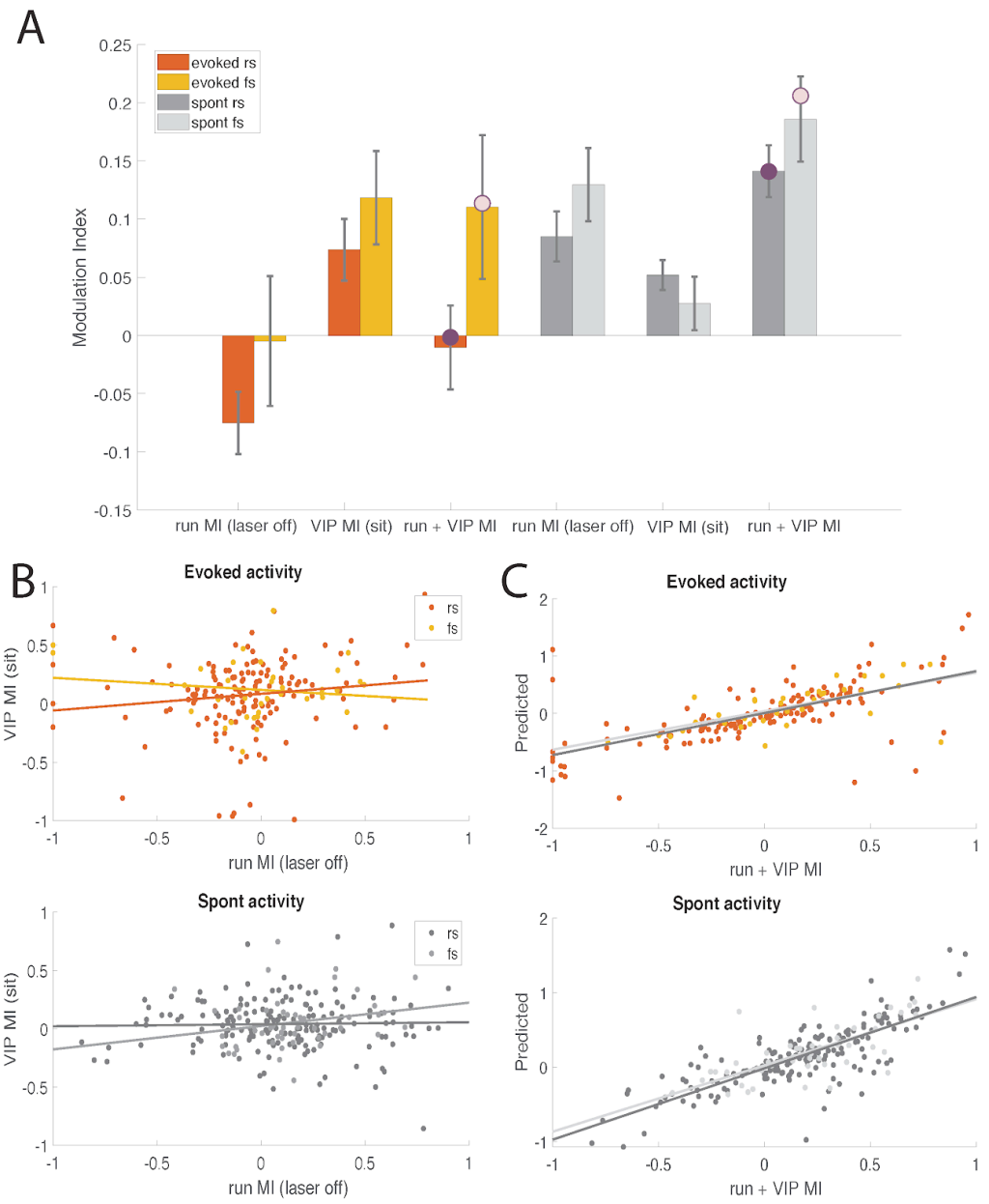

Figure 13. VIP modulation and locomotion modulation do not interact. A. Mean ± SEM modulatory indices by cell type (rs, fs), conditions (running, VIP activation, or both) and activity type (evoked, spontaneous). Modulation indices are separated into three trial types: running during laser off trials (run MI), VIP activation during sitting trials (VIP MI), and running during laser on trials (run + VIP). Mean predicted values for run + VIP condition for each response and cell types are indicated by magenta dots. **B.** Correlations between running modulation and VIP activation. Evoked: rs rho = 0.18, p = 0.03, fs rho =0.09, p = 0.06; spont: rs rho = -0.01,p = 0.88, fs = 0.25, p = 0.08. **C.** Correlation between predicted values for run + VIP condition and actual recorded values. Evoked: rs rho = 0.71, p < 0.001, fs rho = 0.68, p < 0.001; spont: rs rho = -0.80 p < 0.001 fs = 0.71 p < 0.001. Predicted values are not statistically different from recorded values for each cell. Running, evoked: rs signrank z = 0.25, p = 0.80, n = 203, fs z = -1.34, p = 0.18, n = 53; spont: rs singrank z = 1.00, p = 0.31, n = 283, fs signrank z = -0.04, p = 0.98, n = 71.

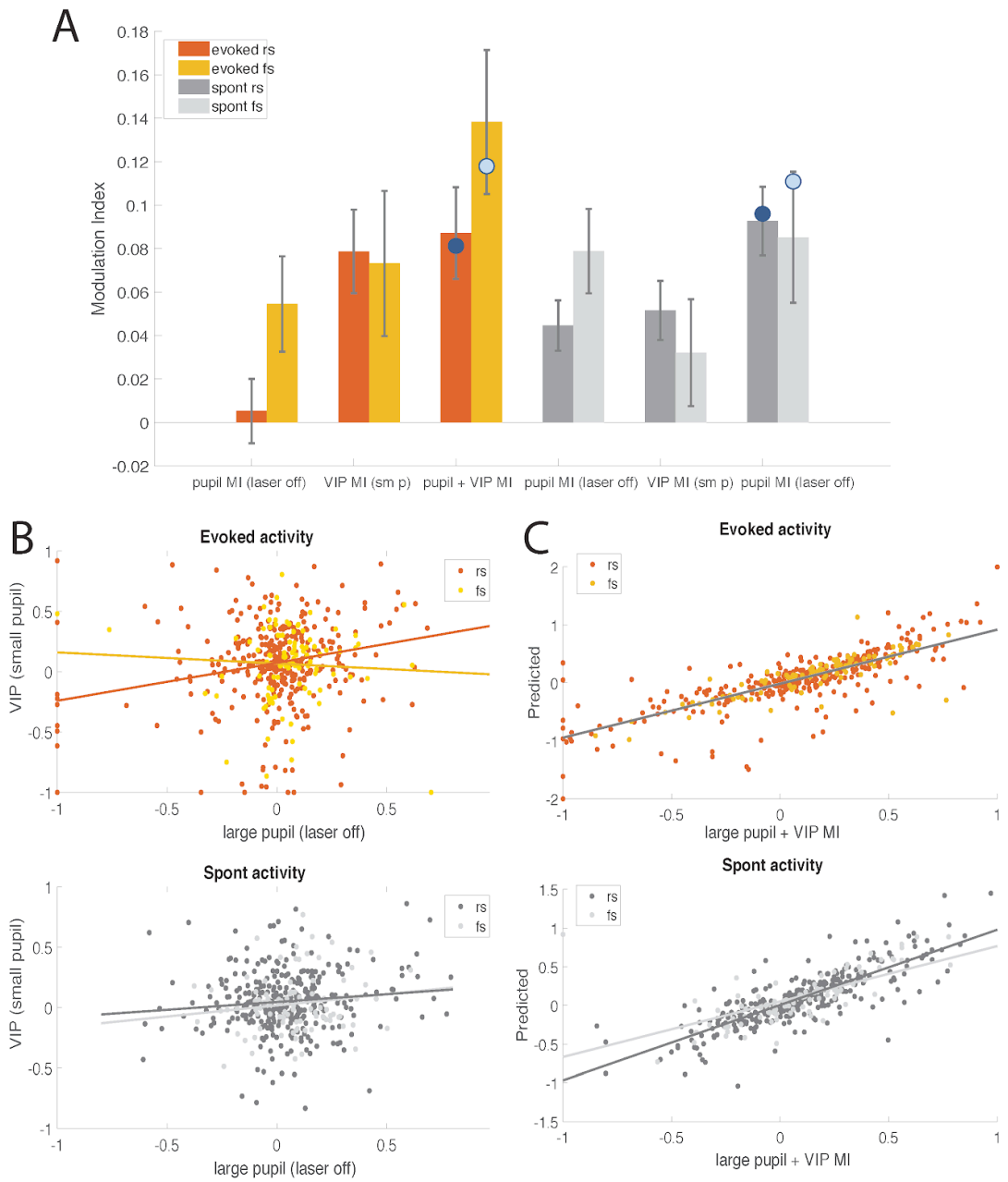

Figure 14. VIP modulation and changes in arousal do not interact. A. Mean ± SEM modulatory indices by cell type and conditions and response type. Modulation indices are separated into three trial types: large pupil size during laser off trials (pupil MI), VIP activation during small pupil trials (VIP MI), and high arousal during laser on trials (pupil + VIP). Mean predicted values for pupil + VIP for each response and cell types are indicated by blue dots. **B.** Correlations between arousal modulation and VIP activation. Evoked: rs rho = 0.12, p = 0.03, fs rho = 0.09, p = 0.38; spont: rs rho = 0.09, p = 0.09, fs = 0.09 p = .38. **C**. Correlation between predicted values for pupil + VIP condition and actual recorded values. Evoked: rs rho = 0.80 p < 0.001, fs rho = 0.83 p < 0.00; spont: rs rho = 0.82 p= 0.00, rho = 0.76, p <0.001. Predicted values are not statistically different from recorded values for each cell. Arousal, evoked: signrank z = 0.47, p = 0.63, n = 348, fs signrank z = -0.15, p = 0.87, n = 96; spont: rs signrank z = -0.40, p = 0.68, n =400, fs z = -0.29, p = 0.77, n = 109.

DISCUSSION

Auditory cortical neurons show diverse effects of modulation by behavioral state and VIP activation. These effects seem to be widespread, indicating that both VIP network and behavioral states modulate cortical neurons of all types and across all layers. Despite these differences, familiar trends can be noted in both VIP activation and state modulation.

VIP has predominantly inhibitory effect in superficial layers and a disinhibitory effect in infragranular layers. Though VIP neurons provide strong inhibition to SOM cells in L2/3, previous work has known that their main GABA+ targets are in layers 5 and 6 (Zhou et al. 2017). Infragranular layers are also known to have large number of low-threshold spiking Martinotti cells, a subgroup of SOM-expressing interneurons (Wang et al. 2004). Research has also shown that SOM neurons in deep layers provide inhibitory feedback to excitatory neurons in the same layers that can increase supralinearly with an activation of even a few excitatory cells (Kapfer et al. 2007; Silberberg and Markram 2007). Strong disinhibitory effect of evoked responses in infragranular layers by VIP activation thus may be the result of unbalanced excitation when SOM neurons are suppressed, allowing excitatory sound-evoked activity to spread.

Previous research has shown that SOM interneurons can provide lateral inhibition in visual cortex leading to a strong suppression of evoked visual activity (Adesnik et al. 2012). Because SOM neurons in L2/3 pool activity from excitatory neurons in that layer, the strength of the suppression they provide is proportional to the increase in activity of the excitatory cells. In visual cortex, presenting stimulus that spans a large portion of the visual field leads to a strong recruitment of SOM neurons, causing a reduction of a stimulus evoked response. In our study, we used white noise to evoke auditory responses, which is the auditory equivalent of a large visual stimulus. If lateral inhibition is affected during VIP activation, one would expect that wide-spread evoked activity in combination with SOM inhibition would lead to a much stronger response, which is the opposite of what we see. In contrast, by inhibiting both inhibitory and excitatory neurons, VIP may scale down sound evoked input to neurons in superficial layers, leading to a strong suppression of sound evoked activity while having only modest effects on spontaneous firing rate. Additionally, the suppression of evoked responses in supragranular layer can

be mediated by recruitment of PV interneurons in infragranular layer. Previous research in visual cortex revealed a subset of layer 6 excitatory neurons, activity of which can have a strong inhibitory effect on evoked responses in superficial layers via recruitment of fast spiking interneurons in layer 6 (Bortone et al. 2014). Our results show that VIP activation increases spontaneous and evoked activity in both regular and spiking cells in layer 6, suggesting that a subset of those neurons can contribute to the inhibitory effects in superficial layers.

Differential effects on VIP on cortical layers can be either a results of their direct inhibition of excitatory neurons or differential connectivity of SOM neurons that are disinhibited during VIP activation. SOM interneurons are known to provide inhibition to PV cells. Though previous work has reported disinhibitory effects of VIP-SOM network (Lee et al., 2013; Pfeffer et al., 2013; Pi et al., 2013), it's likely that some of those SOM neurons in this circuit also inhibit PV cells, leading to a mixture of inhibitory and disinhibitory effects. Activating VIP modulates spontaneous and evoked activity of both regular and fast spiking neurons suggesting that though few in numbers they can still have a large effect on cortical activity.

Processing of auditory streams by subcortical and cortical regions is influenced by a high degree of interconnectivity of those regions, creating complex thalamocortical, corticocortical, and corticothalamic circuits. Though layer 4 is considered to be the main input layer for thalamic neurons, most cortical layers receive at least some thalamic input (Lee and Winer 2008; Huang and Winer 2000; Zhang and Bruno 2019; Constantinople and Bruno 2013; Schoonover et al. 2014). Significant portion of neurons in layers 5 and 6 project back to the thalamus and provide modulatory feedback of medial geniculate nucleus (MGN) responses (Lee 2013; Llano and Sherman 2008). Layer 5 neurons are also known for dendritic projections that can extend cortical columns up to layer 1, suggesting that corticothalamic feedback that they provide contains integrated information across cortical layers (Gao and Zheng 2004). The functional role of reciprocal connections between auditory cortex and thalamus is still not fully understood, though previous research has shown that corticothalamic projections from layer 6 play an important role in perceptual grouping (Homma et al. 2017). Combined with our findings, strong disinhibition of neurons in infragranular layers by VIP suggests that they may

provide important control of inhibition of feedback corticothalamic projections that are likely influenced by intracortical processing as well as corticocortical modulatory input.

Similarly to VIP activation, changes in behavioral state, such as running or changes in arousal, produce diverse inhibitory and excitatory effects on cortical neurons. Running leads to a widespread increase in spontaneous activity in both regular and fast spiking neurons while simultaneously suppressing sound evoked responses (Fig. 6A). This dichotomy of running effect is present throughout cortical layers, though it varies in its strength. One interesting question that arises from these results is what are the possible mechanisms that lead to differential effects on spontaneous and evoked activity? Previous has shown that running can suppress auditory cortical evoked and spontaneous activity via M2 - PV inhibitory network (Nelson et al. 2013; Schneider et al. 2014), though this suppression is inconsistent with an increase in spontaneous activity that we see. Additionally to motor cortex, running can activate basal forebrain projections that target most inhibitory cell subtypes as well as excitatory neurons (Nelson and Mooney 2016). In contrast to motor cortex, activation of these projections leads to a widespread increase in the firing rate of auditory neurons via nicotinic acetylcholine receptors. Because these areas receive different inputs, the two pathways for running modulation are likely providing different types of feedback to auditory cortex. Activity in basal forebrain has been associated with arousal, attention, and learning related plasticity in auditory cortex (Hangya et al. 2015; Sarter et al. 2005; Everitt and Robbins 1997; Metherate et al. 1990) while motor cortex is involved in movement- related planning (Eliades and Wang 2003). The interaction of these two pathways remains unclear, though some data suggests that changes in behavioral state might have a biphasic effect on auditory neurons. Neurons in auditory cortex show a depolarizing effect at the beginning of heightened arousal that's followed by a hyperpolarizing period (Shimaoka et al. 2018), while running still had an overall suppression of evoked responses. The biphasic effect of arousal suggests that some of the differences in reported results can be attributed to timing differences of measurements of modulatory effects.

Though our results show an overall increase in spontaneous and decrease in evoked activity, these effects were quite variable across neurons, with fast spiking neurons showing no net change in a group mean. The diversity of running effects may

reflect that motor cortex input targets only a subset of PV-expressing neurons. Because PV neurons are also the main source of balanced inhibition in the cortex, it is likely that PV inhibition is recruited as needed to reduce the amount of excitatory drive in the cortical cells, after which their activity continues to fluctuate in unison with neighboring excitatory cells. Additionally, cortical neurons receive a variety of modulatory signals that can interact with one another. Brainstem reticular formation (RF) provides critical glutamatergic drive necessary for cortical activation and behavioral arousal via direct input to cortex as well as indirect stimulation of the forebrain (Jones and Yang 1985; Parvizi 2003).

BRIDGE TO CHAPTER III

The work described in Chapter II showed that VIP interneurons can have a potent disinhibitory effect on infragranular layers. Additionally, we provided evidence that modulation by running and changes in arousal do not interact with VIP activation effects, suggesting that VIP are unlikely to be the cellular mechanisms of cortical state modulation. A different cellular subtype, SOM interneurons, which receive strong inhibitory input from VIP, can also be differentially modulated by behavioral state depending on their class, sensory system, and behavioral paradigm. The functional effects of such modulation have been studied with optogenetic manipulation of SOM cells, which produces effects on learning and memory, task performance, and the integration of cortical activity. In the Chapter III, we review the evidence that shows that SOM neurons perform unique neural computations, forming not only distinct molecular but also functional subclasses of cortical inhibitory interneurons. Chapter III was published as an invited review for Frontiers in Neural Circuits (Yavorska and Wehr 2016).

III. ROLE OF SOMATOSTATIN-EXPRESSING INTERNEURONS IN CORTICAL CIRCUITS

INTRODUCTION

Inhibitory interneurons represent about 20-30% of all cortical cells in mammals ranging from mice to humans (Tamamaki et al., 2003; Markram et al., 2004; Sherwood et al., 2010; Hendry et al., 1987). Interneurons exhibit remarkable diversity in their morphology, histochemistry, intrinsic membrane properties, and connectivity. This diversity strongly suggests that different types of interneurons play distinct roles in cortical computation, although only the first glimmers of these functional roles have so far been brought to light. Although inhibitory interneurons can be classified by many different characteristics, a widely used approach is to identify unique molecular markers such as neuropeptides or calcium binding proteins. This method has gained increasing popularity in recent years, because the promoters for such cell-type-specific genes provide access for targeting the expression of genetic tools to specific subsets of cells. Based on histochemical markers, we can divide cortical inhibitory cells into three non-overlapping categories in mice: those that express parvalbumin (PV) , somatostatin (SOM), or vasointestinal peptide (VIP). These categories vary across species; in rats, for example, PV, SOM, and calretinin (CR) cells form non-overlapping categories (Gonchar and Burkhalter, 1991; Kawaguchi and Kubota, 1997), whereas mice show overlapping expression of SOM and CR (Ascoli et al., 2008; Fishell and Rudy, 2011; Freund and Buzsaki, 1996; Rudy et al., 2011; Somogyi and Klausberger, 2005). While these 3 major classes don't account for all inhibitory interneurons (a small number of interneurons express other less common markers), these 3 major classes do account for the vast majority (80-90%) of all inhibitory cells (Gonchar and Burkhalter, 1997; Pfeffer et al., 2013; Rudy et al., 2011).

In this review, we focus on SOM cells in cerebral cortex, with an emphasis on mice. For an excellent recent review of SOM interneurons in cortical circuits, see Urban-Ciecko and Barth, 2016. Because SOM cells differ markedly in many respects from PV and VIP cells, we will briefly review some of the distinctive characteristics of those cell types. PV cells are by far the largest category of inhibitory cells, representing 30-50% of all inhibitory interneurons (Tamamaki et al., 2003; Rudy et al., 2011). Although PV cells

are not a homogenous population, they do appear to share several features. PV cells are found throughout cortical layers 2-6 and are typically fast spiking (FS) cells with narrow spike waveforms. However, not all PV cells are FS cells, and not all FS cells are PV cells (Cauli et al., 2000; Markram et al., 2004; Moore and Wehr, 2013). PV cells tend to target the somata and proximal dendrites of both excitatory cells and other PV cells (Kubota et al., 2016). They provide powerful inhibition, but since they form depressing synapses, this inhibition is relatively short-lived (Beierlein et al., 2003). Although it is still unclear whether PV cells perform similar functions in different sensory regions, current evidence suggests that they most likely provide gain control in cortical networks by indiscriminately pooling locally available excitatory input and feeding this back to both PNs and other PV cells (Cruikshank et al., 2010; Gabernet et al., 2005; Higley and Contreras, 2006; Miller et al., 2001; Pinto et al., 1996, Moore and Wehr, 2013). In sensory cortical areas with columnar organization, PV cells are thought to pool local input from similarly-tuned PNs, and are therefore well-tuned. For example, auditory cortex has columnar organization for sound frequency and PV cells there are well-tuned for frequency (Moore and Wehr, 2013). In contrast, mouse visual cortex does not have columnar organization for orientation, and PV cells pool input from heterogeneously-tuned PNs, and are therefore more broadly tuned for orientation than PNs (Niell and Stryker, 2008; Atallah et al., 2012; Kerlin et al., 2010).

While VIP cells comprise only 1-2% of all cortical cells, recent studies in a number of cortical areas have revealed that VIP cells provide weak inhibition to PV networks and strong inhibition to SOM networks, and thus indirectly regulate the activity of the local population of PNs (Lee et al., 2012, Pi et al., 2013, Pfeffer et al., 2013, Karnani et al., 2016a; Hioki et al., 2013). In the context of understanding SOM networks, VIP cells are of particular interest because they target SOM cells strongly in layers 2/3 (and also weakly in layer 5), forming robust disinhibitory circuits (Lee et al., 2013; Pfeffer et al., 2013; Karnani et al., 2016a). These disinhibitory circuits appear to be engaged under specific behavioral conditions including associative learning, reinforcement, locomotion, and attention (Letzkus et al., 2011, Kepecs et al., 2014, Pi et al., 2013, Pala and Petersen, 2015; Fu et al., 2014, Uematsu et al., 2008). The axons of VIP cells extend vertically within a narrow column, thereby inhibiting mainly local SOM

cells. VIP cells may therefore "open holes in the blanket of inhibition" that is provided by SOM cells to local PNs (Karnani et al., 2016a). VIP cells also belong to a subgroup of neurons that express the 5HT3a serotonin receptor, which also includes neurogliaform and late-spiking as well as a subset of cholecystokinin (CCK), CR, or neuropeptide Y (NPY) expressing neurons (Ruby et al., 2011; Lee et al., 2010).

How Many Distinct Kinds of SOM Cells Are There?

SOM cells compose 30% of all inhibitory cells in the cortex (Xu et al., 2009; Rudy et al., 2011), and these can be further subdivided into smaller distinct groups based on layer, physiology, morphology, co-expression of other markers, and synaptic targets. These approaches typically produce partially overlapping categories, producing an inevitable tension between the tendency to be a "lumper" or a "splitter." Anatomically, for example, the most distinctive type of SOM cell is the Martinotti cell (Ma et al., 2006; Wang et al., 2004; Karube et al., 2004; Martinotti, 1889). The most striking feature of Martinotti cells is their characteristic axonal projection to layer 1, where they make extensive lateral arborizations (Ma et al., 2006; Wang et al., 2004; Gentet, 2012). All Martinotti cells are SOM-positive, however not all SOM-positive cells are Martinotti cells. Martinotti cells are mostly located in supragranular layers 2 and 3, but can also be found sparsely in layers 4, 5 and 6. Their dendrites branch locally or down to deeper layers (Wang et al., 2004). Because Martinotti cells make up the largest and best-studied category of SOM cells, it is tempting to to lump together all other SOM cells as "non-Martinotti," a category that would include multiple anatomical classes such as subsets of basket cells, bitufted, horizontal, and multipolar cells as well as long-projecting GABAergic neurons (Reyes et al., 1998; McGarry et al., 2010; Rogers, 1992; Ma et al., 2006; Suzuki and Bekkers, 2010; Kubota et al., 2011).

A complementary categorization approach has been to take advantage of transgenic mouse lines such as the GIN, X94, and X98 lines (Ma et al., 2006). These three different lines of transgenic GAD67-eGFP mice were generated by pronuclear injection (i.e., not by knock-in), and fortuitously label subsets of SOM cells (most likely due to insertional effects depending on where GAD67-eGFP randomly inserted into the genome). These lines are an excellent tool for restricting GFP expression to SOM cells.

But because they label only subsets of SOM cells, one must be careful not to infer relative proportions of SOM subtypes from studies using these lines. The GIN line labels mostly Martinotti cells, and most of these are found in L2/3, with sparse labeling in L5. GIN cells account for 35% of SOM cells (Ma et al., 2006; Oliva et al., 2000). Targeted patching of these cells reveals that most of them have intrinsic firing properties characteristic of regular-spiking (RS) cells with generally depolarized membrane potentials, which distinguishes them from other types of SOM cells (Ma et al., 2006; Kinnischtzke et al., 2012; McGarry et al., 2010*)*. L2/3 GIN cells are also likely to be electrically coupled to each other (with 66% likelihood) and are strongly activated by cholinergic signaling (Fanselow et al., 2008).

The X98 line labels Martinotti cells in L5 and upper L6, accounting for 20% of all SOM cells. X98 cells have distinctive intrinsic firing properties — 40% of them are low-threshold spiking (LTS) cells. These cells are neither fast spiking nor regular spiking, but instead fire a characteristic rebound spike when depolarized from a relatively hyperpolarized holding potential, often in bursts. All LTS cells are inhibitory, but only about half of LTS cells are SOM-positive, and of those most are Martinotti cells (Gibson et al., 1999; Beierlein et al., 2003; Goldberg et al., 2004). Morphologically, Martinotti cells in L5 are mostly similar to Martinotti cells in L2/3, except for a tendency to send their axons either to L4 or deeper layers in addition to L1 (Wang et al., 2004).

The X94 line labels only non-Martinotti cells in layers 4 and 5a. Thus X94 cells are a completely distinct population from GIN and X98 cells, whereas the GIN and X98 populations partially overlap with each other. X94 cells account for about half of L4 SOM cells and have a basket-like morphology with mostly local axonal projections (unlike the striking L1 projection seen in Martinotti cells). Unlike Martinotti cells, which target PNs, X94 cells target PV-positive FS interneurons in layer 4. X94 cells fire narrow action potentials at high rates, and therefore resemble FS cells, but unlike FS cells they have a distinctive “stuttering” firing pattern in which their spike trains are interrupted by seemingly random periods of silence. These firing properties have therefore been called “FS-like” or “quasi-FS” (Ma et al., 2006; Large et al., 2016). In piriform cortex, SOM-positive cells can also exhibit tonic fast spiking firing properties and PV-positive neurons

can be stuttering fast spiking, which indicates that different cells types can have similar

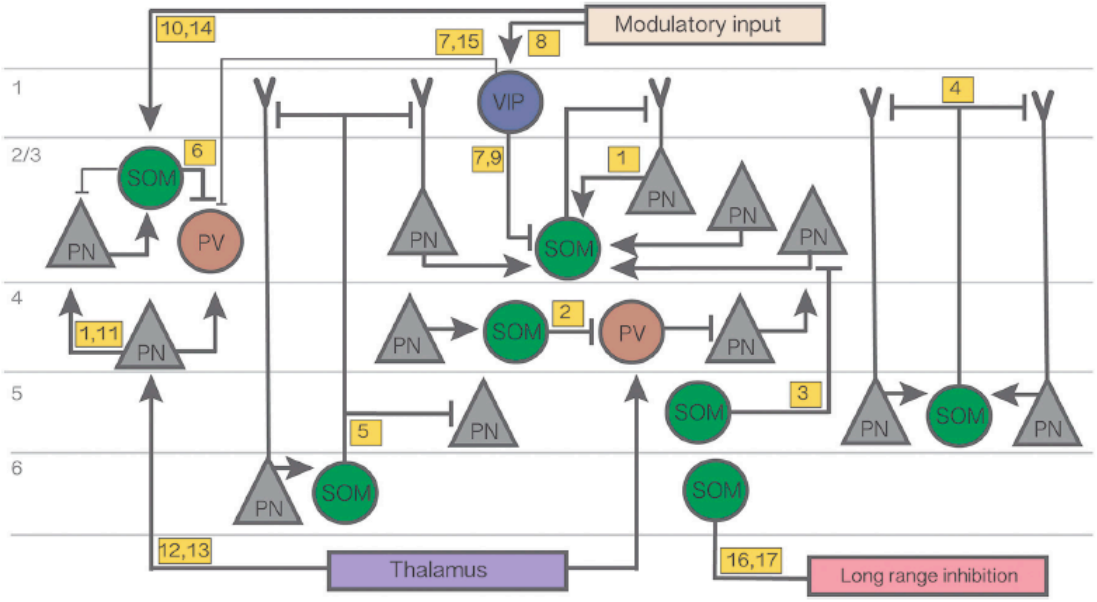

Figure 1. Summary diagram of the cortical circuits in which SOM cells participate. Number in yellow boxes refer to the references below. Some microcircuits combine results from different studies and include speculative connections. Connections not mentioned in the main text or not pertaining to SOM networks are omitted for simplicity. This lines indicate weaker connections. Figure references: 1. Adesnik et al. (2012); 2. Xu et al.(2013); 3. Kafer et al. (2007); 4. Silberberg and Markram, (2007); 5. Wang et al., (2004); 6. Cottam et al., (2013); 7. Pi et al. (2013); 8. Fu et al. (2014); 9. Karnani et al. (2016a); 10. Kawaguchi et al. (1997); 11. Li et al. (2015); 12. Cruikshank et al. (2010); 13. Beierlein et al. (2003); 14. Fanselow et al. (2008); 15. Letzkus et al. (2011); 16. Tomioka et al. (2005); Endo et al. (2006).

firing properties and thus this criterion alone can not be used to reliably identify a specific cell type (Large et al., 2016). Interestingly, the SOM cells in layer 4 that are not labelled in the X94 line are similar to X94 cells in all of these respects: they have only local axons that target L4 PV-positive cells, and have the stuttering FS-like firing type. Thus it appears that L4 SOM cells may be a single population, with no apparent functional correlates of their segregation into X94 and non-X94 categories (Ma et al., 2006; Xu et al., 2013; McGarry et al., 2010). However, some Martinotti cells are found sparsely in L4, at least in rat (Wang et al., 2004).

Another genetic tool increasingly used to investigate SOM neurons is the SOM-Cre line (Taniguchi et al., 2011; Lovett-Barron et al., 2012), which allows researchers to use optogenetic or other Cre reporters to manipulate or record SOM cell activity across cortical layers. The SOM-Cre lines target all SOM cells, and have recently been used to study a number of specific brain regions (Sturgill and Isaacson, 2015; Cottam et al.,

2013; Polack et al., 2013; Neske et al., 2015; Chen, Helmchen et al., 2015). It is important to note that at least one SOM-Cre line (Taniguchi et al., 2011; Jax Stock No. 013044) also erroneously marks a small subset (6-10%) of fast spiking PV neurons (Hu et al., 2013), perhaps due to transient SOM expression during embryonic development in a small subpopulation of FS PV cells (although this has not yet been tested). It is not yet known whether this is also true for the other SOM-Cre line (Lovett-Barron et al., 2012). It is also important to note that about 5% of GFP-expressing neurons in the X94 and X98 lines, and 3% of cells in the GIN line, are not SOM-positive (Ma et al., 2006). This could be attributed to low expression of SOM in some cells which might be below the detectability threshold for immunohistochemistry, highlighting the point that immunohistochemistry results should be interpreted with caution. Although the percentages of this off-target labelling are low, they should still be taken into consideration in experiments. More generally, it is important to note that immunohistochemistry is a relatively difficult technique, and standards for antibody validation have been adopted relatively recently. This likely contributes to sometimes contradictory results for peptide expression in different studies.

A small subset (6-9%) of SOM cells that express NPY, nitric oxide synthase (NOS), and the Substance P receptor (SPR) form a distinct morphological class with long distance axonal projections. Although few in number, they can project to multiple brain regions both horizontally and vertically, making them good candidates for synchronizing neural activity across multiple cortical and subcortical regions (Kubota et al., 2016; Kubota, 2014; Kubota et al., 2011; Endo et al., 2016; Caputi et al., 2013; Tomioka et al., 2005). These cells have high spine density early in development, which is greatly reduced during maturation (Kubota et al., 2011). Additionally, since NOS-positive neurons are highly active during sleep, while most SOM neurons are not, SOM/NOS/SPR neurons are likely to form a distinct subclass with different morphology and activity patterns (Kilduff et al., 2011; for review see Tricoire et al., 2012).

Adding to this diversity are distinct laminar distributions of many of these cell types, as detailed below. In addition, SOM cells co-express a variety of other molecular markers such as CB (calbindin; Ma et al., 2006; Kubota and Kawaguchi, 1994; Wang et al., 2004; Suzuki and Bekkers, 2010), NPY (Ma et al., 2006; Kubota and Kawaguchi,

1994), CR (Xu et al., 2006; 2009), CCK (Gonchar and Burkhalter, 1997), NOS (Xu et al., 2006; Perrenoud et al., 2012; Gonchar and Burkhalter, 1997; Kubota and Kawaguchi, 1994; Kawaguchi and Kubota, 1997; Kilduff et al., 2011), and SPR (Kubota et al., 2011; Kubota et al., 2016; Caputi et al., 2013; Tomioka et al., 2005). Because most studies have used only a subset of these categorization methods (indeed, some methods are mutually exclusive, such as the transgenic lines), it is still not clear how many distinct combinatorial types of SOM cells are found in the cerebral cortex. Nevertheless, it may be informative to attempt to estimate upper and lower bounds on the number of distinct SOM subtypes. At a minimum there are 4 distinct types: (1) L2/3 Martinotti cells, which are mostly regular-spiking, labelled by GIN, and target PNs, (2) L5 Martinotti cells, which include LTS, are labelled by X98, and target PNs, (3) L4 SOM cells, which are FS-like and target L4 PV+ cells, and some of which are labelled by X94, and (4) NOS/SPR long-projecting GABAergic cells that can make either cortico-cortical or corticofugal projections (Table 1). This estimate undoubtedly lumps together subtypes of cells that can be distinguished by at least some criteria, but represents a lower bound on the number of functionally distinct SOM subtypes.

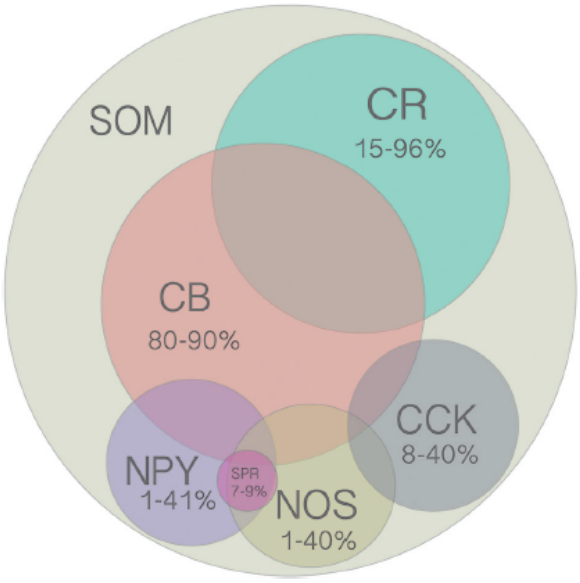

Figure 2. Venn diagram of all molecular markers that are colocalized with SOM (CB, CR, NPY, NOS, CCK). Numbers indicate the range of reported percentages of SOM-positive cells that coexpress a given marker across studies in different species (mouse or rat), cortical layer (2–6),and cortical region (frontal, visual, or somatosensory). For more details, see **Table2**. Area of each circle approximately represents the average range. Overlap of circles indicates known coexpression of depicted markers, however the area of the overlap does not indicate the extent of coexpression.

Although there are no reports of SOM cells coexpressing more than two other molecular markers, this possibility has not been ruled out since it was rarely tested for.

What about the other extreme, an upper bound estimate of the maximum possible number of SOM cell types? Estimating such an upper bound requires several assumptions about whether classification criteria can vary independently (producing all possible combinations) or whether there are correlations that reduce the number of combinations. These assumptions are poorly constrained by data because most studies have measured only a subset of these criteria. In addition, we assume here that these criteria are static, although it's likely that some criteria could change over time. For example, cellular firing properties (such as bursting) can change under certain conditions in some cells (Bahrey et al., 2002), and molecular expression likely changes during development. Based on the ranges of classification criteria (detailed in Table 2), we estimated an upper bound of 100 on the number of possible subtypes of SOM cells. For example, in layer 2/3 there are two types of firing properties (RS and bursting) and 6 molecular markers (CB, CR, NPY, CCK, NOS, and SPR) in SOM cells. These belong mostly to one of two morphological classes, Martinotti cells and multipolar long-projecting neurons that express NOS/SPR. Cells are exclusively RS or bursting, but molecular markers can be expressed in various combinations (but are rarely tested for co-expression, providing little constraint on the number of possible combinations that could occur in SOM cells). Thus there are 2 morphological types, 2^6 potential combinations of molecular markers, and 2 firing-property classes, leading to 256 possible subtypes of SOM cells ($2 \cdot 2^6 \cdot 2$). Of these 256 possible combinations, bursting cells are known not to express NPY, and there is evidence against co-expression for 6 of the 15 possible binary combinations of markers (Table 3). This puts an upper bound of 25 on the number of potential SOM subtypes in L2/3. Following similar logic for layers 2-6 (see Table 2 for details), we estimate the overall number of distinct subtypes of cortical SOM cells is likely no greater than 100. Additional data that further constrains the number of possible combinations would reduce this number. Thus while the true number of distinct subtypes of SOM cells is unknown, we estimate that it most likely lies somewhere between 4 and 100 subtypes.

Another important means of categorizing SOM cells is by the layer in which their cell bodies reside. Here, we consider each of these layers in turn.

Table 1. Four main subtypes of SOM cells (including 3 labeled by specific transgenic lines) with a minimal degree of overlap.

Line	Morphology	Layer	Firing properties	Marker expression
GIN	Martinotti	L2/3, L5	RS	30% CB 27% NPY
X94	Non-Martinotti	L4, L5	FS-like	None
X98	Martinotti	L5	LTS	96% CB 40% NPY
None	Non-Martinotti Long-projecting	L2, L5+6	RS/BS LTS	100% NPY+NOS+SPR

Subtype differences are based on morphology, cortical layer, firing properties, and co- expressed markers. Numbers in the Marker Expression column are the percentage of cells labeled in that subtype that express a given marker.

Layer 2/3

Multiple studies have shown that layer 2/3 SOM cells provide strong inhibition to L2/3 PNs (Xu et al., 2013; Cottam et al., 2013; Fino and Yuste, 2011; Adesnik et al., 2012). However, there is disagreement over how much inhibition L2/3 SOM cells provide to other inhibitory cells in L2/3. In somatosensory cortex, L2/3 SOM neurons provide only weak inhibition to other inhibitory cells (Xu et al., 2013). A quite different pattern was observed in the visual cortex. There, SOM neurons strongly inhibit PV cells (twice as potently as PNs), and this inhibition causes PV cells to be more tuned to orientation (Cottam et al., 2013; Pfeffer et al., 2013). The difference between these findings may indicate different circuits in somatosensory and visual cortex, but it is important to note that these studies also used different methods. Xu et al. performed slice experiments using current injections in single SOM neurons and optogenetic suppression of SOM neurons, whereas Cottam et al. looked at neural firing rate *in vivo* in behaving animals with and without presentation of visual stimuli while optogenetically activating many SOM neurons. Considering that brain states can strongly affect neural activity, it is quite possible that the reported differences in the inhibitory contribution of L2/3 SOM cells to neighboring neurons could be explained by different cortical states and the number of SOM cells recruited.

L2/3 SOM cells avoid inhibiting each other, and instead receive most of their inhibition from VIP and PV cells (Pfeffer et al., 2013). Layer 2/3 SOM neurons have also been shown to participate in a form of lateral inhibition in visual cortex, pooling excitatory input from adjacent PNs and thereby contributing to surround suppression (Adesnik et al., 2012). Indeed, stimulation of a single L2/3 PN in visual cortex can activate 30% of SOM neurons within a 100 micron radius (Kwan and Dan, 2013). This activation of SOM cells by PNs was more strongly distance-dependent than PN→PN activation (Kwan and Dan, 2013). Activity of the SOM network also increases supralinearly as the number of active L2/3 PNs increases. Compared to activating a single PN, activation of just two L2/3 PNs causes a 10-fold increase in the strength of recruited SOM inhibition (Kapfer et al., 2007). Interestingly, in barrel cortex SOM cells are suppressed during stimulus presentation, and thus are anti-correlated with network activity, a feature which has not been observed in other sensory regions (Gentet et al., 2012). In contrast, strong activation of PNs is accompanied by a linear recruitment of PV-mediated inhibition (Xue et al., 2014). Thus, it appears that the most important contribution of SOM inhibition in L2/3 is likely to be driven by high-frequency activation of just a few surrounding PNs.

In visual and auditory cortex, L2/3 SOM cells respond much later than other neurons to input from L4, and have lower spontaneous firing rates than other inhibitory cells (Ma et al., 2010; Li et al., 2015). These late responses have been attributed to the fact that SOM cells in L2/3 do not receive input directly from L4, but rather pool from L2/3 PNs. In general, SOM cells respond with a delay, even if they are receiving input from neighbouring L2/3 PNs (Kwan and Dan, 2013; Kapfer et al., 2007). This delay probably also arises in part from the integration of inputs from facilitating synapses.

L2/3 SOM neurons participate in both feedforward as well as feedback inhibition, and primarily target the dendrites of L2/3 pyramidal neurons (Karnani et al., 2016). Paired *in vitro* recordings of SOM cells (in the GIN line) revealed that both their subthreshold and suprathreshold activity is highly synchronous and they exhibit persistent firing more frequently than other cell types (Fanselow et al., 2008). During spontaneous activity *in vivo*, however, SOM cells do not correlate with oscillatory network activity, whereas PV cells do (Kwan and Dan, 2013). These results support the idea that PNs and

PV cells receive similar input (dominated by thalamic activation), whereas SOM cells are modulated by distinct pathways (including top-down and subcortical input).

Layer 4

Most SOM cells in layer 4 are strikingly different from the typical Martinotti SOM cells in other layers. The X94 line sparsely labels L4 and L5a SOM neurons (Ma et al., 2006; Xu et al., 2013), and these neurons do not send their axons to layer 1, but instead target other inhibitory cells (i.e. PV cells) in layer 4. In fact, unitary IPSPs from SOM cells onto L4 PV cells are much larger than those in L4 excitatory cells (Xu et al., 2013). The morphology of L4 SOM cells also differs from other SOM neurons. They are typically described as bitufted or multipolar cells that keep their axons and dendrites in the same layer (Gonchar and Burkhalter, 1997; Ma et al., 2006). These cells rarely co-express other markers and have been characterized as either quasi-FS (Ma et al., 2006) or bursting (Kubota and Kawaguchi, 1994; Wang et al., 2004). While thalamocortical axons in L4 provide strong and direct input to pyramidal and fast spiking cells, L4 SOM cells are only weakly excited by thalamic input (Cruikshank et al., 2010). Synaptically coupled SOM-FS pairs in L4 of barrel cortex can show synchronous spiking activity, even in the presence of glutamate antagonists (but not when $GABA_A$ receptors are blocked), indicating that inhibitory $GABA_A$-mediated synaptic transmission is both necessary and sufficient to induce synchronous activity between SOM and FS cells (Hu et al., 2011). A small number of SOM cells with Martinotti morphology are also found in L4, at least in juvenile rat (Wang et al., 2004). Due to differences in their targets, it appears that FS-like and RS SOM cells are members of different circuits in L4. In the frontal cortex, these cells also show different patterns of activity during a foraging task (Kvitsiani et al., 2013).

Layer 5

Layer 5 SOM cells represent 19% of all inhibitory cells in L5, some of which also co-express NPY and/or CB (Kawaguchi and Kubota, 1997; Ma et al., 2006) and which are labeled in the X98 mouse line. Layer 5 pyramidal neurons form disynaptic inhibitory circuits with one another via the L5 SOM network (Silberberg and Markram, 2007).

Activation of a L5 PN typically produces inhibition in neighboring PNs, and 40-90% of this inhibition comes from a single L5 Martinotti cell (Silberberg and Markram, 2007). Layer 5 SOM cells also inhibit a subpopulation of L2/3 PNs, consistent with the translaminar projections that are the hallmark of Martinotti cells (Kapfer et al., 2007; Xu et al., 2009). 50% of SOM cells in L5 are low-threshold spiking cells. LTS SOM cells differ in their connectivity to one another compared with other SOM neurons. About 40% of LTS SOM cells make inhibitory connections with one another (Fino and Yuste, 2011). A small percentage of X94 line SOM neurons are also found in L5a (Ma et al., 2006). These neurons create a disinhibitory network by targeting PV cells and, at least, in motor cortex, hyperactivity of SOM cells in L5 leads to excitotoxicity and death of excitatory neurons (Zhang et al., 2016).

Table 2. Diversity of SOM cells across cortical layers 2-6.

Layer	Co-expression	Morphology	Firing properties	Targets	Max Number
2/3	CB[6] (32–92%[7]; 93%[9]; 20%[11];86%[2]; 85%[17]) NPY[6] (15–27%[7]; 18%[11]) CR (57–96%[12,13,22]) CCK (10%[2,11,22]) NOS[8,20,24] (0.5%[2]; 1–40%[12]) SPR[23,20] (6.6%)	Martinotti[2,5,7,13,16,18,19,21,22] Non-Martinotti[20,21,22,23]	RS[5,7] Bursting[11]	L2/3 PNs[1,18] L2/3 INs[1]	25
4	CB (31%[11]) NPY (5%[11]) CR (10%[11]; 18–44%[12,22]) CCK (8%[2,11,22])	Non-Martinotti[7,18,19] Martinotti[2,11]	LTS[14,15] FS-like[7] Bursting[11]	L4 INs[18] L4 PNs[14]	9
5	CB[5,6] (49–96%[7];15%[11];92%[9];86%[2];92%[17]) NPY(1.4–41%[7]; 40%[11]) CR(12–19%[12,22]) NOS[8,20,24] (0.5%[2]; 1–40%[12]) SPR[23] (8.6%)	Martinotti[2,10,16,18,19,21,22,23] Non-Martinotti[7,21]	RS(<50%)[5,7,22] LTS (<50%)[3,7] FS-like[7] Bursting[5,11,22]	L5 PNs[10] L2/3 PNs[4]	27
6	CB[6] (49–96%[7];92%[9];86%[2];92%[17]) NPY[6] (1.4–41%[7]; 40%[11]) CR (15–17%[12,22]) CCK (40%[2,11,22]) NOS[8,20,24] (0.5%[2]; 1–40%[12]) SPR[23,20] (8.4%)	Non-Martinotti[9,21,23] Martinotti[2,7,11,19,21]	RS[11] LTS[15] Bursting[11]	PNs[15]	39
Total					100

No SOM cells are found in L1. The Co-expression column lists known molecular markers that co-localize with SOM in each layer, with the percentage of SOM cells that co-express each marker in parentheses. We included both bursting and LTS as distinct firing types, as reported in separate studies 3, 7, 11, 14, 15*, but considered these as a single category for the purposes of calculating an upper bound on the number of distinct SOM cell types (Max Number column). We determined the upper bound by counting the number of possible combinations of markers, morphology, and firing type, given the constraints on marker co-expression detailed in* ***Table3****, known correspondences between morphology and firing properties, and the observations that bursting SOM cells don't express NPY and that L4 non-Martinotti (X94) cells don't express CB or NPY. 1. Cottam et al. (2013) mouse, visual; 2. Gonchar and Burkhalter (1997) rat, visual cortex; 3. Goldberg et al. (2004) mouse, visual and somatosensory cortex; 4. Kapfer et al. (2007) mouse,*

somatosensory cortex; 5. Kawaguchi and Kubota (1996) rat, frontal cortex; 6. Kawaguchi and Kubota (1997) rat, frontal cortex; 7. Ma et al. (2006) mouse (GIN, X94, X98), somatosensory cortex; 8. Perrenoud et al. (2012) mouse, barrel cortex; 9. Rogers (1992) rat, visual cortex; 10. Silberberg and Markram (2007) rat, somatosensory cortex; 11.Wang et al. (2004) rat, somatosensory cortex; 12. Xu et al. (2006) mouse GIN, frontal (high % NOS), somatosensory, and visual cortex; 13. Xu and Callaway (2009) mouse GIN, somatosensory; 14. Beierlein et al. (2003) rat, barrel cortex; 15. Gibson et al. (1999) rat, somatosensory cortex; 16. Karube et al. (2004) rat, frontal cortex; 17. Kubota and Kawaguchi (1994) rat, frontal cortex; 18. Xu et al. (2013) mouse, somatosensory cortex; 19, McGarry et al. (2010) mouse, frontal, somatosensory, and visual cortex; 20. Endo et al. (2016) mouse, visual cortex; 21. Kawaguchi and Kubota (1998) rat, frontal cortex; 22. Uematsu et al. (2008) rat, frontal cortex; 23. Kubota et al. (2011) rat, frontal cortex; 24. Tomioka et al. (2005) mouse, motor, somatosensory, and visual cortex.

Layer 6

SOM neurons in layer 6 consist mainly of Martinotti cells that coexpress variable combinations of molecular markers such CB and NOS in rat (Kubota and Kawaguchi, 1994) as well as NPY and CCK in mouse (Wang et al., 2004). These cells send axons to layer 1, but about half of the SOM cells in L6 also make axonal arborizations in layers 5 and 6, suggesting less specific laminar targeting than layer 2/3 Martinotti cells (Ma et al., 2006; Wang et al., 2004).

Several studies have now identified a small population of GABAergic projection neurons, i.e., GABAergic inhibitory neurons that are not interneurons (McDonald and Burkhalter, 1993; Gonchar et al., 1995; Tomioka et al., 2005). These cells, while few in number (only 7-9% of SOM cells), project axons outside of the local area, can travel up to several mm, can cross areal boundaries, and in some cases project through the corpus callosum to the contralateral hemisphere (Gonchar et al., 1995). The vast majority of these cells express SOM, NPY, NOS, and substance P receptor (SPR), and are found in layer 6 (and to a lesser extent, in L2 and L5; Caputi et al., 2013; Tomioka et al., 2005; Kubota et al., 2011). Recent work has shown that these long inhibitory projections can regulate the output of medium spiny neurons in striatum, thereby modulating the activity of both direct (D1-type dopamine receptors) and indirect (D2-type dopamine receptors) reward pathways (Rock et al., 2016). NOS-positive projection neurons are a small subpopulation of neurons that is active during slow wave sleep, suggesting that they could play a major role in homeostatic sleep regulation by influencing global neuronal activity (Kilduff et al., 2011; for review see Tamamaki and Tomioka, 2010).

Firing Properties

Cortical SOM cells differ in their firing properties and electrophysiology. In particular, several distinct categories have been reported, including regular spiking (RS) cells, LTS, bursting, and FS-like or stuttering cells (Fanselow et al., 2008; Ma et al., 2006; Goldberg et al., 2004; Wang et al., 2004, Kawaguchi and Kubota, 1996; Large et al., 2016). There is some disagreement about the prevalence of FS-like or stuttering SOM cells in different layers; one possible reason for this is that FS-like SOM cells might have been categorized as FS cells in some studies (Ma et al., 2006; Wang et al., 2004; Beierlein et al., 2003). SOM cells have also been classified as either accommodating or non-accommodating (Wang et al., 2004). Accommodating cells (the vast majority, at 90% of SOM cells) include both RS and bursting types, whereas non-accommodating cells (only 8% of SOM cells) have been described as analogous to FS cells based on their ability to fire at high rates without adaptation. Regular spiking and bursting firing types were originally described for cortical pyramidal neurons (Connors et al., 1982), and it is important to note that the firing properties of RS or bursting SOM cells are analogous but not identical to those classically observed in pyramidal neurons. For example, *in vivo* whole cell studies show that average action potential waveform of SOM neurons is somewhat narrower than pyramidal cells and wider than fast spiking cells recorded both in CRE-IRES-SOM and GIN transgenic lines, thus putting them in a different category than RS neurons (Gentet et al., 2012; Polack et al., 2013). But in slice recordings from younger animals, the waveform of SOM neurons is comparable in width to excitatory neurons (McGarry et al., 2010). This discrepancy so far has not be investigated and could arise from either differences in recording methods or animal age.

It is still not clear whether LTS and bursting SOM cells form two distinct categories or instead are a single class that lie along a continuum. LTS cells are Martinotti cells, and are found in cortical layers 4, 5, and 6 (Beierlein et al., 2000; 2003; Goldberg et al., 2004; Wang et al., 2004; Ma et al., 2006; Kawaguchi and Kubota, 1996). They are so-named because they have very low thresholds for action potential initiation. Because of this low threshold, single-axon inputs to layer 5 LTS cells can generate spikes (Kozloski et al., 2001). In addition, LTS cells have a strong tendency to fire spikes or bursts on rebound from hyperpolarization. These rebound spikes/bursts are mediated by

T-type calcium channels, similar to those found in thalamic relay neurons (Goldberg et al., 2004, Ma et al., 2006). Like relay neurons, L5 LTS cells can fire in either tonic or bursting mode, depending on their membrane potential. In contrast, L4 LTS cells fire tonically under control conditions, and only fire bursts in the presence of metabotropic glutamate agonists (Goldberg et al., 2004, Beierlein et al., 2000; 2003). This suggests that LTS cells in layer 4 and 5 probably form two distinct classes.

Table 3. Co-expression of molecular markers in SOM cells.

	NPY	CR	NOS	CCK	SPR
CB	+[7,24]	+[12,13]	+[2,8,24]	+[11]	+[23]
NPY		−[2]	+[8,24]	−[11]	+[23]
CR			−[2]	−[2]	−[23]
NOS				+[8]	+[20,23]
CCK					−[23]
SPR					

Reported co-expression of binary combinations is indicated by +, reported absence of co-expression is indicated by −. Markers have been reported to co-express in at least some SOM cells for all binary combinations except NPY-CR, NPY-CCK, CR-NOS, CR- CCK, CR-SPR, and CCK-SPR. We pooled data from all layers and did not distinguish betweenNOS-1andNOS-2. Numbers refer to references in ***Table2****.*

Upon release from hyperpolarization, LTS cells can fire either a single spike or a burst of spikes, which in some studies has led to them being categorized as two distinct groups (Ma et al., 2006, Wang et al., 2004). However, it is possible that this difference is due only to variation in input resistance along a continuum (Ma et al., 2006), which would instead suggests that they form only a single group. Different studies have adopted different terminology (either bursting or LTS), and report somewhat different laminar distributions, which is further complicated by the fact that some studies are in rat while others are in mouse (Ma et al., 2006, Wang et al., 2004). Bursting SOM cells exhibit a prominent after-depolarization, which is almost certainly mediated by an I_h current because these cells express HCN channel genes. Pharmacological blockade of the the I_h

current in GIN and X94 cells eliminates rebound depolarization, indicating that I_h likely contributes to bursting in those types of SOM cells. But blockade of the low-threshold T-type calcium channel (but not I_h) eliminates rebound bursting in only X98 cells, indicating that T-type channels are essential for this distinctive firing property of L5 LTS cells (Ma et al., 2006). Thus, based on the channels involved, LTS and bursting SOM cells described in different studies probably represent at least partially distinct populations. It seems likely that classification of SOM cells based on firing properties alone (such as the tendency to burst) could lump together distinct classes or erroneously split a single class, depending on the sample being studied.

LTS cells are notable because they have been shown to form gap-junction coupled networks in layer 4 of barrel cortex (Amitai et al., 2002; Gibson et al., 1999; Beierlein et al., 2000; 2003; Ma et al., 2011). Electrical coupling was also observed in L2/3 SOM neurons in the GIN line, although these are usually not categorized as LTS cells (Fanselow et al., 2008). Electrical coupling of SOM cells likely has a substantial impact on the net effect of the SOM network, because SOM inhibition increases supralinearly when more than one SOM neuron is activated (Kapfer et al., 2007). Adding to the importance of electrical coupling to SOM network activity is the fact that SOM cells don't receive thalamic input, and instead are mostly driven by intracortical input (Cruikshank et al., 2010; Beierlein et al., 2003). Although individual SOM neurons in L2/3 and L4 don't provide as strong or reliable inhibition to PNs as do PV cells (Pfeffer et al., 2013; Beierlein et al., 2003), together as a unified network they may act as a powerful inhibitory force when activity in the local cortical excitatory population increases.

Synaptic Physiology and Input

Unlike strongly depressing PN→FS and FS→PN synapses, L4 and L2/3 SOM cells typically receive strongly facilitating synaptic input from PNs and weakly facilitating synaptic input from FS and VIP cells (Ma et al., 2012; Reyes et al., 1998; Thomson and Deuchars, 1997; Markram et al., 1998; Pi et al., 2013; Karnani et al., 2016b). This suggests that SOM neurons are strongly but transiently inhibited at the onset of a new stimulus, but likely recover during prolonged activity. Facilitating input to SOM cells

also means that they would be more sensitive to a sustained train of input from a single cell than to simultaneous but transient input from multiple PNs. Consistent with this, activation of SOM cells is quite different from other inhibitory cells depending on cortical network state. Synaptic input received by LTS SOM cells tends to be weaker and less reliable at low stimulation frequencies (<20 Hz) compared to input received by FS cells (Beierlein et al., 2003; Ma et al., 2012). At higher stimulation frequencies (>10-20 Hz), LTS cells are powerfully recruited at the same time that synapses onto other inhibitory cells become depressed. As a result, SOM cells are unlikely to be recruited during periods of low cortical activity, but become strongly activated during high cortical network activity. Congruent with these effects of network dynamics on SOM activation, SOM cells make weakly facilitating synapses onto both PNs and FS cells. Thus SOM-mediated inhibition tends to be weak and unreliable at low frequencies, but will become robust at higher frequencies, making SOM cells an important player in shaping neural responses to prolonged stimuli (Beierlein et al., 2003; Ma et al., 2012; Hayut et al., 2011, Pfeffer et al., 2013; Gupta et al., 2007; Kapfer et al., 2007). Tonic firing of SOM neurons regulates spontaneous activity of principal cells via slow $GABA_B$ receptors (Urban-Ciecko et al., 2015), while also contributing fast $GABA_A$-mediated synaptic input onto the distal dendrites of PNs (Silberberg and Markram, 2007; Wang et al., 2004). This indicates that SOM neurons contribute to spontaneous and evoked cortical responses.

Input to SOM cells is also unique since it does not appear to follow the canonical pattern of ascending thalamocortical information flow. Activation of thalamic fibers evokes a strong feedforward and depressing inhibitory current in L4 PNs, suggesting a recruitment of FS neurons by the thalamus. Intracortical stimulation, on the other hand, recruits disynaptic SOM-mediated inhibition (Beierlein et al., 2003). Additionally, stimulation of thalamic projections evokes robust EPSPs in FS INs and RS PNs but only weak excitatory current in SOM neurons in L4 and L5/6 (Cruikshank et al., 2010; Beierlein et al., 2003). Whatever weak thalamic input makes it to SOM neurons is still mediated by depressing rather than facilitating synapses, making thalamic drive to SOM neurons even less impactful (Cruikshank et al., 2010). Within cortex, stimulation of L4 neurons evokes much stronger EPSPs in L2/3 PV cells and PNs than in SOM cells, whereas stimulation of surrounding L2/3 PNs leads to a strong recruitment of L2/3 SOM

neurons (Adesnik et al., 2012). These results from visual cortex indicate that SOM cells in L2/3 are modulated more by within-layer input than translaminar input. SOM neurons in L2/3 of auditory cortex tend to have delayed EPSPs during presentation of sound, also suggesting that they are not directly connected to thalamorecepient neurons in L4, but rather pool input from neighbouring L2/3 PNs (Li et al., 2015). Weak but facilitating input would take longer to integrate and produce a measurable EPSP, which could explain why excitatory currents in SOM cells are delayed. Although more systematic recordings from different layers and cortical regions are necessary to clarify the nature of the input that drives SOM neurons, it is clear that SOM neurons do not respond with the same dynamics as other neurons.

In visual cortex, different subtypes of interneurons are frequently coactive with other neurons within their class. Thus SOM neurons are more likely to be recruited when other SOM neurons are firing. An interesting pattern emerges when co-inhibition between different inhibitory subclasses and their excitatory input are examined. Subclasses that exhibit strong co-inhibition (such as VIP-SOM) tend to receive non-overlapping excitatory input, whereas those with weak co-inhibition (such VIP-PV) have highly correlated membrane potentials (Karnani et al., 2016b).

What Does the Somatostatin Neuropeptide Do?

Somatostatin is not just a cell-type specific marker, but also an inhibitory 14-amino-acid neuropeptide released by the subset of GABAergic neurons that express the somatostatin gene. Somatostatin activates 5 distinct G-protein coupled receptors (Hoyer et al., 1995). The cellular and synaptic effects of somatostatin are fairly well-understood, but less is known about the network, cognitive, and behavioral effects (for review see Baraban and Tallent, 2004; Liguz-Lecznar et al., 2016). Unlike GABA, which is released from conventional synaptic vesicles at axonal boutons, somatostatin is released from dense-core vesicles from both axons and dendrites (Ludwig and Pittman, 2003). Neuropeptide release requires repetitive high-frequency firing (Kits and Mansvelder, 2000), suggesting that GABA and SOM are likely to be released under different conditions. Indeed, in the hippocampus, GABA and SOM are differentially released during the different oscillatory activities accompanying sleep and movement, suggesting the possibility of distinct

functional roles (Katona et al., 2014). The functional interactions of SOM and GABA can be complex. In hippocampus, both SOM and GABA produce postsynaptic hyperpolarization, with SOM augmenting multiple K+ currents and reducing voltage-gated Ca++ currents (Schweitzer et al., 1998; Moore et al., 1988; Ishibashi and Akaike, 1995; Viana and Hille, 1996; Pittman and Siggins, 1981). SOM also acts via presynaptic receptors to inhibit glutamate release by excitatory neurons (Boehm and Betz, 1997; Tallent and Siggins, 1997; Dutar et al., 2002, Sun et al., 2002). Repeated release of SOM also reduces the density of dendritic spines and excitatory synapses, which depends on activation of SOM receptor subtype 4 (Hou and Yu, 2013). All of these actions would be expected to work in concert with GABA release to reduce the firing probability of downstream neurons. However, there is some evidence that SOM also decreases GABA-mediated IPSPs and can lead to depolarization, which would counteract the inhibitory effects of GABA (Greene and Mason, 1996; Leresche et al., 2000; Scharfman and Schwartzkroin, 1989; Dodd and Kelly, 1978). The cellular and synaptic effects of SOM release in cortex have not been studied.

The effects of the somatostatin neuropeptide on network activity and cognition have been studied by intracerebral injections of agonists and antagonists, and also with SOM knockout mice. SOM appears to have an antiepileptic effect, reducing epileptiform activity and seizures in a number of different epilepsy models (Halabisky et al., 2010; Sun et al., 2002). This makes sense because of the inhibitory effects of SOM and the fact that it is released only under conditions of sustained high-frequency firing. Consistent with this, SOM knockout mice show increased severity of kainate-induced and sensory-triggered seizures (Buckmaster et al; 2002; Tomioka et al., 2014). Together these findings suggests that one function of SOM may be to act as a protective neuropeptide system to prevent runaway activity. SOM also appears to play a role in learning and memory. SOM receptor knockout mice show spatial learning deficits (Guillou et al., 1993; Dutar et al. 2002; Tuboly and Vécsei, 2013), whereas hippocampal or ventricular injections of SOM facilitate spatial learning in a variety of tasks (Lamirault et al., 2001; Vécsei et al., 1984; 1988). Cysteamine, a SOM-depleting agent, leads to deficits in memory retention in rats (Vecsei, 1984, 1988; Fitzgerald and Dokla, 1989; Nakagawasai et al., 2003). Cortical expression levels of SOM are reduced in aging in both rats and

humans, and this is correlated with learning deficits in rats (Dournaud et al., 1995). SOM levels are also reduced in the brains of Alzheimer's disease patients examined postmortem, specifically in cortical layers 3 and 5 (Davies et al., 1980; Vécsei and Klivenyi, 1995). However, it's worth noting that many of these studies are relatively old and have not been replicated recently, despite broad interest in the topic. Based on the available evidence, it thus appears that SOM has a potential neuroprotective role in preventing epileptic activity, and also appears to be involved in both learning and memory retention.

Functional and Computational Roles of SOM Cells

Receptive Field Properties

In general, the tuning of inhibitory neurons is very similar among different subtypes, and typically a bit more broad compared to excitatory cells. In L2/3, at least, SOM neurons appear to provide inhibition to nearly all PNs in the local neighborhood, and likewise appear to pool input indiscriminately from the local population (Fino and Yuste, 2011). SOM cells are thus very likely to have the same tuning as the net tuning of the local population, such that their effect on the receptive fields of PNs may not be obvious just from measuring their tuning (Li et al., 2015; Karnani et al., 2016a). In visual cortex, there is evidence that SOM cells are more orientation-tuned than PV neurons (Ma et al., 2010). Their frequency tuning in auditory cortex is also sharper than that of PV cells but does not differ from the tuning of excitatory cells (Li et al., 2015). These differences in tuning at the population level are quite small, however, and are much smaller in magnitude than the variability in tuning across individual cells. Together, these results are largely consistent with the idea that SOM cells, like PV cells, pool input from the local population. This "local pooling hypothesis" explains why inhibitory interneurons tend to reflect the general tuning of the area and the neurons they pool from (Kerlin et al., 2010; Fino and Yuste, 2011; Moore and Wehr, 2013). This idea also explains the minor differences in tuning of IN subtypes, since there are some differences in their input and the size of the area they pool from. For example, PV neurons in L4 receive thalamic input as well as excitatory input from surrounding PNs within about 100 μm, and as a result are highly correlated with local network activity (Beierlein et al., 2003; Scholl et al., 2015).

PV neurons provide equal inhibition to PNs located both near and far from them (within a range of about 400 μm). VIP cells, in contrast, provide very local columnar inhibition to SOM cells within about 120 μm (Zhang et al., 2011; Karnani et al., 2016a). SOM neurons receive little or no thalamic input, and pool mostly from PNs in the same layer within about 550 μm (Fino and Yuste, 2011; Zhang et al., 2014). The peak of their inhibitory contribution is seen in PNs located approximately 200 μm away, making them ideal inhibitors of competing neural activity (Fino and Yuste, 2011; Zhang et al., 2014). SOM neurons often form disynaptic inhibitory circuits between PNs, thus contributing strongly to lateral inhibition (Adesnik et al., 2012; Silberberg and Markram, 2007; Fino and Yuste, 2011; Zhang et al., 2014). For example, SOM-mediated lateral inhibition contributes to surround suppression in L2/3 visual cortical neurons, conferring tuning for stimulus size (Adesnik et al., 2012). The fact that SOM cells form a disinhibitory network with VIP neurons, which are activated by locomotion, predicts that surround suppression should be modulated by locomotion (Ayaz et al., 2013; Fu et al., 2014). Indeed, locomotion alters spatial integration in V1 in mice, leading to a decrease in surround suppression (Ayaz et al., 2013). This suggests that effects of SOM cells on the receptive fields of neighboring PNs could depend in complex ways on behavioral state or task context, and may not be revealed by studies in anesthetized animals. For example, SOM neurons in visual cortex have been reported to be much less visually responsive under anesthesia (Adesnik et al., 2012). In addition, since SOM cells appear to integrate input from within their own layer, and have unique interlaminar connectivity, it is possible that specific contributions of SOM inhibition to PN receptive field properties might only be seen under conditions in which cortical layers are differentially activated, as is seen for example during habituation in auditory cortex (Kato et al., 2016).

Divisive and Subtractive Inhibition

A number of studies have examined the functional role of SOM neurons and their effect on both PNs as well as interneurons using optogenetic activation or suppression of SOM or PV cells (Duguid et al., 2012; Cottam et al., 2013; Atallah et al., 2012; Lee et al., 2012; Wilson et al., 2012 ; Seybold et al., 2015). A common theme is that SOM cells provide gain control for cortical circuitry, but perhaps not surprisingly, a diversity of

results have been reported. Gain control in this context refers to the general enhancement or suppression of PN responses, independent of specific transformations of stimulus selectivity. For example, moderate suppression or activation of PV neurons in layer 2/3 causes a multiplicative scaling up or down of PN responses in visual cortex, without altering their orientation tuning (Atallah et al., 2012; Wilson et al., 2012). Such scaling is referred to as divisive gain control, which is often contrasted with subtractive gain control. In subtractive gain control, all activity (both spontaneous and evoked) is increased or decreased by a constant amount. In contrast to the findings of Atallah and of Wilson, stronger activation of visual PV neurons appears to produce a subtractive instead of divisive effect on PNs, which narrows their orientation tuning instead of leaving it unaffected (Lee et al., 2012). These conflicting results can best be understood in the context of the "iceberg effect," which refers to the idea that firing rates cannot go below zero (i.e., the water level), which hides the subthreshold tuning curve. Stronger suppression of PN spiking can narrow tuning curves, even with purely divisive inhibition, because of this effect of spike threshold (Xue et al., 2014; El-Boustani and Sur, 2014; Lee et al., 2014). These studies illustrate that inferring the presence of divisive or subtractive inhibition from optogenetic manipulations can be problematic (Seybold et al., 2015; Kumar 2013).

Because PV cells provide fast and powerful proximal inhibition, they appear to be ideally positioned to provide divisive inhibition, whereas the dendritic targeting by Martinotti cells seems better suited to providing subtractive inhibition (Kubota et al., 2016; Kubota et al., 2015). Consistent with this, SOM cells provide subtractive inhibition to PNs in olfactory cortex, and moreover provide divisive inhibition to PV cells there (Sturgill and Isaacson, 2015). In visual cortex, conflicting results have been reported for activation of SOM cells. One study found that SOM activation sharpened PN orientation tuning, consistent with subtractive inhibition (Wilson et al., 2012), whereas a similar study reported that SOM activation reduced PN spiking without any effect on tuning, consistent with divisive inhibition (Lee et al., 2012). A key to reconciling these disparate results may lie in the relative timing, size, and durations of sensory and optogenetic stimulation. In particular, inhibition may be more likely to be divisive when it is co-active with strong PN activity, and more likely to be subtractive when PNs and INs are not co-

active. Importantly, one of these studies used brief activation (Wilson et al., 2012), whereas the other used prolonged activation (Lee et al., 2012). Brief SOM activation (which would result in less co-activation) produced a subtractive effect, whereas prolonged SOM activation (with more co-activation) produced a divisive effect (Lee and Dan, 2014; El-Boustani and Sur, 2014). Due to their facilitating input and the fact that they pool broadly from PNs, SOM cells are likely to be only weakly activated by brief or small visual stimuli, whereas prolonged and large visual stimuli are likely to strongly activate the SOM network. Indeed, SOM cells were found to provide late, subtractive inhibition to PNs for small visual stimuli, but switched to fast, divisive inhibition for large visual stimuli (El-Boustani and Sur, 2014). This illustrates that whether gain control is divisive or subtractive is dynamic and stimulus-dependent, rather than a fixed property of a given cell type. In addition, SOM activation suppresses PV cells up to twice as powerfully as PNs, which will have its own effects on network activity and PN tuning (Cottam et al., 2013). A diverse mixture of subtractive and divisive effects during activation of SOM or PV neurons is seen in auditory cortex as well, even in simultaneously recorded neurons within the same column (Seybold et al., 2015). This degree of variability in the effects of SOM network perturbations makes sense given the broadly interconnected and recurrent nature of cortical networks. Indeed, modeling of these networks has shown that inhibitory gain control can shift from being divisive to subtractive depending on the spike threshold of PNs and the strength of the optogenetic suppression. This suggests that these forms of gain control may not be determined by the type of interneuron, but rather by intrinsic properties of a target neuron (Seybold et al., 2015). The picture that emerges from these studies is that whether gain control is divisive or subtractive is a flexible and dynamic feature of inhibitory circuits.

Surprisingly, functional properties of SOM neurons in barrel cortex appear strikingly different from those in auditory and visual cortex. Unlike SOM cells in V1, which have unremarkable responses to visual stimuli, SOM cells in L2/3 of S1 are tonically active in the absence of whisker stimulation but become hyperpolarized and cease firing in response to either active or passive whisker stimulation (Gentet et al., 2012). Optogenetic activation of SOM cells during stimulus presentation might therefore produce unnatural results that would be markedly different from what is seen in the non-

perturbed circuit. Optogenetic suppression of SOM cells in S1, however, is easier to interpret, and leads to increased burst firing in nearby PNs (Gentet et al., 2012). Tonically active SOM cells likely provide tonic inhibition to cortical neurons, especially to apical dendrites (the distinctive target of Martinotti cells). Tonic inhibition remains poorly understood in cerebral cortex, but has been shown to improve the signal-to-noise ratio in cerebellum, allowing reliable transmission of sensory information (Duguid et al., 2012). Reducing tonic inhibition in cerebellum mainly results in increased spontaneous activity, with little effect on evoked responses, consistent with results seen in barrel cortex (Gentet et al., 2012). In hippocampus, silencing SOM (but not PV) neurons increased the probability of burst spiking in PNs (Royer et al., 2012), similar to the effect seen in barrel cortex. Burst spiking in cortical regions has been hypothesized to carry more information than single spikes (Livingstone et al., 1996; Lisman, 1997) and is associated with improved stimulus detection in the visual system (Mukherjee and Kaplan, 1995; Guido et al., 1995). This suggests a mechanism by which the hyperpolarization of SOM cells by whisker stimulation might enhance sensory information processing.

In cortex, excitation is typically balanced by inhibition that is proportionally scaled depending on the strength of excitatory input (Wehr and Zador, 2003; Wilent and Contreras, 2005, Okun and Lampl, 2008; Anderson et al., 2000). In order for inhibition to scale proportionately with excitation, both sources must receive at least some overlapping sensory input. Since PV neurons, but not SOM cells, receive thalamic input, they appear to be best positioned to provide balanced inhibition via feedforward circuitry, as has been shown in the visual cortex (Xue et al., 2014). SOM cells, on the other hand, seem more likely to provide modulatory inhibitory input that is pooled from the activity of surrounding PN population, hence providing feedback inhibition (Murayama et al., 2009). Both sources likely contribute to balanced inhibition in PNs.

Gain Control by Locomotion

Behavioral states can profoundly change how sensory neurons respond to a stimulus (Kato et al., 2016; Niell and Stryker, 2010). A powerful new model for studying these effects has been to study the effects of locomotion on sensory processing, typically by recording stimulus-evoked responses in mice that are free to run on a ball or wheel. The

effects of locomotion are strikingly different across sensory systems. In the visual cortex, for example, running enhances neural responses without changing their orientation tuning (Niell and Stryker, 2010). The opposite effects are seen in the auditory cortex, where projections from secondary motor cortex suppress sensory responses during locomotion (Schneider et al., 2014). Similarly, both the neural circuitry and the neuromodulatory systems underlying locomotion effects also appear to differ across sensory regions. In visual cortex, running depolarizes both PNs and inhibitory cells. The resulting increase in both excitation and inhibition in PNs reduces membrane potential variance, and leads to more stimulus-evoked spikes without any increase in spontaneous activity (Polack et al., 2013). Whereas cholinergic input affects membrane potential fluctuations during quiescent periods, the effect of locomotion on membrane potential variance is mostly dependent on noradrenergic input. Interestingly, SOM neurons do not show decreased membrane potential variability during running, suggesting a differential influence of norepinephrine on SOM neurons and PNs (Polack et al., 2013). Different classes of inhibitory neurons show marked differences in how they are modulated by locomotion in the visual cortex. VIP neurons are depolarized throughout the entire running period, while PV cells only respond transiently at the beginning. SOM neurons are typically suppressed during running, and fire mostly at the end of the running period (Fu et al., 2014). These results suggest that the effect of locomotion is mediated by a disinhibitory circuit, in which VIP cells inhibit SOM cells and thereby increase the activity of neighboring PNs. VIP cells are known to be activated by basal forebrain stimulation, via nicotinic acetylcholine receptors (nAChRs). The basal forebrain projects extensively to V1, and nAChR antagonists strongly reduce the locomotion-induced depolarization of VIP cells. These results suggest that cholinergic projections are a key element of the circuitry underlying the locomotion effect in V1, but because nAChR blockade did not completely abolish this effect, there must be additional pathways involved (Fu et al., 2014). Multiple interacting modulatory pathways could explain the apparent contradiction between the results of Polack and of Fu about the relative importance of norepinephrine and acetylcholine for the locomotion effect in V1. Acetylcholine and norepinephrine modulation can interact in complex ways; for example, it is possible that acetylcholine predominantly affects the gain of evoked responses, while norepinephrine

produces shifts in baseline activity, as seen in barrel cortex (Constantinople and Bruno, 2011). Interestingly, ACh also affects SOM neurons, but acts through muscarinic receptors (Fanselow et al., 2008; Xu and Rudy, 2013; Kawaguchi et al., 1997), suggesting that the influence of ACh on activity of cortical neurons may be complex and depend on the type of activated receptor and neuronal subtype.

One exciting but still speculative possibility is that this disinhibitory circuit operates in much the same fashion to increase gain during selective attention or similar top-down enhancement. For example, VIP cells have been proposed to mediate attentional enhancement by opening local holes in the blanket of inhibition (Karnani et al., 2016a; Zhang et al., 2014). One difference between this idea and the disinhibitory effects of locomotion is that all VIP cells in V1 are activated by running, which is consistent with the observation that the effects of locomotion are distributed broadly across all of visual cortex. This contrasts with the idea of very local disinhibition achieved by activating one or a few VIP cells. It is possible that the same underlying circuitry could operate in these two distinct modes in different functional contexts.

A similar (but not identical) disinhibitory circuit modulates activity in barrel cortex. Unlike V1, somatosensory cortex receives strong M1 input, particularly to VIP cells that express 5HT3aR serotonin receptors (Lee et al., 2013; Fu et al., 2014). While PNs and other types of INs also receive weak input from M1, VIP neurons in all layers are strongly recruited by M1 activation. Whisking reliably activates VIP neurons that in turn suppress SOM activity (Lee et al., 2013). This disinhibitory circuit therefore explains how SOM cells cease their tonic firing and become hyperpolarized during whisking (Gentet et al., 2012). This suggests that the same disinhibitory circuit motif that underlies the locomotion effect in V1 also modulates S1 sensory responses during active whisking, although the source of VIP activation is different in the two systems. Considering that 5HT3aR-expressing VIP cells are strongly depolarized by serotonin and acetylcholine as well, an intriguing possibility is that other behavioral states and contexts could additionally influence sensory responses during whisking (Moreau et al., 2010; Rudy et al., 2011; Lee et al., 2013).

Although auditory neurons also exhibit depolarization and decreased membrane potential variability during running, effects of locomotion on auditory cortex are distinct,

since locomotion mostly suppresses sound-evoked responses instead of enhancing them (Schneider et al., 2014). These changes also tend to precede movement, indicating that modulation comes from a motor planning region rather than from muscle feedback. Interestingly, in auditory cortex, M2 projections inhibit PN responses via the PV network, bypassing the VIP→SOM disinhibitory circuit (Schneider et al., 2014). While running desynchronizes auditory cortex and depolarizes PNs, optimal performance on an auditory task is associated with an intermediate state of arousal and hyperpolarized membrane potentials in PNs, in an attentive but quiescent behavioural state (McGinley et al., 2015). Thus the state of arousal falls along a continuum, and different points of this spectrum are likely mediated by different modulatory systems, not all of which involve SOM inhibitory networks. Taken together, these studies demonstrate that each sensory system integrates information about movements through different local and global circuits.

Salience and Behavioral Relevance

A number of recent studies have looked at the responses of SOM neurons during more complex forms of contextual stimulus presentation. In auditory cortex, SOM inhibition contributes to stimulus-specific adaptation and habituation. In both of these phenomena, SOM neurons appear to be sensitive to the statistics of stimulus presentation, and suppress the responses to frequently presented tones. However, the time scales and contextual structure of the two paradigms suggests that they engage distinct processes. Stimulus-specific adaptation describes how auditory neurons respond in an "oddball" paradigm, in which a frequent stimulus is interleaved with a rare stimulus. Responses to the frequent stimulus are suppressed, but responses to the rare stimulus are not. Stimulus-specific adaptation is seen across all cortical layers, and in all cell types, including SOM neurons. The phenomenon can be seen in anesthetized animals, and develops within a few presentations of brief tone stimuli (Natan et al., 2015; Chen, Helmchen et al., 2015; Szymanski et al., 2009). Suppression of SOM neurons reduces stimulus-specific adaptation in other cortical neurons, increasing PN responses to the frequent tone. Thus SOM cells contribute to stimulus-specific adaptation, even while experiencing stimulus-specific adaptation themselves (Natan et al., 2015). SOM neurons also contribute to a

form of habituation to tones that develops over several days. In this paradigm, daily exposure to repeatedly presented long tones (9 s duration) gradually reduces tone-evoked responses in L2/3 PNs. This habituation can be partially relieved if mice are engaged in a sound detection task (Kato et al., 2016). Tone-evoked responses in L2/3 SOM cells are increased as both PN and PV cell responses are decreased, suggested that SOM cells mediate the habituation in other cortical neurons. This increase in SOM responsiveness contrasts with the decreased SOM responsiveness during stimulus-specific adaptation. However, what causes the increase in SOM inhibition is still unclear. One possibility is that frequently-repeated stimuli might increase SOM activation via facilitating synapses. This mechanism could explain short-term stimulus-specific adaptation in cortical neurons, but cannot explain habituation effects that persist across days. This suggests that there could be long-term cellular or synaptic changes that lead to a 'memory' of a frequent tone. Another possibility is that SOM cells might receive specific input that is not adapted during habituation paradigms. Interestingly, however, thalamorecipient L4 neurons did not show the habituation seen in L2/3 PNs, which makes them unlikely candidates for enhanced SOM activation (Kato et al., 2016). This is consistent with the fact that L2/3 SOM cells get little or no input from L4 (Li and Zhang, 2015), and also suggests that this form of habituation is not inherited from subcortical auditory structures. Yet another possibility is that enhancement of SOM cell responses during habituation may be generated by top-down input. For example, SOM cells in visual cortex receive weak but measurable input from cingulate cortex (Zhang et al., 2014). Modulation of VIP neurons, as occurs in different behavioral states (Pi et al., 2013; Fu et al., 2013; Karnani et al., 2016a), is also a plausible candidate for the habituation signal.

Inhibition of SOM cells via VIP neurons, as seen during locomotion, also seems to play central role in modulating SOM activity during task performance and behavioral relevance (Pi et al., 2013; Karnani et al., 2016a; Zhang et al., 2014). Although locomotion changes activity broadly across visual cortex, disinhibitory effects of VIP neurons might also be local to a region of specific tuning (Karnani et al., 2016a). A highly localized disinhibitory network could provide a mechanism for selectively enhancing visual processing in a small part of the visual field, without affecting inhibition in other regions. A similar circuit motif can also enhance the signal-to-noise ratio in

cortical neurons during task performance. Indeed, V1 receives strong localized input from the cingulate cortex that enhances VIP activity (Zhang et al., 2014). A top-down control signal from an executive region would be an ideal candidate to selectively modulate visual responses. In auditory cortex, neurons that are tuned to target frequency display enhanced selectivity during performance of a tone-in-noise detection task, while neurons that are tuned to other frequencies suppress their responses (Atiani et al., 2009). All cortical neurons showed a dramatic gain reduction during the task, which, in combination with sharpened receptive fields for target frequency, leads to a dramatic reduction in noise and better task performance (Atiani et al., 2009; Otazu et al., 2009; Sadagopan and Wang, 2010). Although it is unclear whether the VIP→SOM network is responsible for this short-term receptive field plasticity, reinforcement signals are known to activate VIP-positive neurons in auditory cortex, which in turn results in strong suppression of SOM neurons and of a small fraction of PV cells (Pi et al., 2013).

The modulatory signals that underlie differential recruitment of various cell types during task performance are still unclear. In visual cortex, VIP neurons receive modulatory input from cingulate cortex, basal ganglia, and to a weaker extent M1 (Fu et al., 2014, Zhang et al., 2014, Lee et al., 2013). Slice experiments show that ACh increases input resistance in regular and burst spiking VIP and SOM neurons, resulting in increased firing, whereas fast and late spiking cells remain unaffected (Kawaguchi et al., 1997). Moreover, norepinephrine increases spike probability in regular spiking and bursting SOM neurons in rat frontal cortex (Kawaguchi and Shindou, 1998). Additionally, VIP cells belong to a subgroup of neurons that express 5HT3a receptors, thus making them a primary target of serotonergic projections (Rudy et al., 2011). Adding to this complexity, these modulatory inputs also have different effects on cortical activity. ACh and serotonin desynchronize cortical network activity, whereas norepinephrine synchronizes cortical activity (for review see Lee and Dan, 2012). Cortical neurons can also be desynchronized by tonic glutamatergic input from the thalamus (Hirata and Castro-Alamancos, 2010). Interestingly, ACh can synchronize coupled LTS cells, although it is important to remember that LTS cells are only a subset of SOM neurons (Beierlein et al., 2000). Awake behaving mice typically show desynchronized cortical activity, whereas quiet wakefulness, sleep, and anesthesia are

associated with synchronized activity featuring up and down states. Evidence from barrel cortex suggest that non-fast-spiking inhibitory cells tend to correlate with the membrane potential of excitatory cells during quiet wakefulness states, but show dramatic increases in depolarization and firing during active whisking, thus suppressing cortical responses (Gentet et al., 2010). By receiving either direct or disynaptic input from other brain regions, SOM-mediated inhibition could play a role in selective attention of sensory processing during task engagement and dictate changes in cortical network activity during specific behavioral states. Norepinephrine and acetylcholine could have opposing effects because the former activates SOM cells, whereas the latter inhibits them through the VIP→SOM circuit. In summary, an intriguing but still speculative possibility is that different neuromodulators might act via SOM networks to promote synchronized or desynchronized network states, in much the same way as they modulate gain during locomotion.

Learning

SOM neurons also appear to play an important role in memory formation. Classical fear conditioning of a whisker stimulus increases the number of inhibitory synapses in L4 of the corresponding barrel in S1 (Jasinska et al., 2010; Siucinska, 2006). Recently, upregulation of GABA was shown to be accompanied by an increase in the number of SOM-expressing neurons in L4 of barrel cortex after conditioning (Cybulska-Klosowicz et al., 2013; Gierdalski et al., 2001). This presumably results from an increase in SOM expression by SOM cells, bringing them above immunostaining detection threshold, rather than an increase in the number of SOM cells per se. Thus SOM cells express more GABA and somatostatin after associative learning, suggesting that increased SOM-mediated inhibition may play a role in circuit plasticity during learning. In cortical slices from naive animals, SOM neurons exhibit lower levels of GABA expression compared to other classes of inhibitory cells (Gonchar and Burkhalter, 1997). Upregulation of GABA after associative learning may allow the SOM inhibitory network to shape cortical responses that represent a newly behaviorally-relevant stimulus after learning. A quite different pattern of changes has been demonstrated in motor cortex, where motor learning induces reorganization of dendritic spines on the apical tufts of L2/3 PNs. This

reorganization coincides with a decrease in axonal boutons of SOM cells in layer 1 shortly after the beginning of training (Chen, Kim, et al., 2015). Indeed, SOM activation during motor learning destabilizes spines on PN apical tufts, whereas SOM suppression hyperstabilized those spines. These two results — fewer SOM synapses after motor learning, but more synapses after associative learning — appear at first glance to be contradictory. However, the decrease after motor learning was seen for L1 synapses onto L2/3 apical dendrites, whereas the increase after associative learning was seen in L4. The former are almost certainly synapses from Martinotti cells, which target PNs, whereas the relevant L4 SOM cells could be non-Martinotti cells that target PV interneurons in L4. The net effect of these changes could therefore be in the same direction — a disinhibition of PNs. Much remains to be understood about exactly how these SOM inhibitory networks are involved in learning. Yet the differential activation of these networks during learning paradigms illustrates that SOM cells do not merely relay sensory information, but rather modify cortical sensory responses based on an animal's previous experience.

Challenges in Studying Interneuron Populations

Although new optogenetic tools have been indispensable in understanding the role of specific cell types in intact cortical circuits *in vivo*, they do have important limitations that must be considered when interpreting the results. Variability in illumination intensity and duration, transgenic vs. viral expression, and the details of sensory stimuli or task parameters can interact in complex ways that affect how neurons respond to optogenetic manipulation even in the same cortical region. In the case of Arch-mediated suppression, for instance, depending on the cell type and region of inactivation, it can be extremely difficult to completely silence neural responses. For example, spontaneous or low-amplitude evoked activity can show 65-80% suppression, whereas strong evoked bursting activity remains unchanged even with high-power Arch activation (Cardin, 2012). Expression of ChR2 can also produce variable responses of a given cell to the same light pulse, ranging from robust spiking responses to less reliable prolonged responses (Cardin, 2012). Misinterpretation of ChR2 manipulation may also come from atypical firing patterns evoked in cells that show late or suppressed responses under control conditions. In S1 SOM cells, for example, which are normally hyperpolarized by sensory

stimulation, optogenetic activation would produce highly unnatural activity (Gentet et al., 2012). Recent advances in genetic calcium imaging techniques (such as GCaMP) have provided a new approach to the study of inhibitory neuronal populations such as SOM networks (Karnani et al., 2016a; Karnani et al., 2016b; Jackson et al., 2016). Two caveats to this approach are that SOM cells are known to have high basal firing rates, and TdTomato labelling in high concentrations can contaminate the fluorescence signal. Both of these caveats could lead this technique to underestimate neuronal firing rates, and thus care should be taken when inferring neural activity from fluorescence changes. Lastly, high levels of interconnectivity in cortical circuits make it challenging to study the effects of only a single interneuron subtype. In particular, it is virtually impossible to perturb the activity of the SOM network without changing firing patterns in other inhibitory neurons, which may lead to conflicting and misleading results (Cottam et al., 2013; Gibson et al., 1999). Nevertheless, the past few years have seen tremendous advances in knowledge about interneuron function in general, and SOM cell function in particular. It is important to remember that SOM cells are not a single population, but rather consist of several distinct classes of inhibitory cells; new methods for targeting these specific subpopulations will only accelerate discoveries in the near future. It is also exciting that much of the progress in recent years has come not from studying SOM cells and sensory cortex in isolation, but rather from taking account of behavioral state, task context, learning, and sensorimotor integration — in other words, how SOM cells participate in large-scale interactions between sensory cortex and the rest of the brain.

CHAPTER IV
DISCUSSION

Research in animals points to diverse effects of neuromodulatory systems, arousal, and movements on auditory sensory processing. The discrepancies in reported results have been a challenge for interpretation. Some of those differences can be attributed to different animal models used in experiments (monkeys, ferrets, mice, etc., (Fritz et al. 2010; Pi et al. 2013; Peters and Sethares 1991), experimental methods (single cell imaging, extracellular or intracellular recording, (Nelson et al. 2013; Zagha et al. 2013; Fu et al. 2014; Niell and Stryker 2010), and the type of behavioral state changes that were observed during any given experiment (task engagement vs spontaneous changes in arousal levels, (Schneider, Nelson, and Mooney 2014; Lee et al. 2013; Fu et al. 2014)). From numerous experiments has become clear that modulation of sensory processing cannot be attributed to one type of mechanism; multiple neuromodulatory signals and projection pathways are often engaged, interacting in nonlinear ways at different timescales leading to diversity of outcomes.

The work described here provides the evidence for the disinhibitory effects of VIP interneurons in cortical circuits in mice. However, this disinhibitory effect shows an organized pattern and is mostly found in infragranular layers, suggesting that selective disinhibition by VIP may be involved in the corticothalamic feedback circuit. Moreover, evidence from our studies suggests that changes in arousal and locomotion do not modulate cortical circuits exclusively by VIP network. Additionally, we review the studies describing the intricacies of local cortical inhibition by different neuronal subtypes, which may lead to unexpected outcomes of delicate balance of excitation and inhibition.

In the mouse auditory cortex, cortical neurons are tuned to ranges of sound frequencies (Bizley et al. 2005; Bandyopadhyay, Shamma, and Kanold 2010; Moore and Wehr 2013; Guo et al. 2012). In the auditory and other sensory cortices, this tuning is shaped by tuned thalamocortical input (Li et al. 2014) as well as the interaction of excitatory and inhibitory intracortical inputs, with cortical inhibition playing a crucial role in refining stimulus selectivity (Priebe and Ferster, 2008; Isaacson and Scanziani, 2011). Whereas previous studies have established the role of synaptic excitation and

inhibition on sound frequency tuning, the modulatory signaling mechanisms that fine-tune cortical specificity to sound frequencies are not well understood. Modulatory and sound-evoked signals target both excitatory and inhibitory neurons (Nelson et al. 2013; Fu et al. 2014; Wehr and Zador 2003; Pi et al. 2013; Stokes and Isaacson 2010). These signals are processed by highly interconnected circuits of feedforward and recurrent inhibition, resulting in recruitment of GABAergic neurons regardless of the source of input. The exact dynamics of inhibition that balances out excitation in the circuit can be affected by numerous factors such as synaptic physiology (depressing or facilitating synapses), cellular target cites (dendrites or soma), electrophysiological properties (low threshold spiking or fast spiking), as well as recurrent excitatory feedback that inhibitory neurons receive (Jia et al. 2010; Silberberg and Markram 2007; Li et al. 2014) . For instance, suppressing PV interneurons results in a net increase in excitation and inhibition in downstream neurons due potent excitatory feedback current that effectively recruits PV inhibitory network when it's left unbalanced (Moore et al. 2018). On the other hand, SOM inhibition is recruited gradually with an increase in excitation (Adesnik et al. 2012). Their suppression leads to predominantly disinhibitory effect which makes them more suited for fine-tuned modulation of sensory responses (Natan, Rao, and Geffen 2017). These differences provide best-suited roles for different inhibitory cells, though they do not suggest they these interneurons are working separately. GABAergic cells make inhibitory contacts onto each other suggesting that they pull together to harmonize cortical dialogue (Gibson, Beierlein, and Connors 1999; Galarreta and Hestrin 2002; Lee et al. 2013).

Though neuromodulation has been mostly studied in neurons, it's likely that glial cells are contributing to changes in cortical activity as well. NE receptors are known to be expressed in astrocytes and during locomotion, activity of NE neurons globally increases astrocytic Ca-transients (Ding et al. 2013; Paukert et al. 2014). Astrocytes perform many vital functions for healthy cortical processing including neurotransmitter clearance, ion buffering, metabolite delivery. In visual cortex, astrocyte activity was really associated with visual stimulus alone, though when paired with NE, astrocytes became primed to detect changes in neural activity, suggesting that modulatory signals engage a variety of cortical systems, some of which cannot be detected with a measurement of electrical

activity change. Thus, our understanding of modulatory effects on neural activity will always be limited by our understanding of functional contributions of glial cells to neural computations as well as neurotransmitter effect on glial cells.

APPENDIX

SUPPLEMENTARY FIGURES AND VIDEOS FOR CHAPTER II

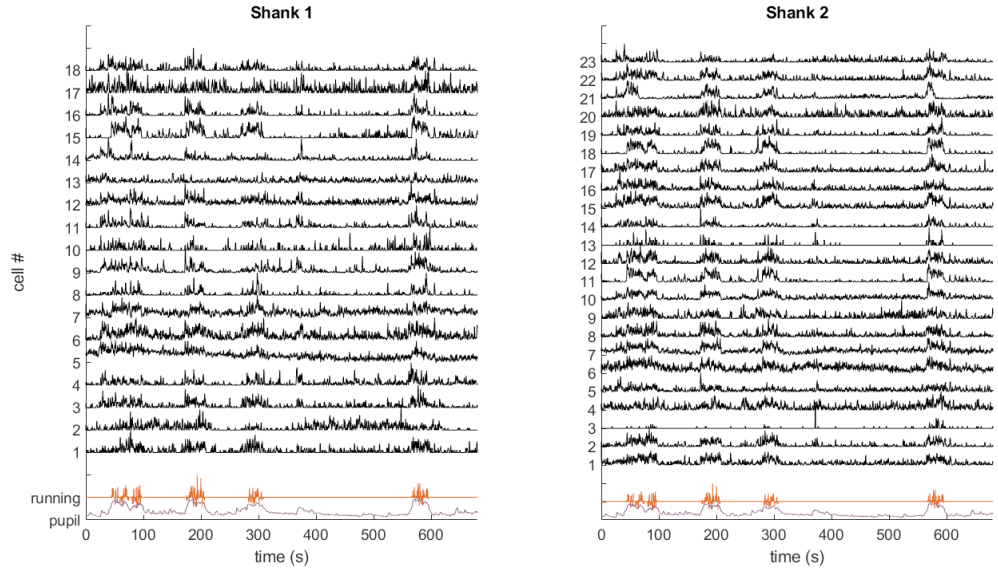

Figure S1. Modulation of activity by locomotion and arousal level. Each trace represents normalized firing rate of a single neuron (total n = 41) arranged by the recording sites on a silicon probe, depth increases incrementally upwards. Neurons were simultaneously recorded with a 64-channel silicon probe (two 32-channel shanks, shank 1 and shank 2). Bottom traces show normalized running speed and normalized pupil size.

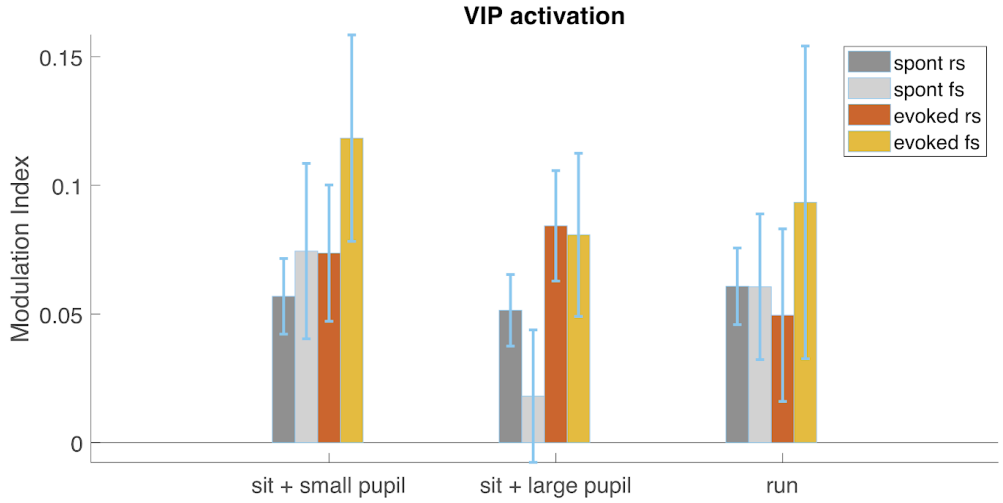

Figure S2. Effects of VIP activation are similar across behavioral conditions. VIP activation modulates neuronal activity similarly Two-way ANOVA, conditions p = 0.52, cell types p = 0.48, interaction p = 0.43.

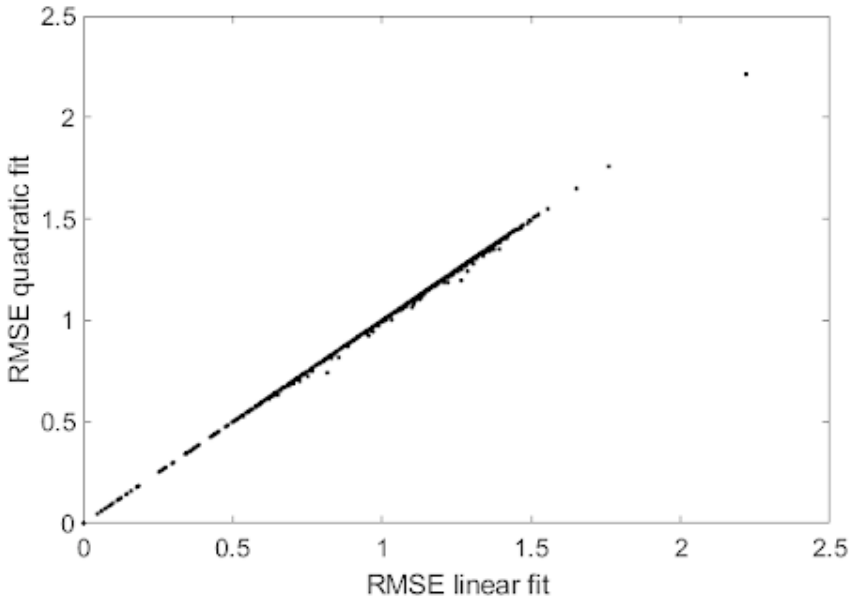

Figure S3. Pupil had a linear relationship with neural activity. Residual mean squared errors of linear and quadratic fits among recorded neurons and pupil traces show that both fits perform similarly.

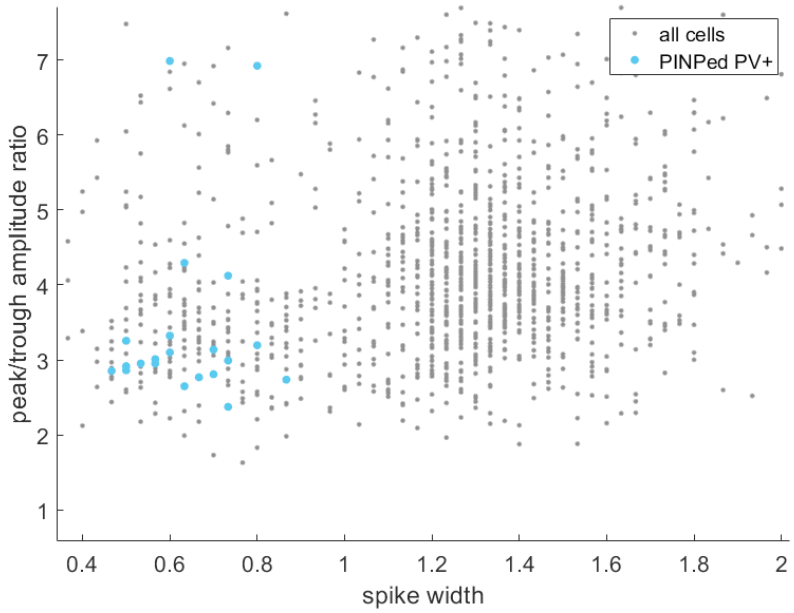

Figure S4. Identification of fast-spiking neurons. Scatter plot shows distribution of spike waveform measurements for recorded neurons. Neurons were considered to be fast-spiking if their spike width was less 0.9 ms, which is consistent with waveform measurements of photo-identified (PINPed) PV+ interneurons from PV-ChR2 mice. Neuron that had spike width of 0.9 ms or greater were considered to belong to be regular spiking.

REFERENCES CITED

CHAPTER II

Adesnik, Hillel, William Bruns, Hiroki Taniguchi, Z. Josh Huang, and Massimo Scanziani. 2012. "A Neural Circuit for Spatial Summation in Visual Cortex." *Nature* 490 (7419): 226–31.

Bandyopadhyay, Sharba, Shihab A. Shamma, and Patrick O. Kanold. 2010. "Dichotomy of Functional Organization in the Mouse Auditory Cortex." *Nature Neuroscience* 13 (3): 361–68.

Bayraktar, T., E. Welker, T. F. Freund, K. Zilles, and J. F. Staiger. 2000. "Neurons Immunoreactive for Vasoactive Intestinal Polypeptide in the Rat Primary Somatosensory Cortex: Morphology and Spatial Relationship to Barrel-Related Columns." The Journal of Comparative Neurology 420 (3): 291–304.

Bizley, Jennifer K., Fernando R. Nodal, Israel Nelken, and Andrew J. King. 2005. "Functional Organization of Ferret Auditory Cortex." *Cerebral Cortex* 15 (10): 1637–53.

Chen, Naiyan, Hiroki Sugihara, and Mriganka Sur. 2015. "An Acetylcholine-Activated Microcircuit Drives Temporal Dynamics of Cortical Activity." Nature Neuroscience 18 (6): 892–902.

Cohen, Marlene R., and John H. R. Maunsell. 2009. "Attention Improves Performance Primarily by Reducing Interneuronal Correlations." Nature Neuroscience 12 (12): 1594–1600.

Ding, Fengfei, John O'Donnell, Alexander S. Thrane, Douglas Zeppenfeld, Hongyi Kang, Lulu Xie, Fushun Wang, and Maiken Nedergaard. 2013. "α1-Adrenergic Receptors Mediate Coordinated Ca2+ Signaling of Cortical Astrocytes in Awake, Behaving Mice." *Cell Calcium* 54 (6): 387–94.

Fritz, Jonathan B., Stephen V. David, Susanne Radtke-Schuller, Pingbo Yin, and Shihab A. Shamma. 2010. "Adaptive, Behaviorally Gated, Persistent Encoding of Task-Relevant Auditory Information in Ferret Frontal Cortex." *Nature Neuroscience* 13 (8): 1011–19.

Froemke, Robert C., Ioana Carcea, Alison J. Barker, Kexin Yuan, Bryan A. Seybold, Ana Raquel O. Martins, Natalya Zaika, et al. 2013. "Long-Term Modification of Cortical Synapses Improves Sensory Perception." Nature Neuroscience 16 (1): 79–88.

Fu, Yu, Jason M. Tucciarone, J. Sebastian Espinosa, Nengyin Sheng, Daniel P. Darcy, Roger A. Nicoll, Z. Josh Huang, and Michael P. Stryker. 2014. "A Cortical Circuit for Gain Control by Behavioral State." *Cell* 156 (6): 1139–52.

Galarreta, Mario, and Shaul Hestrin. 2002. “Electrical and Chemical Synapses among Parvalbumin Fast-Spiking GABAergic Interneurons in Adult Mouse Neocortex.” *Proceedings of the National Academy of Sciences of the United States of America* 99 (19): 12438–43.

Galazyuk, Alexander. 2015. “Sound-Triggered Suppression of Neuronal Firing in the Auditory Cortex: Implications to the Residual Inhibition of Tinnitus.” The Journal of the Acoustical Society of America. https://doi.org/10.1121/1.4933488.

Galazyuk, A. V., S. V. Voytenko, and R. J. Longenecker. 2017. “Long-Lasting Forward Suppression of Spontaneous Firing in Auditory Neurons: Implication to the Residual Inhibition of Tinnitus.” Journal of the Association for Research in Otolaryngology: JARO 18 (2): 343–53.

Gentet, Luc J., Michael Avermann, Ferenc Matyas, Jochen F. Staiger, and Carl C. H. Petersen. 2010. “Membrane Potential Dynamics of GABAergic Neurons in the Barrel Cortex of Behaving Mice.” Neuron 65 (3): 422–35.

Gibson, J. R., M. Beierlein, and B. W. Connors. 1999. “Two Networks of Electrically Coupled Inhibitory Neurons in Neocortex.” *Nature* 402 (6757): 75–79.

Gonchar, Yuri, Quanxin Wang, and Andreas Burkhalter. 2007. “Multiple Distinct Subtypes of GABAergic Neurons in Mouse Visual Cortex Identified by Triple Immunostaining.” Frontiers in Neuroanatomy 1: 3.

Guo, Wei, Anna R. Chambers, Keith N. Darrow, Kenneth E. Hancock, Barbara G. Shinn-Cunningham, and Daniel B. Polley. 2012. “Robustness of Cortical Topography across Fields, Laminae, Anesthetic States, and Neurophysiological Signal Types.” *The Journal of Neuroscience: The Official Journal of the Society for Neuroscience* 32 (27): 9159–72.

Hangya, Balázs, Sachin P. Ranade, Maja Lorenc, and Adam Kepecs. 2015. “Central Cholinergic Neurons Are Rapidly Recruited by Reinforcement Feedback.” Cell 162 (5): 1155–68.

Harris, Kenneth D., and Alexander Thiele. 2011. “Cortical State and Attention.” Nature Reviews. Neuroscience 12 (9): 509–23.

Herrero, J. L., M. J. Roberts, L. S. Delicato, M. A. Gieselmann, P. Dayan, and A. Thiele. 2008. “Acetylcholine Contributes through Muscarinic Receptors to Attentional Modulation in V1.” Nature 454 (7208): 1110–14.

Herrero, Jose L., Marc A. Gieselmann, and Alexander Thiele. 2017. “Muscarinic and Nicotinic Contribution to Contrast Sensitivity of Macaque Area V1 Neurons.” Frontiers in Neural Circuits 11 (December): 106.

Jia, Hongbo, Nathalie L. Rochefort, Xiaowei Chen, and Arthur Konnerth. 2010. "Dendritic Organization of Sensory Input to Cortical Neurons in Vivo." *Nature* 464 (7293): 1307–12.

Joshi, Siddhartha, Yin Li, Rishi M. Kalwani, and Joshua I. Gold. 2016. "Relationships between Pupil Diameter and Neuronal Activity in the Locus Coeruleus, Colliculi, and Cingulate Cortex." Neuron 89 (1): 221–34.

Kato, Hiroyuki K., Shea N. Gillet, and Jeffry S. Isaacson. 2015. "Flexible Sensory Representations in Auditory Cortex Driven by Behavioral Relevance." Neuron 88 (5): 1027–39.

Lee, Soohyun, Illya Kruglikov, Z. Josh Huang, Gord Fishell, and Bernardo Rudy. 2013. "A Disinhibitory Circuit Mediates Motor Integration in the Somatosensory Cortex." *Nature Neuroscience* 16 (11): 1662–70.

Letzkus, Johannes J., Steffen B. E. Wolff, Elisabeth M. M. Meyer, Philip Tovote, Julien Courtin, Cyril Herry, and Andreas Lüthi. 2011. "A Disinhibitory Microcircuit for Associative Fear Learning in the Auditory Cortex." Nature 480 (7377): 331–35.

Li, Ling-Yun, Xu-Ying Ji, Feixue Liang, Ya-Tang Li, Zhongju Xiao, Huizhong W. Tao, and Li I. Zhang. 2014. "A Feedforward Inhibitory Circuit Mediates Lateral Refinement of Sensory Representation in Upper Layer 2/3 of Mouse Primary Auditory Cortex." *The Journal of Neuroscience: The Official Journal of the Society for Neuroscience* 34 (41): 13670–83.

Liu, Bao-Hua, Guangying K. Wu, Robert Arbuckle, Huizhong W. Tao, and Li I. Zhang. 2007. "Defining Cortical Frequency Tuning with Recurrent Excitatory Circuitry." Nature Neuroscience 10 (12): 1594–1600.

McGinley, Matthew J., Stephen V. David, and David A. McCormick. 2015. "Cortical Membrane Potential Signature of Optimal States for Sensory Signal Detection." Neuron 87 (1): 179–92.

Mesik, Lukas, Wen-Pei Ma, Ling-Yun Li, Leena A. Ibrahim, Z. J. Huang, Li I. Zhang, and Huizhong W. Tao. 2015. "Functional Response Properties of VIP-Expressing Inhibitory Neurons in Mouse Visual and Auditory Cortex." Frontiers in Neural Circuits 9 (May): 22.

Moore, Alexandra K., and Michael Wehr. 2013. "Parvalbumin-Expressing Inhibitory Interneurons in Auditory Cortex Are Well-Tuned for Frequency." *The Journal of Neuroscience: The Official Journal of the Society for Neuroscience* 33 (34): 13713–23.

Moore, Alexandra K., Aldis P. Weible, Timothy S. Balmer, Laurence O. Trussell, and Michael Wehr. 2018. “Rapid Rebalancing of Excitation and Inhibition by Cortical Circuitry.” *Neuron* 97 (6): 1341–55.e6.

Natan, Ryan G., Winnie Rao, and Maria N. Geffen. 2017. “Cortical Interneurons Differentially Shape Frequency Tuning Following Adaptation.” *Cell Reports* 21 (4): 878–90.

Nelson, Anders, David M. Schneider, Jun Takatoh, Katsuyasu Sakurai, Fan Wang, and Richard Mooney. 2013. “A Circuit for Motor Cortical Modulation of Auditory Cortical Activity.” *The Journal of Neuroscience: The Official Journal of the Society for Neuroscience* 33 (36): 14342–53.

Niell, Cristopher M., and Michael P. Stryker. 2010. “Modulation of Visual Responses by Behavioral State in Mouse Visual Cortex.” *Neuron* 65 (4): 472–79.

Otazu, Gonzalo H., Lung-Hao Tai, Yang Yang, and Anthony M. Zador. 2009. “Engaging in an Auditory Task Suppresses Responses in Auditory Cortex.” Nature Neuroscience 12 (5): 646–54.

Paukert, Martin, Amit Agarwal, Jaepyeong Cha, Van A. Doze, Jin U. Kang, and Dwight E. Bergles. 2014. “Norepinephrine Controls Astroglial Responsiveness to Local Circuit Activity.” *Neuron* 82 (6): 1263–70.

Pachitariu, Marius, Nicholas Steinmetz, Shabnam Kadir, Matteo Carandini, and Kenneth D. Harris. 2016. “Kilosort: Realtime Spike-Sorting for Extracellular Electrophysiology with Hundreds of Channels.” https://doi.org/10.1101/061481.

Peters, A., and C. Sethares. 1991. “Organization of Pyramidal Neurons in Area 17 of Monkey Visual Cortex.” *The Journal of Comparative Neurology* 306 (1): 1–23.

Pfeffer, Carsten K., Mingshan Xue, Miao He, Z. Josh Huang, and Massimo Scanziani. 2013. “Inhibition of Inhibition in Visual Cortex: The Logic of Connections between Molecularly Distinct Interneurons.” Nature Neuroscience 16 (8): 1068–76.

Pi, Hyun-Jae, Balázs Hangya, Duda Kvitsiani, Joshua I. Sanders, Z. Josh Huang, and Adam Kepecs. 2013. “Cortical Interneurons That Specialize in Disinhibitory Control.” *Nature* 503 (7477): 521–24.

Prönneke, Alvar, Bianca Scheuer, Robin J. Wagener, Martin Möck, Mirko Witte, and Jochen F. Staiger. 2015. “Characterizing VIP Neurons in the Barrel Cortex of VIPcre/tdTomato Mice Reveals Layer-Specific Differences.” Cerebral Cortex 25 (12): 4854–68.

Reimer, Jacob, Matthew J. McGinley, Yang Liu, Charles Rodenkirch, Qi Wang, David A. McCormick, and Andreas S. Tolias. 2016. “Pupil Fluctuations Track Rapid Changes in Adrenergic and Cholinergic Activity in Cortex.” Nature Communications 7 (1). https://doi.org/10.1038/ncomms13289.

Rudy, Bernardo, Gordon Fishell, Soohyun Lee, and Jens Hjerling-Leffler. 2011. “Three Groups of Interneurons Account for Nearly 100% of Neocortical GABAergic Neurons.” Developmental Neurobiology 71 (1): 45–61.

Saunders, Jonny L., and Michael Wehr. 2019. “Mice Can Learn Phonetic Categories.” The Journal of the Acoustical Society of America 145 (3): 1168.

Schneider, David M., Anders Nelson, and Richard Mooney. 2014. “A Synaptic and Circuit Basis for Corollary Discharge in the Auditory Cortex.” *Nature* 513 (7517): 189–94.

Silberberg, Gilad, and Henry Markram. 2007. “Disynaptic Inhibition between Neocortical Pyramidal Cells Mediated by Martinotti Cells.” *Neuron* 53 (5): 735–46.

Stokes, Caleb C. A., and Jeffry S. Isaacson. 2010. “From Dendrite to Soma: Dynamic Routing of Inhibition by Complementary Interneuron Microcircuits in Olfactory Cortex.” *Neuron* 67 (3): 452–65.

Takesian, Anne E., Luke J. Bogart, Jeff W. Lichtman, and Takao K. Hensch. 2018. “Inhibitory Circuit Gating of Auditory Critical-Period Plasticity.” Nature Neuroscience, January. https://doi.org/10.1038/s41593-017-0064-2.

Wehr, Michael, and Anthony M. Zador. 2003. “Balanced Inhibition Underlies Tuning and Sharpens Spike Timing in Auditory Cortex.” *Nature* 426 (6965): 442–46.

Wójcik, Daniel K. 2014. “Current Source Density (CSD) Analysis.” In Encyclopedia of Computational Neuroscience, 1–10.

Xu, Xiangmin, Keith D. Roby, and Edward M. Callaway. 2010. “Immunochemical Characterization of Inhibitory Mouse Cortical Neurons: Three Chemically Distinct Classes of Inhibitory Cells.” The Journal of Comparative Neurology 518 (3): 389–404.

Zhou, Mu, Feixue Liang, Xiaorui R. Xiong, Lu Li, Haifu Li, Zhongju Xiao, Huizhong W. Tao, and Li I. Zhang. 2014. “Scaling down of Balanced Excitation and Inhibition by Active Behavioral States in Auditory Cortex.” Nature Neuroscience 17 (6): 841–50.

Zhou, Xiaojuan, Michael Rickmann, Georg Hafner, and Jochen F. Staiger. 2017. "Subcellular Targeting of VIP Boutons in Mouse Barrel Cortex Is Layer-Dependent and Not Restricted to Interneurons." Cerebral Cortex 27 (11): 5353–68.

Zagha, Edward, Amanda E. Casale, Robert N. S. Sachdev, Matthew J. McGinley, and David A. McCormick. 2013. "Motor Cortex Feedback Influences Sensory Processing by Modulating Network State." *Neuron* 79 (3): 567–78.

CHAPTER III

Adesnik, H., Bruns, W., Taniguchi, H., Huang, Z. J., and Scanziani, M. (2012). A neural circuit for spatial summation in visual cortex. Nature, 490(7419), 226–231. oi: 10.1038/nature11526

Anderson, J. S., Carandini, M., and Ferster, D. (2000). Orientation tuning of input conductance, excitation, and inhibition in cat primary visual cortex. Journal of Neurophysiology, 84(2), 909–26.

Amitai, Y., Gibson, J. R., Beierlein, M., Patrick, S. L., Ho, A. M., Connors, B. W., et al. (2002). The spatial dimensions of electrically coupled networks of interneurons in the neocortex. The Journal of Neuroscience : The Official Journal of the Society for Neuroscience, 22(10), 4142–4152. doi: 20026371

Atallah, B. V, Bruns, W., Carandini, M., and Scanziani, M. (2012). Parvalbumin-expressing interneurons linearly transform cortical responses to visual stimuli. Neuron, 73(1), 159–70. doi: 10.1016/j.neuron.2011.12.013

Atiani, S., Elhilali, M., David, S. V., Fritz, J. B., and Shamma, S. A. (2009). Task Difficulty and Performance Induce Diverse Adaptive Patterns in Gain and Shape of Primary Auditory Cortical Receptive Fields. Neuron, 61(3), 467–480. doi: 10.1016/j.neuron.2008.12.027

Ayaz, A., Saleem, A. B., Schölvinck, M. L., and Carandini, M. (2013). Locomotion controls spatial integration in mouse visual cortex. Current Biology, 23(10), 890–894. doi: 10.1016/j.cub.2013.04.012

Bahrey, H. L. P., Moody, W. J., Bahrey, H. L. P., and Moody, W. J. (2002). Early Development of Voltage-Gated Ion Currents and Firing Properties in Neurons of the Mouse Cerebral Cortex Early Development of Voltage-Gated Ion Currents and Firing Properties in Neurons of the Mouse Cerebral Cortex. Journal of Neurophysiology, 89(December), 1761–1773. doi: 10.1152/jn.00972.2002

Baraban, S. C., and Tallent, M. K. (2004). Interneuron Diversity series: Interneuronal neuropeptides - Endogenous regulators of neuronal excitability. Trends in Neurosciences, 27(3), 135–142. doi: 10.1016/j.tins.2004.01.008

Beierlein, M., Gibson, J. R., and Connors, B. W. (2003). Two Dynamically Distinct Inhibitory Networks in Layer 4 of the Neocortex. J. Neurophysiol., 90(J), 2987–3000.

Beierlein, M., Gibson, J. R., and Connors, B. W. (2000). A network of electrically coupled interneurons drives synchronized inhibition in neocortex. Nature Neuroscience, 3(9), 904–910. doi: 10.1038/78809

Boehm, S., and Betz, H. (1997). Somatostatin inhibits excitatory transmission at rat hippocampal synapses via presynaptic receptors. Journal of Neuroscience, 17(11), 4066–4075.

Buckmaster, P. S., Otero-Corchon, V., Rubinstein, M., and Low, M. J. (2002). Heightened seizure severity in somatostatin knockout mice. Epilepsy Research, 48(1-2), 43–56. doi: 10.1016/S0920-1211(01)00318-7

Caputi, A., Melzer, S., Michael, M., and Monyer, H. (n.d.). The long and short of GABAergic neurons. Current Opinion in Neurobiology, 23(2), 179–186. doi: 10.1016/j.conb.2013.01.021

Cardin, J. A. (2012). Dissecting local circuits in vivo: integrated optogenetic and electrophysiology approaches for exploring inhibitory regulation of cortical activity. Journal of Neurophysiology, 106(3-4), 104–111. doi: 10.1016/j.jphysparis.2011.09.005.Dissecting

Cauli, B., Porter, J. T., Tsuzuki, K., Lambolez, B., Rossier, J., Quenet, B., et al. (2000). Classification of fusiform neocortical interneurons based on unsupervised clustering. Proceedings of the National Academy of Sciences of the United States of America, 97(11), 6144–6149. doi: 10.1073/pnas.97.11.6144

Chen, I.-W., Helmchen, F., and Lutcke, H. (2015). Specific Early and Late Oddball-Evoked Responses in Excitatory and Inhibitory Neurons of Mouse Auditory Cortex. Journal of Neuroscience, 35(36), 12560–12573. doi: 10.1523/JNEUROSCI.2240-15.2015

Chen, S. X., Kim, A. N., Peters, A. J., and Komiyama, T. (2015). Subtype-specific plasticity of inhibitory circuits in motor cortex during motor learning. Nature Neuroscience, 18(8), 1109–1115. doi: 10.1038/nn.4049

Connors, B. W., Gutnick, M. J., and Prince, D. A. (1982). Electrophysiological properties of neocortical neurons in vitro. Journal of Neurophysiology, 48(6), 1302–1320.

Constantinople CM, Bruno RM. (2011) Effects and mechanisms of wakefulness on local cortical networks. Neuron, Mar 24;69(6):1061-8.

Cottam, J. C. H., Smith, S. L., and Hausser, M. (2013). Target-Specific Effects of Somatostatin-Expressing Interneurons on Neocortical Visual Processing. Journal of Neuroscience, 33(50), 19567–19578. doi: 10.1523/JNEUROSCI.2624-13.2013

Cruikshank, S. J., Urabe, H., Nurmikko, A. V., and Connors, B. W. (2010). Pathway-Specific Feedforward Circuits between Thalamus and Neocortex Revealed by Selective Optical Stimulation of Axons. Neuron, 65(2), 230–245. doi: 10.1016/j.neuron.2009.12.025

Cybulska-Klosowicz, A., Posluszny, A., Nowak, K., Siucinska, E., Kossut, M., and Liguz-Lecznar, M. (2013). Interneurons containing somatostatin are affected by learning-induced cortical plasticity. Neuroscience, 254, 18–25. doi: 10.1016/j.neuroscience.2013.09.020

Davies, P., Katzman, R., and Terry, R. D. (1980). Reduced somatostatin-like immunoreactivity in cerebral cortex from cases of Alzheimer disease and Alzheimer senile dementa. Nature. doi: 10.1038/288279a0

Dodd, J., and Kelly, J. S. (1978). Is somatostatin an excitatory transmitter in the hippocampus? Neuroscience Abstracts, 273, 674–675. doi: 10.1038/273674a0

Dournaud, P., Delaere, P., Hauw, J. J., and Epelbaum, J. (1995). Differential correlation between neurochemical deficits, neuropathology, and cognitive status in Alzheimer's disease. Neurobiology of Aging, 16(5), 817–823. doi: 10.1016/0197-4580(95)00086-T

Duguid, I., Branco, T., London, M., Chadderton, P., and Hausser, M. (2012). Tonic Inhibition Enhances Fidelity of Sensory Information Transmission in the Cerebellar Cortex. Journal of Neuroscience, 32(32), 11132–11143. doi: 10.1523/JNEUROSCI.0460-12.2012

Dutar, P., Vaillend, C., Viollet, C., Billard, J. M., Potier, B., Carlo, A. S., et al. (2002). Spatial learning and synaptic hippocampal plasticity in type 2 somatostatin receptor knock-out mice. Neuroscience, 112(2), 455–466 . doi: 10.1016/S0306-4522(02)00074-X

El-Boustani, S., and Sur, M. (2014). Response-dependent dynamics of cell-specific inhibition in cortical networks in vivo. Nature Communications, 5, 5689. doi: 10.1038/ncomms6689

Endo, T., Yanagawa, Y., and Komatsu, Y. (2016). Substance P Activates Ca 2 + -Permeable Nonselective Cation Channels through a Phosphatidylcholine-Specific Phospholipase C Signaling Pathway in nNOS-Expressing GABAergic Neurons in Visual Cortex, 67(February), 669–682. doi: 10.1093/cercor/bhu233

Fanselow, E. E., Richardson, K. A, and Connors, B. W. (2008). Selective , State-Dependent Activation of Somatostatin-Expressing Inhibitory Interneurons in Mouse Neocortex. Journal of Neurophysiology, 100, 2640–2652. doi: 10.1152/jn.90691.2008.

Fino, E., and Yuste, R. (2011). Dense Inhibitory Connectivity in Neocortex. Neuron, 69(6), 1188–1203. doi: 10.1016/j.neuron.2011.02.025

Fishell, G., and Rudy, B. (2011). Mechanisms of inhibition within the telencephalon:"where the wild things are." Annual review of neuroscience. doi: 10.1146/annurev-neuro-061010-113717.Mechanisms

Fitzgerald, L. W.; Dokla, C. P. (1989) Morris water task impairment and hypoactivity following cysteamine-induced reductions of somatostatin- like immunoreactivity. Brain Res, 505(2), 246-250.

Fomby, P., Cherlin, A. J., and Yuste, R. (2014). A blanket of inhibition: functional inferences from dense inhibitory circuit structure. Current Opinion in Neurobiology, 72(2), 181–204. doi: 10.1038/nature13314.A

Freund, T. F., and Buzsáki, G. (1996). Interneurons of the hippocampus. Hippocampus, 6(4), 347–470.

Fu, Y., Tucciarone, J. M., Espinosa, J. S., Sheng, N., Darcy, D. P., Nicoll, R. A., et al. (2014). A cortical circuit for gain control by behavioral state. Cell, 156(6), 1139–1152. doi: 10.1016/j.cell.2014.01.050

Gabernet, L., Jadhav, S. P., Feldman, D. E., Carandini, M., and Scanziani, M. (2005). Somatosensory integration controlled by dynamic thalamocortical feed-forward inhibition. Neuron, 48(2), 315–327. doi: 10.1016/j.neuron.2005.09.022

Gentet, L. J. (2012). Functional diversity of supragranular GABAergic neurons in the barrel cortex. Frontiers in Neural Circuits, 6(August), 1–13. doi: 10.3389/fncir.2012.00052

Gentet, L. J., Avermann, M., Matyas, F., Staiger, J. F., and Petersen, C. C. H. (2010). Membrane Potential Dynamics of GABAergic Neurons in the Barrel Cortex of Behaving Mice. Neuron, 65(3), 422–435. doi: 10.1016/j.neuron.2010.01.006

Gentet, L. J., Kremer, Y., Taniguchi, H., Huang, Z. J., Staiger, J. F., and Petersen, C. C. (2012). Unique functional properties of somatostatin-expressing GABAergic neurons in mouse barrel cortex. Nat Neurosci, 15(4), 607–612. doi: 10.1038/nn.3051

Gibson, J. R., Beierlein, M., and Connors, B. W. (1999). Two networks of electrically coupled inhibitory neurons in neocortex. Nature, 402(6757), 75–79. doi: 10.1038/47035

Gierdalski, M., Jablonska, B., Siucinska, E., Lech, M., Skibinska, A., and Kossut, M. (2001). Rapid regulation of GAD67 mRNA and protein level in cortical neurons after sensory learning. Cerebral Cortex, 11(9), 806–15. doi: 10.1093/cercor/11.9.806

Goldberg, J. H., Lacefield, C. O., and Yuste, R. (2004). Global dendritic calcium spikes in mouse layer 5 low threshold spiking interneurones: implications for control of pyramidal cell bursting. The Journal of Physiology, 558(Pt 2), 465–478. doi: 10.1113/jphysiol.2004.064519

Greene, J. R., and Mason, A. (1996). Neuronal diversity in the subiculum: correlations with the effects of somatostatin on intrinsic properties and on GABA-mediated IPSPs in vitro. Journal of Neurophysiology, 76(3), 1657–1666.

Guido, W., Lu, S. M., Vaughan, J. W., Godwin, D. W., and Sherman, S. M. (1995). Receiver operating characteristic (ROC) analysis of neurons in the cat's lateral geniculate nucleus during tonic and burst response mode. Visual Neuroscience, 12(4), 723–741. doi: 10.1017/S0952523800008993

Guillou, J.-L., Micheau, J., and Jaffard, R. (1993). Effects of intrahippocampal injections of somatostatin and cysteamine on spatial discrimination learning in mice. Psychobiology, 21(4), 265–271. doi: 10.3758/BF03327144

Gupta, A., Wang, Y., and Markram, H. (2007). Organizing Principles for a Diversity of GABAergic Interneurons and Synapses in the Neocortex. Science, 273(2000). doi: 10.1126/science.287.5451.273

Halabisky, B., Parada, I., Buckmaster, P. S., and Prince, D. A. (2010). Excitatory input onto hilar somatostatin interneurons is increased in a chronic model of epilepsy. Journal of Neurophysiology, 104(4), 2214–2223. doi: 10.1152/jn.00147.2010

Hayut, I., Fanselow, E. E., Connors, B. W., and Golomb, D. (2011). LTS and FS inhibitory interneurons, short-term synaptic plasticity, and cortical circuit dynamics. PLoS Computational Biology, 7(10), e1002248. doi: 10.1371/journal.pcbi.1002248

Hendry, S. H. C., Schwark H. D., Jones E. G., Yan J. (1987) Number and proportions of GABA-immunoreactive neurons in different areas of monkey cerebral cortex. J. Neurosci. 7, 1503–1519.

Higley, M. J., and Contreras, D. (2006). Balanced Excitation and Inhibition Determine Spike Timing during Frequency Adaptation. Journal of Neuroscience, 26(2), 448–457. doi: 10.1523/JNEUROSCI.3506-05.2006

Hioki, H., Okamoto, S., Konno, M., Kameda, H., Sohn, J., Kuramoto, E., et al. (2013). Cell Type-Specific Inhibitory Inputs to Dendritic and Somatic Compartments of Parvalbumin-Expressing Neocortical Interneuron. Journal of Neuroscience, 33(2), 544–555. doi: 10.1523/JNEUROSCI.2255-12.2013

Hirata, A., and Castro-Alamancos, M. A. (2010). Neocortex network activation and deactivation states controlled by the thalamus. Journal of Neurophysiology, 103(3), 1147–1157. doi: 10.1152/jn.00955.2009

Hou, Z.-H., and Yu, X. (2013). Activity-regulated somatostatin expression reduces dendritic spine density and lowers excitatory synaptic transmission via postsynaptic somatostatin receptor 4. The Journal of Biological Chemistry, 288(4), 2501–9. doi: 10.1074/jbc.M112.419051

Hoyer, D., Bell, G. I., Berelowitz, M., Epelbaum, J., Feniuk, W., Humphrey, P. P., et al. (1995). Classification and nomenclature of somatostatin receptors. Trends Pharmacol Sci, 16(3), 86–88. doi: 10.1016/S0165-6147(00)88988-9

Hu, H., Ma, Y., and Agmon, A. (2011). Submillisecond Firing Synchrony between Different Subtypes of Cortical Interneurons Connected Chemically But Not Electrically. Journal of Neuroscience, 31(9), 3351–3361. doi: 10.1523/JNEUROSCI.4881-10.2011

Hu, H., Cavendish, J. Z., and Agmon, A. (2013). Not all that glitters is gold: off-target recombination in the somatostatin–IRES-Cre mouse line labels a subset of fast-spiking interneurons. Frontiers in Neural Circuits, 7(December), 1–4. doi: 10.3389/fncir.2013.00195

Ishibashi, H., and Akaike, N. (1995). Somatostatin modulates high-voltage-activated Ca2+ channels in freshly dissociated rat hippocampal neurons. Journal of Neurophysiology, 74(3), 1028–1036.

Jackson, J., Ayzenshtat, I., Karnani, M. M., Yuste, R. (2016). VIP + interneurons control neocortical activity across brain states Methods to Understand Brain Connections and Neural Function VIP ♀ interneurons control neocortical activity across brain states. Journal of Neurophysiology, 115(March), 3008–3017.doi: 10.1152/jn.01124.2015

Jasinska, M., Siucinska, E., Cybulska-Klosowicz, A., Pyza, E., Furness, D. N., Kossut, M., et al. (2010). Rapid, Learning-Induced Inhibitory Synaptogenesis in Murine Barrel Field. Journal of Neuroscience, 30(3), 1176–1184. doi: 10.1523/JNEUROSCI.2970-09.2010

Jiang, X., Wang, G., Lee, A. J., Stornetta, R. L., and Zhu, J. J. (2013). The organization of two new cortical interneuronal circuits. Nature Neuroscience, 16(2), 210–218. doi: 10.1038/nn.3305

Kapfer, C., Glickfeld, L. L., Atallah, B. V, and Scanziani, M. (2007). Supralinear increase of recurrent inhibition during sparse activity in the somatosensory cortex. Nature Neuroscience, 10(6), 743–753. doi: 10.1038/nn1909

Karnani, M. M., Jackson, J., Ayzenshtat, I., Sichani, X. A. H., Manoocheri, K., Kim, S., et al. (2016a). Opening Holes in the Blanket of Inhibition : Localized Lateral Disinhibition by VIP Interneurons. Journal of Neuroscience, 36(12), 3471–3480. doi: 10.1523/JNEUROSCI.3646-15.2016

Karnani, M. M., Jackson, J., Ayzenshtat, I., Tucciarone, J., Manoocheri, K., and Snider, W. G. (2016b). Cooperative Subnetworks of Molecularly Similar Interneurons in Mouse Neocortex Article Cooperative Subnetworks of Molecularly Similar Interneurons in Mouse Neocortex. Neuron, 90(1), 86–100. doi: 10.1016/j.neuron.2016.02.037

Karube, F., Kubota, Y., and Kawaguchi, Y. (2004). Axon Branching and Synaptic Bouton Phenotypes in GABAergic Nonpyramidal Cell Subtypes. Journal of Neuroscience, 24(12), 2853–2865. doi: 10.1523/JNEUROSCI.4814-03.2004

Katona, L., Lapray, D., Viney, T. J., Oulhaj, A., Borhegyi, Z., Micklem, B. R., et al. (2014). Sleep and Movement Differentiates Actions of Two Types of Somatostatin-Expressing GABAergic Interneuron in Rat Hippocampus. Neuron, 82(4), 872–886. doi: 10.1016/j.neuron.2014.04.007

Kato, H. K., Gillet, S. N., and Isaacson, J. S. (2016). Flexible sensory representations in auditory cortex driven by behavioral relevance. 88(December), 1–13. doi: 10.1016/j.neuron.2015.10.024

Kawaguchi, Y., and Kubota, Y. (1996). Physiological and morphological identification of somatostatin- or vasoactive intestinal polypeptide-containing cells among GABAergic cell subtypes in rat frontal cortex. Journal of Neuroscience. 16(8), 2701–2715.

Kawaguchi, Y., and Kubota, Y. (1997). GABAergic cell subtypes and their synaptic connections in rat frontal cortex. Cerebral Cortex, 7(6), 476–486. doi: 10.1093/cercor/7.6.476

Kawaguchi, Y., and Kubota, Y. (1998). Neurochemical Features and Synaptic Connections of Large Physiologically-Identified Gabaergic Cells In the Rat Frontal Cortex. Neuroscience, 85(3), 677–701.

Kawaguchi, Y., Bavelier, D., Levi, D. M., Li, R. W., Dan, Y., Hensch, T. K., et al. (1997). Selective Cholinergic Modulation of Cortical GABAergic Cell Subtypes. Rapid Communication. 97(May), 1743–1747.

Kawaguchi, Y., and Shindou, T. (1998). Noradrenergic excitation and inhibition of GABAergic cell types in rat frontal cortex. Journal of Neuroscience , 18(17), 6963–6976.

Kerlin, A. M., Andermann, M. L., Berezovskii, V. K., and Reid, R. C. (2010). Broadly tuned response properties of diverse inhibitory neuron subtypes in mouse visual cortex. Neuron, 67(5), 858–71. doi: 10.1016/j.neuron.2010.08.002

Kilduff, T. S., Cauli, B., Gerashchenko, D., Curie, M., and Neurobiologie, L. De. (2011). Activation of cortical interneurons during sleep : an anatomical link to homeostatic sleep regulation ? Trends in Neurosciences, 34(1), 10–19. doi: 10.1016/j.tins.2010.09.005

Kinnischtzke, A. K., Sewall, A. M., Berkepile, J. M., and Fanselow, E. E. (2012). Postnatal maturation of somatostatin-expressing inhibitory cells in the somatosensory cortex of GIN mice. Frontiers in Neural Circuits, 6(May), 1-12. doi: 10.3389/fncir.2012.00033

Kits, K. S. and Mansvelder, H. D. (2000) Regulation of exocytosis in neuroendocrine cells: spatial organization of channels and vesicles, stimulus-secretion coupling, calcium buffers and modulation. Brain Res. Rev. 33, 78–94

Kozloski, J., Hamzei-Sichani, F., and Yuste, R. (2001). Stereotyped Position of Local Synaptic Targets in Neocortex. Science, 293(5531), 868–872. doi: 10.1126/science.293.5531.868

Kvitsiani, D., Ranade, S., Hangya, B., Taniguchi, H., Huang, J. Z., and Kepecs, A. (2013). Distinct behavioural and network correlates of two interneuron types in prefrontal cortex. Nature, 498(7454), 363–366. doi: 10.1038/nature12176

Kubota, Y. (2014). Untangling GABAergic wiring in the cortical microcircuit. Current Opinion in Neurobiology, 26, 7–14. doi: 10.1016/j.conb.2013.10.003

Kubota, Y., Karube, F., Nomura, M., and Kawaguchi, Y. (2016). The Diversity of Cortical Inhibitory Synapses. Frontiers in Neural Circuits, 10(April), 1–15. doi: 10.3389/fncir.2016.00027

Kubota, Y., and Kawaguchi, Y. (1994). Three classes of GABAergic interneurons in neocortex and neostriatum. The Japanese Journal of Physiology, 44March), S145–S148.

Kubota, Y., Shigematsu, N., Karube, F., Sekigawa, A., Kato, S., Yamaguchi, N., et al. (2011). Selective Coexpression of Multiple Chemical Markers Defines Discrete Populations of Neocortical GABAergic Neurons, Cerebral Cortex, (21), 1803-1817. doi: 10.1093/cercor/bhq252

Kubota, Y., Kondo, S., Nomura, M., Hatada, S., Yamaguchi, N., Mohamed, A. A., et al. (2015). Functional effects of distinct innervation styles of pyramidal cells by fast spiking cortical interneurons. eLIFE, (4), 1–27. doi: 10.7554/eLife.07919

Kumar A, Vlachos I, Aertsen A, Boucsein C. (2013). Challenges of understanding brain function by selective modulation of neuronal subpopulations. Trends Neurosci. Oct;36(10):579-86.

Kwan, A. C., and Dan, Y. (2013). Dissection of cortical microcircuits by single-neuron stimulation in vivo. Current Biology, 22(16), 1459–1467. doi: 10.1016/j.cub.2012.06.007.Dissection

Lamirault, L., Guillou, J. L., Micheau, J., and Jaffard, R. (2001). Intrahippocampal injections of somatostatin dissociate acquisition from the flexible use of place responses. European Journal of Neuroscience, 14(3), 567–570. doi: 10.1046/j.0953-816X.2001.01672.x

Large, A. M., Kunz, N. A., Mielo, S. L., Oswald, A. M., and Oswald, A. M. (2016). Inhibition by Somatostatin Interneurons in Olfactory Cortex. Frontiers in Neural Circuits, 10(August), 1–17. doi: 10.3389/fncir.2016.00062

Lee, S. H., and Dan, Y. (2012). Neuromodulation of Brain States. Neuron, 76(1), 109–222. doi: 10.1016/j.neuron.2012.09.012

Lee, S. H., Kwan, A. C., Zhang, S., Phoumthipphavong, V., Flannery, J. G., Masmanidis, S. C., et al. (2012). Activation of specific interneurons improves V1 feature selectivity and visual perception. Nature, 488(7411), 379–83. doi: 10.1038/nature11312

Lee, S. H., Kwan, A. C., and Dan, Y. (2014). Interneuron subtypes and orientation tuning. Nature, 508, E1–E2. doi: 10.1038/nature13128

Lee, S., Hjerling-Leffler, J., Zagha, E., Fishell, G., and Rudy, B. (2010). The largest group of superficial neocortical GABAergic interneurons expresses ionotropic serotonin receptors. J Neurosci, 30(50), 16796–16808. doi: 10.1523/JNEUROSCI.1869-10.2010

Lee, S., Kruglikov, I., Huang, Z. J., Fishell, G., and Rudy, B. (2013). A disinhibitory circuit mediates motor integration in the somatosensory cortex. Nature Neuroscience, 16(11), 1662–1670. doi: 10.1038/nn.3544

Leresche, N., Asprodini, E., Emri, Z., Cope, D. W., and Crunelli, V. (2000). Somatostatin inhibits GABAergic transmission in the sensory thalamus via presynaptic receptors. Neuroscience, 98(3), 513–522. doi: 10.1016/S0306-4522(00)00107-X

Letzkus, J. J., Wolff, S. B. E., Meyer, E. M. M., Tovote, P., Courtin, J., Herry, C., et al. (2011). A disinhibitory microcircuit for associative fear learning in the auditory cortex. Nature, 480(7377), 331–335. doi: 10.1038/nature10674

Li, L. -y., Xiong, X. R., Ibrahim, L. A., Yuan, W., Tao, H. W., and Zhang, L. I. (2015). Differential Receptive Field Properties of Parvalbumin and Somatostatin Inhibitory Neurons in Mouse Auditory Cortex. Cerebral Cortex, 25(7), 1782–1791. doi: 10.1093/cercor/bht417

Liguz-lecznar, M., Urban-ciecko, J., and Kossut, M. (2016). Somatostatin and Somatostatin-Containing Neurons in Shaping Neuronal Activity and Plasticity. Journal of Neurophysiology, 10(June), 1–15. doi: 10.3389/fncir.2016.00048

Lisman, J. E. (1997). Bursts as a unit of neural information: Making unreliable synapses reliable. Trends in Neurosciences, 20(1), 38–43. doi: 10.1016/S0166-2236(96)10070-9

Livingstone, M. S., Freeman, D. C., and Hubel, D. H. (1996). Visual responses in V1 of freely viewing monkeys. Cold Spring Harbor Symposia on Quantitative Biology, 61, 27–37. doi: 10.1101/SQB.1996.061.01.006

Lovett-Barron, M., Turi, G. F., Kaifosh, P., Lee, P. H., Bolze, F., Sun, et al. (2012). Regulation of neuronal input transformations by tunable dendritic inhibition. Nat. Neurosci. 15, 423–430. doi: 10.1038/nn.3024

Ludwig, M. and Pittman, Q. J. (2003) Talking back: dendritic neurotransmitter release. Trends Neurosci. 26, 255–261

Ma, Y., Hang, H., Berrebi, S. A., Mathers, H. P., and Agmon, A. (2006). Distinct Subtypes of Somatostatin-Containing Neocortical Interneurons Revealed in Transgenic Mice. Journal of Neuroscience, 26(19), 5069–5082. doi: 10.1523/JNEUROSCI.0661-06.2006

Ma, Y., Hioki, H., Konno, M., Pan, S., Nakamura, H., Nakamura, K. C., et al. (2011). Expression of Gap Junction Protein Connexin36 in Multiple Subtypes of GABAergic Neurons in Adult Rat Somatosensory Cortex. Cerebral Cortex, (21), 2639–2649. doi: 10.1093/cercor/bhr051

Ma, Y., Hu, H., Agmon, A. (2012). Short-Term Plasticity of Unitary Inhibitory-to-Inhibitory Synapses Depends on the Presynaptic Interneuron Subtype. Journal of Neuroscience, 32(3), 983–988. doi: :10.1523/JNEUROSCI.5007-11.2012

Ma, W. -p., Liu, B. -h., Li, Y. -t., Josh Huang, Z., Zhang, L. I., and Tao, H. W. (2010). Visual Representations by Cortical Somatostatin Inhibitory Neurons--Selective But with Weak and Delayed Responses. Journal of Neuroscience, 30(43), 14371–14379. doi: 10.1523/JNEUROSCI.3248-10.2010

Markram, H., Toledo-Rodriguez, M., Wang, Y., Gupta, A., Silberberg, G., and Wu, C. (2004). Interneurons of the neocortical inhibitory system. Nature Reviews Neuroscience, 5(10), 793–807. doi: 10.1038/nrn1519

Markram, H., Wang, Y., and Tsodyks, M. (1998). Differential signaling via the same axon of neocortical pyramidal neurons. Proceedings of the National Academy of Sciences of the United States of America, 95(9), 5323–5328. doi: 10.1073/pnas.95.9.5323

Martinotti, C. (1889). "Contributo allo studio della corteccia cerebrale, ed all'origine centrale dei nervi". Ann. Freniatr. Sci. Affini. 1: 14–381

McGinley, M. J., David, S. V., and McCormick, D. A. (2015). Cortical Membrane Potential Signature of Optimal States for Sensory Signal Detection. Neuron, 87(1), 179–192. doi: 10.1016/j.neuron.2015.05.038

McGarry, L. M., Packer, A. M., Fino, E., Nikolenko, V., Sippy, T., & Yuste, R. (2010). Quantitative classification of somatostatin-positive neocortical interneurons identifies three interneuron subtypes. Frontiers in Neural Circuits, 4(May), 1–19. doi: 10.3389/fncir.2010.00012

Moore, S.D., Madamba, S.G., Joels, M., Siggins, G.R. (1988). Somatostatin augments the M-current in hippocampal neurons. Science, 239(4837), 278-280.

Moore, A. K., and Wehr, M. (2013). Parvalbumin-Expressing Inhibitory Interneurons in Auditory Cortex Are Well-Tuned for Frequency. Journal of Neuroscience, 33(34), 13713–13723. doi: 10.1523/JNEUROSCI.0663-13.2013

Moreau, W. A., Amar, M., Le Roux, N., Morel, N., and Fossier, P. (2010). Serotoninergic fine-tuning of the excitation-inhibition balance in rat visual cortical networks. Cerebral Cortex, 20(2), 456–467. doi: 10.1093/cercor/bhp114

Mukherjee, P., and Kaplan, E. (1995). Dynamics of neurons in the cat lateral geniculate nucleus: in vivo electrophysiology and computational modeling. Journal of Neurophysiology, 74(3), 1222–1243.

Murayama, M., Perez-Garci, E., Nevian, T., Bock, T., Senn, W., and Larkum, M. E. (2009). Dendritic encoding of sensory stimuli controlled by deep cortical interneurons. Nature Letters, 457(February), 1137–1141. doi: 10.1038/nature07663

Nakagawasai, O., Hozumi, S., Tan-No, K., Niijima, F., Arai, Y., Yasuhara, H., and Tadano, T. (2003). Immunohistochemical fluorescence intensity reduction of brain somatostatin in the impairment of learning and memory-related behaviour induced by olfactory bulbectomy. Behavioural Brain Research, 142(1-2), 63–67. doi: 10.1016/S0166-4328(02)00383-2

Natan, R. G., Briguglio, J. J., Mwilambwe-tshilobo, L., Jones, S. I., Aizenberg, M., Goldberg, E. M., et al. (2015). Complementary control of sensory adaptation by two types of cortical interneurons. eLIFE, (October), 1–27. doi: 10.7554/eLife.09868

Neske, G. T., Patrick, S. L., and Connors, B. W. (2015). Contributions of Diverse Excitatory and Inhibitory Neurons to Recurrent Network Activity in Cerebral Cortex. J. Neurosci., 35(3), 1089–1105. doi: 10.1523/JNEUROSCI.2279-14.2015

Okun, M., and Lampl, I. (2008). Instantaneous correlation of excitation and inhibition during ongoing and sensory-evoked activities. Nature Neuroscience, 11(5), 535–537. doi: 10.1038/nn.2105

Oliva, a a, Jiang, M., Lam, T., Smith, K. L., and Swann, J. W. (2000). Novel hippocampal interneuronal subtypes identified using transgenic mice that express green fluorescent protein in GABAergic interneurons. Journal of Neuroscience, 20(9), 3354–3368. doi: 0270-6474/00/203354-15$15.00/0

Otazu, G.H., Tai, L.H., Yang, Y., and Zador, A.M. (2009). Engaging in an auditory task suppresses responses in auditory cortex. Nature Neuroscience. 12, 646–654.

Pala, A., and Petersen, C. C. H. (2015). In Vivo Measurement of Cell-Type-Specific Synaptic Connectivity and Synaptic Transmission in Layer 2/3 Mouse Barrel Cortex. Neuron, 85(1), 68–76. doi: 10.1016/j.neuron.2014.11.025

Perrenoud, Q., Geoffroy, H., Gauthier, B., Rancillac, A., Alfonsi, F., Kessaris, N., et al. (2012). Characterization of Type I and Type II nNOS-Expressing Interneurons in the Barrel Cortex of Mouse. Frontiers in Neural Circuits, 6(June), 1–17. doi: 10.3389/fncir.2012.00036

Pfeffer, C. K., Xue, M., He, M., Huang, Z. J., and Scanziani, M. (2013). Inhibition of inhibition in visual cortex: the logic of connections between molecularly distinct interneurons. Nature Neuroscience, 16(8), 1068–76. doi: 10.1038/nn.3446

Pi, H.-J., Hangya, B., Kvitsiani, D., Sanders, J. I., Huang, Z. J., and Kepecs, A. (2013). Cortical interneurons that specialize in disinhibitory control. Nature, 503(7477), 521–4. doi: 10.1038/nature12676

Pittman, Q. J., and Siggins, G. R. (1981). Somatostatin hyperpolarizes hippocampal pyramidal cells in vitro. Brain Research, 221(2), 402–408. doi: 10.1016/0006-8993(81)90791-5

Rock, C., Zurita, H., Wilson, C., and Apicella, A. (2016). An inhibitory corticostriatal pathway. eLIFE, (5), 1–17. doi: 10.7554/eLife.15890

Polack, P. O., Friedman, J., and Golshani, P. (2013). Cellular mechanisms of brain state-dependent gain modulation in visual cortex. Nature Neuroscience, 16(9), 1331–9. doi: 10.1038/nn.3464

Reyes, A., Lujan, R., Rozov, A., Burnashev, N., Somogyi, P., and Sakmann, B. (1998). Target-cell-specific facilitation and depression in neocortical circuits. Nature Neuroscience, 1(4), 279–285. doi: 10.1038/1092

Rogers, J. H. (1992). Immunohistochemical markers in rat brain: colocalisation of calretinin and calbindin-D28k with tyrosine hydroxylase. Brain Res., 587(44), 203–210.

Royer, S., Zemelman, B. V, Losonczy, A., Kim, J., Chance, F., Magee, J. C., et al. (2012). Control of timing, rate and bursts of hippocampal place cells by dendritic and somatic inhibition. Nature Neuroscience, 15(5), 1–10. doi: 10.1038/nn.3077

Rudy, B., Fishell, G., Lee, S., and Hjerling-Leffler, J. (2011). Three groups of interneurons account for nearly 100% of neocortical GABAergic neurons. Dev. Neurobiol. 71, 45–61.

Sadagopan, S., and Wang, X. (2010). Contribution of Inhibition to Stimulus Selectivity in Primary Auditory Cortex of Awake Primates. Journal of Neuroscience, 30(21), 7314–7325. doi: 10.1523/JNEUROSCI.5072-09.2010

Scharfman, H. E., and Schwartzkroin, P. A. (1989). Selective depression of GABA-mediated IPSPs by somatostatin in area CA1 of rabbit hippocampal slices. Brain Research, 493(2), 205–211. doi: 10.1016/0006-8993(89)91155-4

Seybold, B. a, Phillips, E. a K., Schreiner, C. E., and Hasenstaub, A. R. (2015). Inhibitory Actions Unified by Network Integration. Neuron, 87(6), 1181–1192. doi: 10.1016/j.neuron.2015.09.013

Sherwood, C. C., Raghanti, M. A., Stimpson, C. D., Spocter, M. a, Uddin, M., Boddy, A. M., et al. (2010). Inhibitory interneurons of the human prefrontal cortex display conserved evolution of the phenotype and related genes. Proceedings. Biological Sciences / The Royal Society, 277(1684), 1011–20. doi: 10.1098/rspb.2009.1831

Scholl B., Pattadkal J. J., Dilly G. A., Priebe N. J., Zemelman B. V. (2015). Local Integration Accounts for Weak Selectivity of Mouse Neocortical Parvalbumin Interneurons. Neuron. 87(2):424-36.

Schweitzer, P., Madamba, S. G., and Siggins, G. R. (1998). Somatostatin increases a voltage-insensitive K+ conductance in rat CA1 hippocampal neurons. Journal of Neurophysiology, 79(3), 1230–1238.

Silberberg, G., and Markram, H. (2007). Disynaptic Inhibition between Neocortical Pyramidal Cells Mediated by Martinotti Cells. Neuron, 53(5), 735–746. doi: 10.1016/j.neuron.2007.02.012

Siucinska, E. (2006). GAD67-positive puncta: Contributors to learning-dependent plasticity in the barrel cortex of adult mice. Brain Research, 1106(1), 52–62. doi: 10.1016/j.brainres.2006.05.061

Somogyi, P., and Klausberger, T. (2005). Defined types of cortical interneurone structure space and spike timing in the hippocampus. The Journal of Physiology, 562, 9–26. doi: 10.1113/jphysiol.2004.078915

Sturgill, J. F., and Isaacson, J. S. (2015). Somatostatin cells regulate sensory response fidelity via subtractive inhibition in olfactory cortex. Nature Neuroscience, 18(4), 531–5. doi: 10.1038/nn.3971

Sun, Q.-Q., Huguenard, J. R., and Prince, D. A. (2002). Somatostatin inhibits thalamic network oscillations in vitro: actions on the GABAergic neurons of the reticular nucleus. The Journal of Neuroscience, 22(13), 5374–86.doi: 20026529

Suzuki, N., and Bekkers, J. M. (2010). Distinctive Classes of GABAergic Interneurons Provide Layer-Specific Phasic Inhibition in the Anterior Piriform Cortex. Cerebral Cortex, 20(12), 2971–2984. doi: 10.1093/cercor/bhq046

Szymanski, F. D., Garcia-Lazaro, J. a, and Schnupp, J. W. H. (2009). Current source density profiles of stimulus-specific adaptation in rat auditory cortex. Journal of Neurophysiology, 102(3), 1483–90. doi: 10.1152/jn.00240.2009

Tallent, M. K., and Siggins, G. R. (1997). Somatostatin depresses excitatory but not inhibitory neurotransmission in rat CA1 hippocampus. Journal of Neurophysiology, 78(6), 3008–3018.

Tamamaki, N., and Tomioka, R. (2010). Long-range GABAergic connections distributed throughout the neocortex and their possible function. Frontiers in Neuroscience, 4(December), 1–8. doi: 10.3389/fnins.2010.00202

Tamamaki, N., Yanagawa, Y., Tomioka, R., Miyazaki, J. I., Obata, K., and Kaneko, T. (2003). Green Fluorescent Protein Expression and Colocalization with Calretinin,

Parvalbumin, and Somatostatin in the GAD67-GFP Knock-In Mouse. Journal of Comparative Neurology, 467(1), 60–79. doi: 10.1002/cne.10905

Taniguchi, H., He, M., Wu, P., Kim, S., Paik, R., Sugino, K., et al. (2011). A Resource of Cre Driver Lines for Genetic Targeting of GABAergic Neurons in Cerebral Cortex. Neuron, 71(6), 995–1013. doi: 10.1016/j.neuron.2011.07.026

Thomson, A. M. (1997). Activity-dependent properties of synaptic transmission at two classes of connections made by rat neocortical pyramidal axons in vitro. Journal of Physiology, 502(1), 131–147. doi: 10.1111/j.1469-7793.1997.131bl.x

Thomson, A. M., and Deuchars, J. (1997). Synaptic interactions in neocortical local circuits: Dual intracellular recordings in vitro. Cerebral Cortex, 7(6), 510–522. doi: 10.1093/cercor/7.6.510

Tomioka, R., Okamoto, K., Furuta, T., Fujiyama, F., Iwasato, T., Yanagawa, Y., et al. (2005). Demonstration of long-range GABAergic connections distributed throughout the mouse neocortex. European Journal of Neuroscience, 21(6), 1587–1600. doi: 10.1111/j.1460-9568.2005.03989.x

Tomioka, N. H., Yasuda, H., Miyamoto, H., Hatayama, M., Morimura, N., Matsumoto, Y., et al. (2014). Elfn1 recruits presynaptic mGluR7 in trans and its loss results in seizures. Nature Communications, 5, 4501. doi: 10.1038/ncomms5501

Tricoire, L., Vitalis, T., and Rudy, B. (2012). Neuronal nitric oxide synthase expressing neurons : a journey from birth to neuronal circuits. Frontiers in Neural Circuits, 6(December), 1–16. doi: 10.3389/fncir.2012.00082

Tuboly, G., and Vécsei, L. (2013). Somatostatin and cognitive function in neurodegenerative disorders. Mini Reviews in Medicinal Chemistry, 13(1), 34–46.

Uematsu, M., Hirai, Y., Karube, F., Kato, M., Abe, K., Obata, K., et al. (2008). Quantitative Chemical Composition of Cortical GABAergic Neurons Revealed in Transgenic Venus-Expressing Rats. Cerebral Cortex, (February), 315–330. doi: 10.1093/cercor/bhm056.

Urban-Ciecko, J., and Barth, A. L. (2016). Somatostatin neurons in cortical networks. Nature Publishing Group, 17(7), 401–409. doi: 10.1038/nrn.2016.53.

Urban-Ciecko, J., Fanselow, E. E., and Barth, A. L. (2015). Neocortical Somatostatin Neurons Reversibly Silence Excitatory Transmission via GABAb Receptors. Current Biology, 25(6), 722–731. doi: 10.1016/j.cub.2015.01.035.

Vécsei, L., Király, C., Bollók, I., Nagy, A., Varga, J., Penke, B., Telegdy, G. (1984). Comparative studies with somatostatin and cysteamine in different behavioral tests on rats. Pharmacol. Biochem. Behav., 21(6), 833-837.

Vécsei, L., Klivenyi, P. (1995). Somatostatin and Alzheimer's disease. Archives of Gerontology and Geriatrics, 21, 35–41.

Vécsei, L., Widerlov, E. (1988). Effects of intracerebroventricularly administered somatostatin on passive avoidance, suttle-box behavior and open-field activity in rats. Neuropeptides, 12(4), 237-242. doi: 10.1016/0143-4179(88)90061-3

Viana, F., Hille, B. (1996). Modulation of high voltage-activated calcium channels by somatostatin in acutely isolated rat amygdaloid neurons. The Journal of Neuroscience : The Official Journal of the Society for Neuroscience, 16(19), 6000–11.

Wang, Y., Toledo-Rodriguez, M., Gupta, A., Wu, C., Silberberg, G., Luo, J., et al. (2004). Anatomical, physiological and molecular properties of Martinotti cells in the somatosensory cortex of the juvenile rat. The Journal of Physiology, 561(1), 65–90. doi: 10.1113/jphysiol.2004.073353

Wehr, M., and Zador, A. M. (2003). Balanced inhibition underlies tuning and sharpens spike timing in auditory cortex. Nature, 426(6965), 442–446. doi: 10.1038/nature02116

Wilent, W. B., and Contreras, D. (2005). Dynamics of excitation and inhibition underlying stimulus selectivity in rat somatosensory cortex. Nature Neuroscience, 8(10), 1364–1370. doi: 10.1038/nn1545

Wilson, N. R., Runyan, C. A., Wang, F. L., and Sur, M. (2012). Division and subtraction by distinct cortical inhibitory networks in vivo. Nature, 488(7411), 343–348. doi: 10.1038/nature11347

Xu, H., Jeong, H.-Y., Tremblay, R., and Rudy, B. (2013). Neocortical Somatostatin-Expressing GABAergic Interneurons Disinhibit the Thalamorecipient Layer 4. Neuron, 77(1), 155–167. doi: 10.1016/j.neuron.2012.11.004

Xu, X., and Callaway, E. M. (2009). Laminar Specificity of Functional Input to Distinct Types of Inhibitory Cortical Neurons. Journal of Neuroscience, 29(1), 70–85. doi: 10.1523/JNEUROSCI.4104-08.2009

Xu, X., Roby, K. D., and Callaway, E. M. (2006). Mouse Cortical Inhibitory Neuron Type That Coexpresses Somatostatin and Calretinin. The Journal of Comparative Neurology, 504(3), 144–160. doi: 10.1002/cne

Xue, M., Atallah, B. V., and Scanziani, M. (2014). Equalizing excitation–inhibition ratios across visual cortical neurons. Nature, 511(7511), 596–600. doi: 10.1038/nature13321.

Zeyda, T., Diehl, N., Paylor, R., Brennan, M. B., and Hochgeschwender, U. (2001). Impairment in motor learning of somatostatin null mutant mice. Brain Research, 906(1-2), 107–114. doi: 10.1016/S0006-8993(01)02563-X

Zhang, W., Zhang, L., Liang, B., Schroeder, D., Zhang, Z., Cox, G. A., et al. (2016). Hyperactive somatostatin interneurons contribute to excitotoxicity in neurodegenerative disorders. Nature Neuroscience, 19(4), 2–6. doi: 10.1038/nn.4257

Zhang, S., Xu, M., Kamigaki, T., Phong Hong Do, J., Chang, W.-C., Jenway, S., et al. (2014). Long-range and local circuits for top-down modulation of visual cortex processing. Science, 660(345), 660–665. doi: 10.1126/science.1254126